



# Crack width in Tunnels

A thesis on the accuracy of the Eurocode 2 crack width calculation of flexural cracks in structures with large thicknesses.

Peter Bart Knuvers (4416406)



# Crack width in Tunnels

A thesis on the accuracy of the Eurocode 2 crack width calculation of flexural cracks in structures with large thicknesses.

By

P.B. Knuvers

in partial fulfilment of the requirements for the degree of

**Master of Science**

in Structural Engineering, Hydraulic Structures

at the Delft University of Technology, Faculty of Civil Engineering,

to be defended publicly on 13 February, 2018 at 15:00 AM.

Supervisor:	Prof. dr. ir. D. A. Hordijk	TU Delft
Thesis committee:	Dr. ir C. R. Braam,	TU Delft
	Ir. K. J. Reinders,	TU Delft
	Ir. C. M. P. 't Hart,	TEC / Royal Haskoning DHV

*This thesis is confidential and cannot be made public until 13 February, 2018.*

An electronic version of this thesis is available at <http://repository.tudelft.nl/>.

Source front image: <http://www.aecom.com/projects/guangzhou-zhouthouzui-immersed-tunnel/>



# Preface

This is the final report of my master's thesis on crack width in Tunnels, which I did at Tunnel Engineering Consultants (TEC) for my study at Delft University of Technology. With this thesis my master in the direction of Structural Engineering with specialisation Hydraulic Structures has been finalized.

The topic of this thesis has been provided by TEC. This organisation is a permanent joint venture partnership between Royal HaskoningDHV and Witteveen+Bos. TEC is used to combine knowledge, experience and expertise in underground project.

At last I want to thank my committee for their guidance, expertise and supervision. During the process they have given me advice and direction, which led to this end result. Next to that I want to thank my colleagues at TEC / Royal HaskoningDHV for their expertise and the facilities they have let me use during my thesis.

Peter Bart Knuvers

*Delft, February 2018*

# Contents

Preface.....	I
Contents.....	II
Abstract.....	VI
List of symbols.....	VIII
List of figures.....	XI
List of tables.....	XIV
1 Introduction .....	1
1.1 General description .....	1
1.1.1 Immersed Tunnels .....	1
1.1.2 Concrete .....	2
1.1.3 Cracks.....	2
1.2 The problem.....	3
1.2.1 Problem description.....	3
1.2.2 Problem analysis.....	3
1.2.3 Problem definition .....	5
1.3 Guide .....	6
I Analytical calculations .....	7
2 Crack width formulas in codes.....	8
2.1 Eurocode 2.....	8
2.2 Model code 2010.....	12
2.3 Other codes.....	15
2.3.1 AASHTO (US).....	15
2.3.2 JSCE (Japan).....	16
2.3.3 JTG D62 (China).....	17
2.4 Differences between the codes .....	18
2.4.1 Eurocode 2 vs Model code 2010 .....	18
2.4.2 Eurocode 2 vs AASHTO.....	19
2.4.3 Eurocode 2 vs JSCE .....	19
2.4.4 Eurocode 2 vs JTG D62.....	20
3 Influence height on crack width .....	22
3.1 Approach calculations .....	22
3.2 Input codes .....	24
3.2.1 Geometry .....	24

3.2.2	Materials .....	24
3.2.3	Reinforcement percentage .....	25
3.2.4	Compression height .....	26
3.3	Influence cover .....	28
3.3.1	Eurocode 2.....	28
3.3.2	Other codes .....	32
3.4	Influence reinforcement percentage .....	34
3.4.1	Eurocode 2.....	34
3.4.2	Other codes .....	36
3.5	Influence concrete tensile strength .....	38
3.5.1	Eurocode 2.....	38
3.5.2	Other codes .....	40
3.6	Influence reinforcement stress.....	41
3.6.1	Eurocode 2.....	41
3.6.2	Other codes .....	44
3.7	Conclusions.....	45
3.7.1	Cover .....	45
3.7.2	Reinforcement percentage .....	45
3.7.3	Concrete tensile strength .....	45
3.7.4	Reinforcement stress .....	45
3.7.5	General conclusion .....	45
II	Numerical calculations.....	46
4	DIANA .....	47
4.1	General description .....	47
4.2	Material models.....	47
4.2.1	Total strain crack model .....	47
4.2.2	Multi directional fixed crack model.....	47
4.2.3	Tensile behaviour of concrete .....	48
4.2.4	Compressive behaviour of concrete .....	49
4.2.5	Bond-slip .....	50
4.3	Elements .....	51
5	Verification .....	52
5.1	Input DIANA .....	52
5.1.1	Concrete .....	52
5.1.2	Reinforcement steel .....	54
5.1.3	Steel plates .....	55

5.1.4	Interfaces .....	55
5.2	Experiment Braam.....	56
5.2.1	Geometry .....	56
5.2.2	Force-Displacement .....	58
5.2.3	Crack pattern.....	59
5.2.4	Crack width .....	60
5.3	Experiment E3.....	62
5.3.1	Geometry .....	62
5.3.2	Force-Displacement .....	64
5.3.3	Crack pattern.....	65
5.3.4	Crack width .....	66
5.4	Experiment VS-C3.....	68
5.4.1	Geometry .....	68
5.4.2	Force-Displacement .....	70
5.4.3	Crack pattern.....	71
5.4.4	Crack width .....	71
5.5	Conclusion .....	72
5.5.1	Force displacement.....	72
5.5.2	Crack pattern.....	72
5.5.3	Crack width .....	72
6	Influence height on crack width .....	73
6.1	DIANA input .....	73
6.2	Influence cover.....	77
6.3	Influence reinforcement percentage .....	80
6.4	Influence concrete tensile strength.....	82
6.5	Influence reinforcement stress.....	84
6.6	Conclusions.....	86
6.6.1	Cover .....	86
6.6.2	Reinforcement percentage .....	86
6.6.3	Concrete tensile strength .....	86
6.6.4	Reinforcement stress .....	86
6.6.5	General conclusion .....	86
III	Comparison, Conclusions and Recommendations .....	87
7	Comparison Analytical and Numerical.....	88
7.1	Influence cover.....	89
7.2	Influence reinforcement percentage .....	92



7.3	Influence concrete tensile strength.....	94
7.4	Influence reinforcement stress.....	96
7.5	Adjusting Eurocode 2.....	98
7.5.1	Crack strain.....	98
7.5.2	Crack spacing.....	100
8	Conclusions and recommendations.....	101
8.1	Conclusions.....	101
8.2	Recommendations.....	103
9	List of literature.....	104
IV	Appendix.....	105

# Abstract

When engineers at Tunnel Engineering Consultants (TEC) used the Eurocode 2 (EC2) for the verification of flexural cracks in cross sections of immersed tunnel elements, they found out that there was more reinforcement needed for crack width limitation than for tensile strength of the reinforced concrete. This raised questions, namely whether the extra reinforcement is needed, how accurate the EC2 calculates the crack width and what the influence is of the construction height on the crack width?

*Are the current rules in the Eurocode 2 for the calculation of flexural cracks too conservative for large thicknesses that are applied in the concrete lining of immersed tunnels?*

In this thesis the crack width calculation of the EC2 has been compared with other codes around the world, namely the AASHTO (United states), the JSCE (Japan), the JTG D62 (China) and the Model code 2010. When these codes are compared with each other it seemed to be that the EC2 is not conservative in comparison with the other codes, however it does not directly mean that this is true.

To check whether the codes, especially the EC2, are conservative, the codes should be compared with laboratory experiments. Since there is little data of experiments available where the cracks are carefully measured, in particular beams with large thicknesses, the finite element program DIANA is used to gain more data sets. A DIANA model is validated with three different experiments with each a different height. The DIANA model is able to predict the crack patterns quite well. Though, the crack widths are a bit off, because the mean of the crack widths in DIANA is in range of the maximum crack width of the experiments. For this reason the mean of the DIANA results is compared with the outcome of the EC2, since the EC2 gives a maximum value.

When the EC2 and the DIANA results are compared, a few differences are found. The predicted crack widths in the EC2 are larger than that of the DIANA results. In the EC2 the crack width is the multiplication of the crack strain and crack spacing. If these values are compared, the EC2 gives a smaller crack strain than DIANA and therefore the crack spacing gives an even larger difference than the crack width. Next to that, the influence of the parameters in the EC2 is analysed. In both the EC2 and the DIANA results the cover is the most important parameter for the crack spacing and the steel stress of the reinforcement is the most important parameter for the strain. In all the results there is almost no effect of the construction height visible, except in the crack strain of the DIANA results when the cover is relatively large. A decrease of strain with an increase of height has been detected.

The differences in crack strain can be explained by the fact that the strain in the EC2 is calculated at reinforcement height, but the strain at the outer fibre is needed. In axial loaded cases these strains are the same, but in cases where the cracks appear due to bending moments, which is the case in this thesis, the strain is bigger at outer fibre. Next to that it seemed that influence factors used in the crack spacing calculation are overestimated, but no clear reason is found for this result.

So eventually the current rules for crack width calculation in the EC2 are slightly conservative. And almost no effect of the increase of thickness/construction height has been observed, except for the crack strain results where a large cover is applied.

# List of symbols

$W_{\max}$	maximum allowable crack width;
$w_k$	crack width;
$S_{r,\max}$	crack spacing;
$f_{ct,eff}$	effective concrete tensile strength;
$\sigma_s$	tension stress in the reinforcement;
$\alpha_e$	ratio $E_s/E_{cm}$ ;
$E_s$	steel young's modulus;
$E_{cm}$	concrete mean young's modulus;
$A_s$	steel area;
$\rho_{p,eff}$	effective reinforcement percentage, ratio $A_s/A_{c,eff}$ ;
$k_t$	Eurocode 2 factor dependent on the duration of the load, 0,6 for short term loading and 0,4 for long term loading;
$A_{c,eff}$	the effective area of concrete in tension around the reinforcement;
$h_{c,eff}$	effective height of concrete in tension, the minimum of $2.5(h-d)$ or $(h-x)/3$ ;
$d$	height of the concrete minus the cover and half of the diameter;
$x$	concrete compression height;
$\emptyset$	reinforcement bar diameter, (or an equivalent diameter);
$c$	the cover to the longitudinal reinforcement;
$k_1$	Eurocode 2 coefficient which takes account of the bond properties of the bonded reinforcement, this is 0.8 for high bond bars;
$k_2$	Eurocode 2 coefficient which takes account of the distribution of strain, which is 0.5 for bending;
$k_3$	recommended value is 3.4 in the Eurocode 2;
$k_4$	recommended value is 0.425 in the Eurocode 2;
$l_{s,\max}$	denotes the length over which slip between concrete and steel occurs;
$\epsilon_{sm}$	the average steel strain;
$\epsilon_{cm}$	the average concrete strain;
$\epsilon_{cs}$	the strain of the concrete due to shrinkage;

$k$	an empirical parameter in the Model code 2010 to take the influence of the concrete cover into consideration, $k = 1$ can be assumed;
$f_{ctm}$	the mean tensile stress of concrete;
$T_{bms}$	mean bond strength between steel and concrete;
$\beta$	an empirical coefficient in the Model code 2010 to assess the mean strain over $l_{s,max}$ depending of the type of loading;
$\sigma_{sr}$	maximum steel stress in a crack in the crack formation stage;
$\eta_r$	Model code 2010 coefficient for considering the shrinkage contribution;
$\epsilon_{sh}$	the shrinkage strain;
$\gamma_e$	exposure factor of the AASHTO;
$\beta_s$	AASHTO influence factor of the tensile stress in the steel reinforcement;
$d_e$	thickness of concrete cover measured from extreme tension fibre to centre of the flexural reinforcement located closest (inches);
$f_{ss}$	tensile stress in steel reinforcement at the service limit state;
$h$	construction height;
$s$	spacing of steel reinforcement in the layer closest to the tension face;
$j_1$	JSCE constant that takes into account the effect of the surface of reinforcement on crack width. This is 1.0 for deformed bars, 1.3 for plain bars;
$j_2$	JSCE constant that takes into account the effect of concrete quality on crack width;
$f_{cc}$	compressive strength of concrete;
$j_3$	JSCE constant to take into account the effect of multiple layers of tensile reinforcement on crack width;
$n$	number of layers of tensile reinforcement;
$c_s$	centre-to-centre distance of tensile reinforcement;
$\epsilon'_{csd}$	compressive strain for evaluation of increment of crack width due to shrinkage and creep of concrete;
$C_1$	JTG D62 shape coefficient of surface of rebar, for ribbed rebar, $C_1=1.0$ ;
$C_2$	JTG D62 coefficient influenced by effect of action for long term, $C_2=1+0.5 N_1/N_2$ . $N_1$ and $N_2$ stands for the value of internal forces of long term and short term respectively;
$C_3$	JTG D62 stands for relating coefficient of member stress, bending member, $C_3=1.0$ ;

$\rho$	JTG D62 ratio of tension reinforcement, if $\rho > 0.02$ , $\rho = 0.02$ is used; if $\rho < 0.006$ , $\rho = 0.006$ is used;
$M_s$	bending moment;
$w$	width of the structure;
$f_y$	steel yield stress;
$N_s$	normal force in steel;
$N_c$	normal force in concrete;
$\eta$	compression strength factor;
$\lambda$	compression height factor;
$A_{s,x\%}$	steel area at a percentage of $x$ ;
$M_r$	moment capacity;
$n_b$	number of bars.

## List of figures

Figure 1-1; Evolution of immersed tunnels.....	1
Figure 1-2; Shear and flexural cracks (Leonhardt & Walther, 1962).....	2
Figure 1-3; Critical parts of the cross section of a Tunnel (Bakker, Huijben, & Vrijling, 2012, p. 3.45).....	3
Figure 1-4; Example results crack width calculations DIANA.....	4
Figure 2-1; Recommended values of crack limits $w_{max}$ Table 7.1 Eurocode 2 (Nederlands Normalisatie-instituut, 2011, p. 127).....	8
Figure 2-2; The exposure class Table 4.1 Eurocode 2 (Nederlands Normalisatie-instituut, 2011, p. 49).....	9
Figure 2-3; Effective area of concrete (Nederlands Normalisatie-instituut, 2011, p. 130).....	11
Figure 2-4; The different stages in cracking of concrete (International Federation for Structural Concrete, 2013, p. 283).....	12
Figure 2-5; Stresses in the crack formation stage (International Federation for Structural Concrete, 2013, p. 284).....	13
Figure 2-6; Values for $\tau_{bms}$ , $\beta$ and $\eta_r$ (International Federation for Structural Concrete, 2013, p. 285).....	14
Figure 2-7; Limit value of the crack width (JSCE 2010 concrete committee, 2007).....	16
Figure 3-1; example results of influence cover on crack width.....	23
Figure 3-2; example trend between cover and crack width.....	23
Figure 3-3; Reinforced concrete beam cross section.....	24
Figure 3-4; Configuration for calculating the compression height of concrete.....	26
Figure 3-5; Values for calculation of the compression height of concrete.....	27
Figure 3-6; Influence of cover on crack width.....	29
Figure 3-7; Increasing crack width with increasing cover.....	29
Figure 3-8; Influence of cover on crack spacing.....	30
Figure 3-9; Increasing crack spacing with increasing cover.....	30
Figure 3-10; Influence of cover on crack strain.....	31
Figure 3-11; Influence of cover in different codes.....	32
Figure 3-12; Influence reinforcement percentage on crack width.....	34
Figure 3-13; Influence reinforcement percentage on crack spacing.....	35
Figure 3-14; Influence reinforcement percentage on strain.....	35
Figure 3-15; Influence of reinforcement percentage is different codes.....	36
Figure 3-16; Influence of concrete tensile strength on crack width.....	38
Figure 3-17; Influence concrete tensile strength on crack strain.....	39
Figure 3-18; Influence of concrete tensile strength in different codes.....	40
Figure 3-19; Influence of reinforcement stress on crack width.....	41
Figure 3-20; Reinforcement stress over crack width.....	42
Figure 3-21; Influence of reinforcement stress on crack strain.....	42
Figure 3-22; Reinforcement stress over crack strain.....	43
Figure 3-23; Influence of reinforcement stress in different codes.....	44
Figure 4-1; Predefined tension softening (DIANA FEA BV, 2016, p. Material library 6.2.2)....	48
Figure 4-2; Predefined compressive softening (DIANA FEA BV, 2016, p. Material library 6.2.3).....	49
Figure 4-3; Bond shear traction slip curves, (DIANA FEA BV, 2016, p. Material library 9.3) ..	50
Figure 4-4; Example mesh.....	51

Figure 4-5; CQ16M and CT12M (DIANA FEA BV, 2016, p. Element library 5.7.4)	51
Figure 4-6; CL12I (DIANA FEA BV, 2016, p. Element library 12)	51
Figure 5-1; Geometry of the beam of the experiment of Braam	56
Figure 5-2; Cross-section of the experiment of Braam	56
Figure 5-3; Geometry DIANA model experiment Braam	57
Figure 5-4; Mesh of the DIANA model of the experiment of Braam	57
Figure 5-5; Part of the beam where crack patterns are recorded	57
Figure 5-6; Force-displacement diagram	58
Figure 5-7; Crack pattern beam 468 kN	59
Figure 5-8; Crack pattern beam DIANA results 468 kN	59
Figure 5-9; Check of crack widths (close view of bottom edge)	60
Figure 5-10; Crack width and crack spacing	60
Figure 5-11; Measure heights of the crack widths	60
Figure 5-12; Results of crack width experiment Braam	61
Figure 5-13; Crack width comparison experiment Braam	61
Figure 5-14; Geometry of the beam of experiment E3	62
Figure 5-15; Cross-section of the beam of experiment E3	62
Figure 5-16; Geometry DIANA model experiment E3 half beam	63
Figure 5-17; Mesh DIANA model experiment E3 half beam	63
Figure 5-18; Force displacement diagram of Experiment E3 and DIANA results	64
Figure 5-19; Failure crack pattern beam experiment E3	65
Figure 5-20; Failure crack pattern DIANA results E3	65
Figure 5-21; Crack width determination, failure crack pattern	66
Figure 5-22; Extended version crack width determination, failure crack pattern	66
Figure 5-23; Crack widths experiment E3	66
Figure 5-24; Crack width comparison experiment E3	67
Figure 5-25; Geometry of the beam of the experiment VS-C3	68
Figure 5-26; Cross-section of the experiment VS-C3	68
Figure 5-27; Geometry DIANA model experiment VS-C3	69
Figure 5-28; Mesh of the DIANA model of the experiment VS-C3	69
Figure 5-29; Force displacement diagram of with result of experiment VS-C3 and DIANA	70
Figure 5-30; Crack pattern experiment VS-C3	71
Figure 5-31; Right part of the crack pattern of experiment VS-C3	71
Figure 5-32; Crack pattern of the DIANA results	71
Figure 6-1; Geometry standard beam	73
Figure 6-2; Mesh standard beam	74
Figure 6-3; Influence of cover on crack width	77
Figure 6-4; Cover over crack width	77
Figure 6-5; Influence of cover on crack spacing	78
Figure 6-6; Cover over crack spacing	78
Figure 6-7; Influence of cover on cracks strain	79
Figure 6-8; Single crack DIANA model, height 900 mm, cover 100 mm	79
Figure 6-9; Influence reinforcement percentage on crack width	80
Figure 6-10; Influence reinforcement percentage on crack spacing	80
Figure 6-11; Influence reinforcement percentage on strain	81
Figure 6-12; Influence concrete tensile strength on crack width	82
Figure 6-13; Influence concrete tensile strength on crack spacing	82
Figure 6-14; Influence concrete tensile strength on crack strain	83



Figure 6-15; Influence reinforcement stress on crack width .....	84
Figure 6-16; Reinforcement stress over crack width .....	84
Figure 6-17; Influence reinforcement stress on crack strain.....	85
Figure 6-18; Reinforcement stress over crack strain.....	85
Figure 7-1; Influence cover on crack width .....	89
Figure 7-2; Comparison cover over crack width.....	89
Figure 7-3; Influence cover on crack spacing .....	90
Figure 7-4; Comparison cover over crack spacing.....	90
Figure 7-5; Influence cover on crack strain.....	91
Figure 7-6; Influence reinforcement percentage on crack width.....	92
Figure 7-7; Influence reinforcement percentage on crack spacing.....	92
Figure 7-8; Influence reinforcement percentage on crack strain .....	93
Figure 7-9; Influence of tensile strength on crack width .....	94
Figure 7-10; Influence tensile strength on crack spacing .....	94
Figure 7-11; Influence tensile strength on crack strain.....	95
Figure 7-12; Influence reinforcement stress on crack width .....	96
Figure 7-13; Comparison reinforcement stress over crack width .....	96
Figure 7-14; Influence reinforcement stress on crack strain.....	97
Figure 7-15; Comparison reinforcement stress over crack strain .....	97
Figure 7-16; Influence cover DIANA model on crack strain.....	98
Figure 7-17; Difference ( $\Delta\varepsilon$ ) in crack strain reinforcement height and outer fibre .....	98
Figure 7-18; Adjusted Eurocode 2 to DIANA model.....	99
Figure 7-20; Comparison cover over crack spacing with factors Eurocode 2 .....	100
Figure 7-21; Comparison cover over crack spacing with adjusted Eurocode 2 .....	100

## List of tables

Table 3-1; Geometry beam Eurocode calculations .....	24
Table 3-2; Concrete material properties.....	24
Table 3-3; Steel material properties.....	24
Table 3-4; Steel area applied for one percent reinforcement .....	25
Table 3-5; Configuration 0.7 percent .....	25
Table 3-6; Configuration 1.5 percent .....	26
Table 3-7; Example calculation table (height 300 mm, cover 50 mm) .....	28
Table 3-8; Maximum allowable crack width in the different codes.....	32
Table 5-1; Parameters and models for the concrete .....	53
Table 5-2; Parameters and models for the reinforcement.....	54
Table 5-3; Parameters and models for modeling elements.....	55
Table 5-4; Parameters for the experiment of Braam .....	56
Table 5-5; Parameters for the experiment of E3 .....	62
Table 5-6; Parameters for the experiment VS-C3.....	68
Table 6-1; Steel area applied for one percent reinforcement .....	74
Table 6-2; Input parameters for the different heights .....	75
Table 6-3; Input parameters for 0.7 % reinforcement percentage .....	75
Table 6-4; Input parameters for 1.5% reinforcement percentage .....	76
Table 6-5; Crack width with distance to reinforcement.....	79
Table 7-1; Factors model code and adjusted Eurocode 2.....	99
Table 7-2; Factors adjusted Eurocode 2 all covers .....	99

# 1 Introduction

In this chapter the topic of this thesis is introduced. After that the problem and the procedure of how the problem is handled will be explained. Then the main question, sub questions and goals will be stated. A guide for reading the report can be found at the end of this chapter.

## 1.1 General description

A description is given about immersed tunnels, concrete and the cracks that can appear in concrete structures.

### 1.1.1 Immersed Tunnels

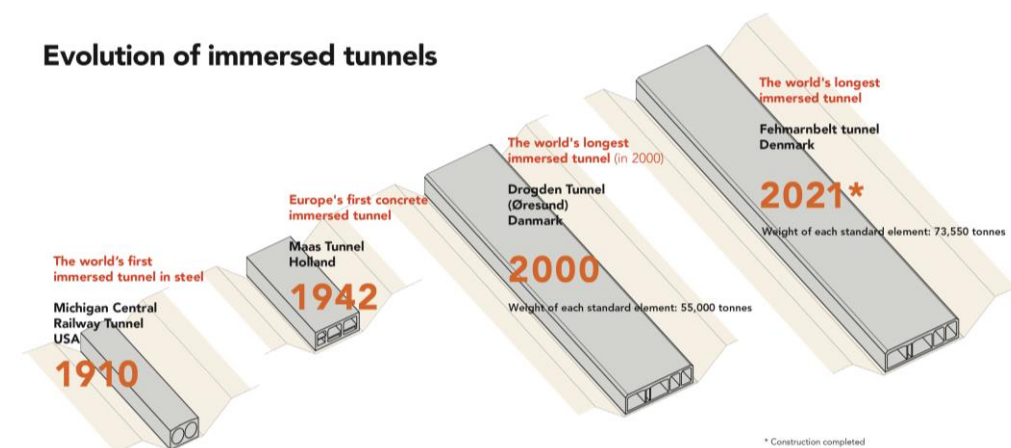
Since 1910 the immersed tunnelling technique is used to cross waterways for larger transportation. This first tunnel was made of two watertight steel tubes, which were placed in a dredged trench and then backfilled with concrete.

The first significant concrete tunnel was the Friedrichshagen tunnel in Germany, which was completed in 1927. In the Netherlands the Maastunnel was the first concrete tunnel, which was completed in 1942. In the Netherlands immersed tunnelling is commonly applied in the past and will be applied in near future projects.

As can be stated out of the previous paragraph there are different kinds of immersed tunnels. Namely tunnels based on steel tubes, backfilled with concrete and tunnels build completely out of reinforced concrete.

The geometry of a tunnel is dependent on the layout of the traffic tubes with the alignment, ventilation system and other measures for safety, but also on placing and settlement tolerances. The thicknesses of the walls, floor and roof are in the first assessment based on the stability and buoyancy of the structure, since it should be able to float stable and in a later stage immerse. The fact that it should be able to immerse is the main reason why the concrete structure is so thick and therefore heavy.

The size of immersed tunnels is increasing; since roads are getting more lanes, and immersed tunnels are applied for longer distances, see Figure 1-1.



(Source: <http://visualarchive.femern.dk/Search.aspx?mi=2842>)

Figure 1-1; Evolution of immersed tunnels

After the first estimate of the tunnel dimensions, calculations are carried out to make it structural reliable. This is done with the different loads that are applied on the structure in the different stages of the construction of the immersed tunnel. The most important permanent loads are the self-weight of the structure, the hydrostatic forces, the permanent ballast, the finishing's and the backfill. Next to that there are some variable loads; vehicles, temperature change, waves and currents, ice and accidents. In Appendix A more information about immersed tunnels can be found.

### 1.1.2 Concrete

Concrete is widely used in immersed tunnels, because the weight is needed to immerse and reinforced concrete is watertight when designed and constructed properly. Several checks have to be done when designing a reinforced concrete structure. There are checks in the ultimate limit state (ULS) and in the serviceability limit state (SLS).

For the ULS the strength is important, logically the structure should be able to withstand all the loads that it is experiencing. Next to that the stability of the structure is checked in the ULS.

In the SLS the stress limitation, crack width and deformations are checked. Cracks are important in immersed tunnels, because they could give leakage when formed through the whole thickness of the concrete lining and when cracks are deep and wide enough they could cause corrosion of the reinforcing steel. Corrosion will cause a decrease of strength in the reinforcement and so the risk of collapse will increase. The formation of corrosion is explained in Appendix B.

### 1.1.3 Cracks

In reinforced concrete it is common practice that small cracks appear, but for named reasons they should be controlled. These tensile cracks appear because of tensile stresses in the concrete which are bigger than the strength of the concrete. In the compression zone this problem is not that significant since concrete is stronger in compression than it is in tension. Therefore the reinforcement bars are mostly applied in the tensile areas. Cracks can be introduced by (obstructed) deformations and external loading. Examples of cracks because of (obstructed) deformations are;

- Drying shrinkage;
- Thermal contraction;
- Restraint to shortening;
- Settlements.

And when the reinforced concrete is loaded by axial tensile forces or bending forces there will also be tension in the concrete. When concrete cracks, the reinforcement will take over the tensile forces that are formed in the crack. These cracks are called flexural cracks, when they are formed due to bending (see Figure 1-2 between the load points) and shear cracks if it's due to shear (Figure 1-2 cracks at an angle). In this thesis the flexural cracks, so cracks due to bending, are investigated.

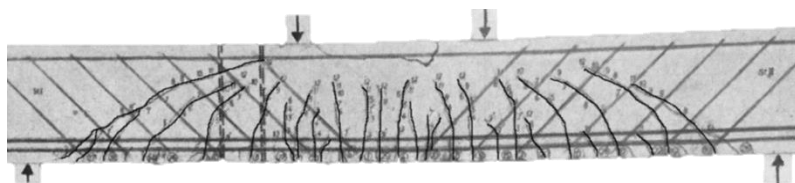


Figure 1-2; Shear and flexural cracks (Leonhardt & Walther, 1962)

## 1.2 The problem

The problem is introduced. Thereafter the way how the problem is addressed is described. At the end the questions and goals are given.

### 1.2.1 Problem description

When engineers perform the SLS check on crack width in the Eurocode 2 they experience problems with the crack width in certain areas in the cross-section of immersed tunnels. These cracks appear because of moments in the structure, which are most critical in the corners and the middle of the tunnel cross section; see red circles in Figure 1-3.

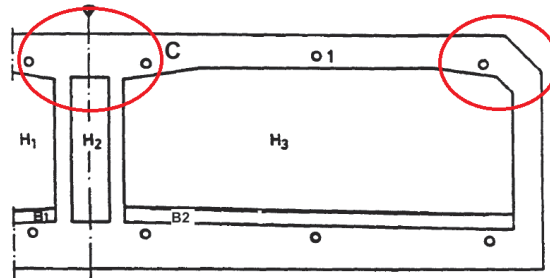


Figure 1-3; Critical parts of the cross section of a Tunnel (Bakker, Huijben, & Vrijling, 2012, p. 3.45)

The cracks in these points appear on the outside of the tunnel and are in direct contact with water, and are submerged impossible to reach. For these reasons the most severe circumstances for the maximum crack width are applied ( $w_{max}=0.2$ ).

The fact that the crack width becomes critical can lead to an increase of reinforcement by an enormous amount (sometimes twice as much as is needed for strength). The question appeared whether this is realistic in such thick concrete structures, so whether the large thickness has influence on the crack width.

### 1.2.2 Problem analysis

First a literature study has been done, the topics that are covered are:

- Immersed tunnels;
- Corrosion of the reinforcement steel;
- Crack width calculations in the guidelines;
- Cracks in DIANA FEA.

General information about immersed tunnels and corrosion of the reinforcement steel do not directly contribute in the determination of crack width. Though, an understanding of these elements can be helpful and are related to the problem. The crack width calculations in several of guidelines are also investigated, with these calculations the crack width can be determined analytically. And to be able to use DIANA to calculate crack width numerically, knowledge of the different material models and elements is required.

After this literature study, the analytical calculations will be covered. The main focus will be on the Eurocode 2, but also a few calculations with other guidelines are made. This is done to gain insight in how different countries handle the crack width check and what the differences are in the calculations. The calculations will be done with different thicknesses, to see what the effect is of increasing construction height. Next to the influence of the height, the influences of four height independent parameters are analysed. This is done for an additional view on differences in the other codes compared to the Eurocode 2 and for the comparison with the numerical results at the end of the report.

Then the numerical part of the thesis will be tackled. First a DIANA model is made and verified with experiments of concrete beams. The force-displacement line, the crack pattern and the crack widths will be compared and the elements and material models within DIANA that give the best comparison will be used.

This DIANA model will be used to investigate the effect of increasing construction height; hereby also influence of the height independent parameters of the Eurocode 2 calculation will be calculated. The results will be compared with the Eurocode 2 results and differences in crack widths, spacing's and strains and the parameter causing this difference can be specified. The correctness of the used parameters and there influence factor in the Eurocode 2 calculation can then be analysed.

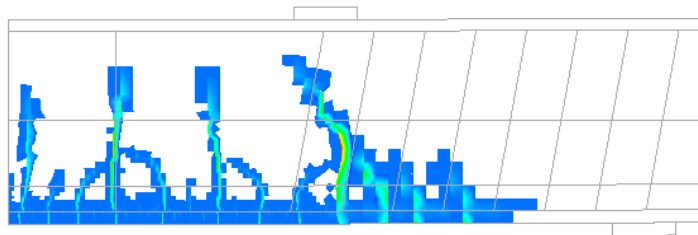


Figure 1-4; Example results crack width calculations DIANA

Eventually the conclusions and recommendations will be given.

### 1.2.3 Problem definition

Are the current rules in the Eurocode 2 for the calculation of flexural cracks too conservative for large thicknesses that are applied in the concrete lining of immersed tunnels?

#### Sub questions:

- How is crack width calculated in the Eurocode 2, and where are these calculations based on?
- How is crack width calculated in other codes, and what are the differences with the Eurocode 2?
- How does DIANA determine the location of the crack?
- How can the crack width be determined in DIANA?
- Can DIANA predict the crack width found in experiments?
- How do the parameters that are used in the Eurocode 2 crack width calculation influence the outcome of both the Eurocode 2 and the DIANA calculations?
- Are the outcomes of the DIANA and Eurocode 2 of the crack width comparable, if not which explanations can be given for the difference?
- What is the influence of the construction height on the crack width?

#### Goals:

- Use DIANA to predict crack width;
- More insight in the way crack width is calculated;
- Determine how accurate the Eurocode 2 can predict the crack width;
- Reducing the needed reinforcement in thick-walled structures.

## 1.3 Guide

In first chapter is the introduction of the thesis, the topic has its introduction. After that the problem and the approach of the problem are explained. Then the main and sub questions and goals are stated. A guide for reading the report can be found at the end of this chapter.

### Section I Analytical calculations

In the second chapter the analytical formulas are covered. First the crack width formulas of the Eurocode 2 and other codes and some information about them are given. Then the differences are discussed. In the third chapter the influence of the height and the parameters in the Eurocode 2 calculation are analysed. These are compared with results of the other codes.

### Section II Numerical calculations

In the fourth chapter the material models and elements in DIANA are explained. The fifth chapter is about the validation of the DIANA model with three experiments. In the following chapter the influence of the height and the influence of the Eurocode 2 parameters in the DIANA calculation are examined.

### Section III Comparison, conclusions and recommendation

In chapter seven the results of the Eurocode 2 and the DIANA model will be compared. Eventually the conclusions and recommendations will be addressed in chapter eight.



# I Analytical calculations

In the first section the analytical calculations are covered. First the formulas of the crack width of the Eurocode 2 and other code, with some information about them, are given. Then the differences are discussed. Next the influence of the height and the parameters in the Eurocode 2 calculation will be analysed. These will be compared with results of the other codes.

## 2 Crack width formulas in codes

In the following chapter the crack width formulas of five codes are discussed, under which the Eurocode 2 (Standard used in the Netherlands), the Model Code 2010 and of other countries (United States, Japan and China). The most important code is the Eurocode 2, since the results of this calculation are going to be compared with Finite Element Analysis results. The different formulas will be compared with the Eurocode 2 at the end of this chapter.

### 2.1 Eurocode 2

Checks for the Serviceability Limit State (SLS) of concrete structures need to be performed as given in the Eurocode 2 chapter 7 (Nederlands Normalisatie instituut, 2011). The limit states that are covered in chapter 7 are:

- Stress limitation;
- Crack control;
- Deflection control.

The crack control formulas (chapter 7.3 Eurocode 2) are discussed:

There are some general considerations made in the Eurocodes.

- Cracks are a normal phenomenon in reinforced concrete structures and they should be limited for proper function, durability and appearance;
- Cracks that are formed by other causes than bending, shear, torsion or tension, such as plastic shrinkage or chemical reactions are outside the scope of this chapter of the Eurocode;
- If the cracks are not jeopardizing the function of the structure they are permitted to form without control;
- The crack width is limited by proposed function, nature of the structure and/or the cost of limiting cracking. The recommended values are in Table 7.1 (Figure 2-1) of the Eurocode, the value of  $w_{max}$  in a Country can be found in its National Annex, these values are based on the Exposure Class. The Exposure Class can be found in table 4.1 of the Eurocode 2 (Figure 2-2).

Exposure Class	Reinforced members and prestressed members with unbonded tendons	Prestressed members with bonded tendons
	Quasi-permanent load combination	Frequent load combination
X0, XC1	0,4 <sup>1</sup>	0,2
XC2, XC3, XC4	0,3	0,2 <sup>2</sup>
<sup>AC2</sup> XD1, XD2, XD3, XS1, XS2, XS3 <sub>AC2</sub>		Decompression
<p><b>Note 1:</b> For X0, XC1 exposure classes, crack width has no influence on durability and <sup>AC1</sup>this limit is set to give generally acceptable appearance. In the absence <sup>AC1</sup> of appearance conditions this limit may be relaxed.</p> <p><b>Note 2:</b> For these exposure classes, in addition, decompression should be checked under the quasi-permanent combination of loads.</p>		

Figure 2-1; Recommended values of crack limits  $w_{max}$  Table 7.1 Eurocode 2 (Nederlands Normalisatie-instituut, 2011, p. 127)

<b>2 Corrosion induced by carbonation</b>		
XC1	Dry or permanently wet	Concrete inside buildings with low air humidity Concrete permanently submerged in water
XC2	Wet, rarely dry	Concrete surfaces subject to long-term water contact Many foundations
XC3	Moderate humidity	Concrete inside buildings with moderate or high air humidity External concrete sheltered from rain
XC4	Cyclic wet and dry	Concrete surfaces subject to water contact, not within exposure class XC2
<b>3 Corrosion induced by chlorides</b>		
XD1	Moderate humidity	Concrete surfaces exposed to airborne chlorides
XD2	Wet, rarely dry	Swimming pools Concrete components exposed to industrial waters containing chlorides
XD3	Cyclic wet and dry	Parts of bridges exposed to spray containing chlorides Pavements Car park slabs
<b>4 Corrosion induced by chlorides from sea water</b>		
XS1	Exposed to airborne salt but not in direct contact with sea water	Structures near to or on the coast
XS2	Permanently submerged	Parts of marine structures
XS3	Tidal, splash and spray zones	Parts of marine structures

Figure 2-2; The exposure class Table 4.1 Eurocode 2 (Nederlands Normalisatie-instituut, 2011, p. 49)

- The outside of a tunnel is permanently submerged and can be scaled in XC1 for that matter, only when submerged in sea water it should be put in XS2. When there are no prestressed members with bonded tendons the  $w_{max}$  is respectively 0.4 mm and 0.3 mm. Though, because it is impossible to reach the external perimeter the most severe exposure conditions are applied. This means that the  $w_{max}$  is 0.2 mm; sometimes designers even lower this criterion to 0.15 mm. The inside of a tunnel can be seen as a moderate humid environment and there are deposits from exhaust fumes and road salt, this creates a corrosive environment. In these conditions exposure class XC3/XD1 is applied with a  $w_{max}$  of 0.3 mm. Though, in practice a  $w_{max}$  of 0.25 is applied; (Lunniss & Baber, 2013, pp. 214, 294)
- When crack control is necessary, a minimum amount of reinforcement is needed to control cracking in tension areas;
- Bonded tendons may be assumed to contribute to crack control, in prestressed members no minimum reinforcement is required where the concrete is compressed or beneath  $\sigma_{ct,p}$ .

In the Eurocode 2 there are two ways to validate the crack width; with tables in 7.3.3 and with calculations in 7.3.4. The tables are more conservative than the calculations. To check whether the Eurocode is conservative, the least conservative method should be used. When this method is found conservative the other method is even more conservative. Therefore the calculations are used.

The calculation for the crack width,  $w_k$ , exists of the multiplication of the crack spacing and the difference between the mean strain of the steel and concrete, which is called the crack strain:

$$w_k = S_{r,max} * (\varepsilon_{sm} - \varepsilon_{cm})$$

2-1

In which:

- $w_k$                     *crack width;*
- $S_{r,max}$                 *crack spacing;*
- $\varepsilon_{sm}$                   *the average steel strain;*
- $\varepsilon_{cm}$                   *the average concrete strain.*

The crack strain term  $\varepsilon_{sm} - \varepsilon_{cm}$  can be calculated with:

$$\varepsilon_{sm} - \varepsilon_{cm} = \frac{\sigma_s - k_t * \frac{f_{ct,eff}}{\rho_{p,eff}} (1 + \alpha_e * \rho_{p,eff})}{E_s} \geq 0.6 \frac{\sigma_s}{E_s}$$

2-2

This formula can be broken down into the part of the mean strain of steel  $\varepsilon_{sm}$ , which is:

$$\varepsilon_{sm} = \frac{\sigma_s - k_t * \frac{f_{ct,eff}}{\rho_{p,eff}}}{E_s} = \frac{\sigma_s - k_t * \frac{f_{ct,eff} * A_{c,eff}}{A_s}}{E_s}$$

2-3

And the mean strain of the concrete:

$$\varepsilon_{cm} = \frac{k_t * \alpha_e * f_{ct,eff}}{E_s} = k_t * \frac{f_{ct,eff}}{E_{cm}}$$

2-4

In which:

- $\sigma_s$                     *tension stress in the reinforcement;*
- $k_t$                         *Eurocode 2 factor dependent on the duration of the load;*
- $f_{ct,eff}$                   *effective concrete tensile strength;*
- $\rho_{p,eff}$                   *effective reinforcement percentage, ratio  $A_s/A_{c,eff}$ ;*
- $A_s$                         *steel area;*
- $A_{c,eff}$                   *the effective area of concrete in tension around the reinforcement;*
- $\alpha_e$                       *ratio  $E_s/E_{cm}$ ;*
- $E_s$                         *steel young's modulus;*
- $E_{cm}$                       *concrete mean young's modulus.*

The steel stress  $\sigma_s$  is the value in which the full tensile force is in the reinforcement. This value is reduced, because cracks first have to appear before a crack strain can develop. Cracks appear just after the maximum tensile stress of concrete is reached. Therefore the reduction exists out of the maximum tensile stress of concrete and the stress in the reinforcement at this point.

The effective area of concrete  $A_{c,eff}$  (Figure 2-3) is dependent on the effective height. The effective height for flexural cracks is:

$$h_{c,eff} = \min(2,5(h - d), (h - x)/3)$$

2-5

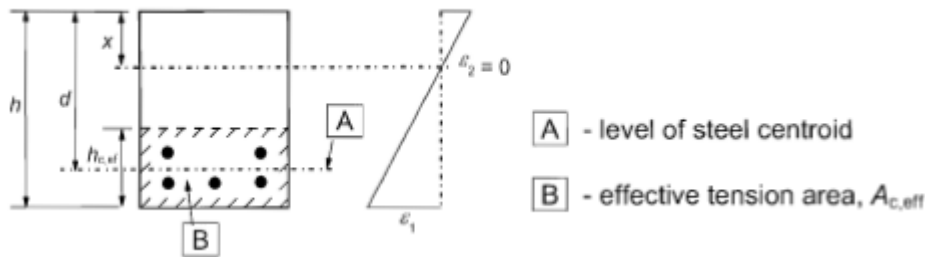


Figure 2-3; Effective area of concrete (Nederlands Normalisatie-instituut, 2011, p. 130)

In which:

- $h_{c,eff}$  effective height of concrete in tension;
- $d$  height of the concrete minus the cover and half of the diameter;
- $x$  concrete compression height;
- $h$  construction height.

The crack spacing is the distance between cracks, in the Eurocode 2 it is calculated with the following formula:

$$S_{r,max} = k_3 * c + k_1 * k_2 * k_4 * \phi / \rho_{p,eff}$$

2-6

The crack spacing is dependent on the cover, the diameter and the effective reinforcement percentage. A larger cover and/or diameter results in a larger crack spacing; a larger effective reinforcement percentage results in a smaller crack spacing. The crack spacing is proportional to the crack width, a larger crack spacing means a larger crack width.

In the national annex of the Netherlands a maximum is applied on the crack spacing, namely:

$$S_{r,max} \leq \max((50 - 0.8 * f_{cc}) * \phi, 15 * \phi)$$

2-7

This implies that at a certain crack spacing the influence of the cover is neglected. This effect has not been taken into account in the calculations in this thesis.

Eventually  $w_k$  should be smaller than  $w_{max}$  before the check for crack width will be approved.

In which:

- $S_{r,max}$  crack spacing;
- $\emptyset$  reinforcement bar diameter, (or an equivalent diameter);
- $c$  the cover to the longitudinal reinforcement;
- $k_1$  Eurocode 2 factor concerning the bond properties of the reinforcement;
- $k_2$  Eurocode 2 coefficient which takes account of the distribution of strain;
- $k_3$  recommended value is 3.4 in the Eurocode 2;
- $k_4$  recommended value is 0.425 in the Eurocode 2;
- $f_{cc}$  compressive strength of concrete.

## 2.2 Model code 2010

According to the model code 2010 (International Federation for Structural Concrete, 2013) there are four stages in the formation of cracks in reinforced concrete:

- The uncracked stage;
- The crack formation stage;
- The stabilized cracking stage;
- The steel yielding stage.

In Figure 2-4 a schematization is presented of these stages for an axial loaded structure.

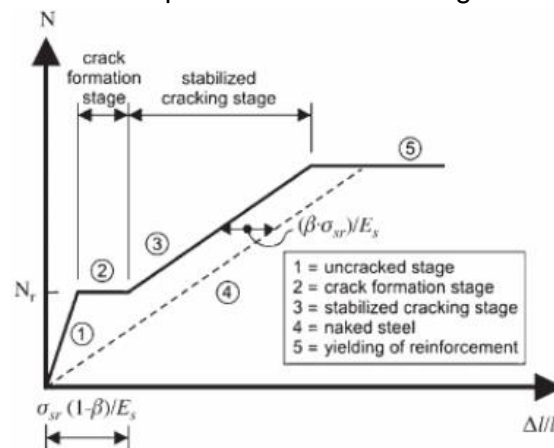


Figure 2-4; The different stages in cracking of concrete (International Federation for Structural Concrete, 2013, p. 283)

The first crack in the concrete will occur when the concrete tensile stress reaches the concrete tensile strength; this is called the crack formation stage. Until this stage the concrete and the steel strain are the same. When concrete cracks, the tension force in the crack is completely in the steel, see Figure 2-5. On both sides of the crack the reinforcement gradually transfers stress to the concrete by the bond between the reinforcement and the concrete. The bond stress occurs because the strains of the concrete and steel differ after cracking. When enough cracks have been formed, the stabilized cracking stage is reached. In this stage there is no place where the concrete can crack anymore. So the existing cracks will widen.

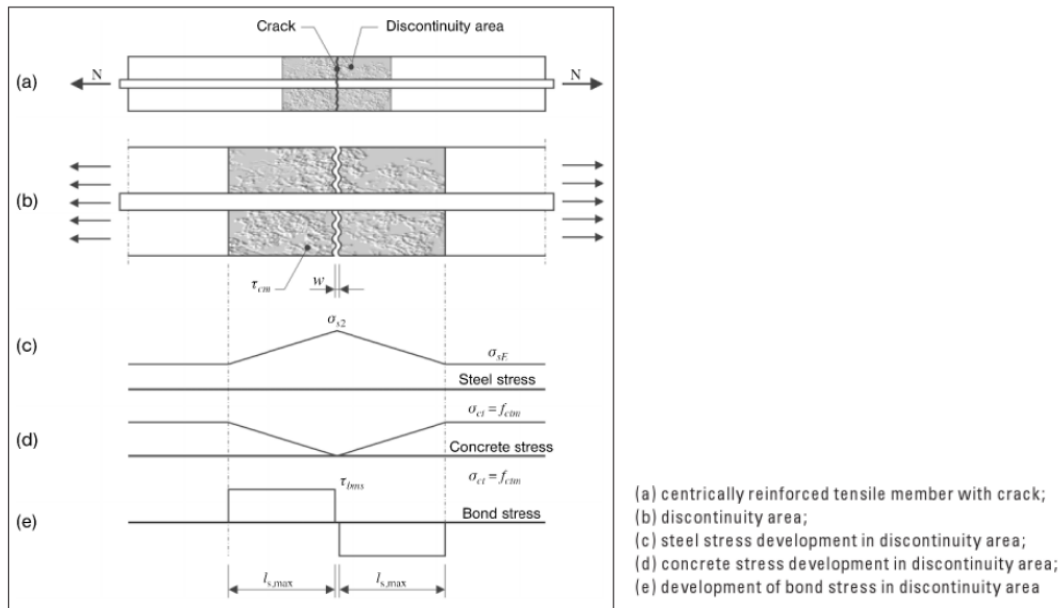


Figure 2-5; Stresses in the crack formation stage (International Federation for Structural Concrete, 2013, p. 284)

The calculation of the crack width for axial loaded members in the model code 2010 is stated as:

$$w_k = 2 * l_{s,max} * (\epsilon_{sm} - \epsilon_{cm} - \epsilon_{cs})$$

2-8

In which:

- $w_k$  crack width;
- $l_{s,max}$  denotes the length over which slip between concrete and steel occurs;
- $\epsilon_{sm}$  the average steel strain;
- $\epsilon_{cm}$  the average concrete strain;
- $\epsilon_{cs}$  the strain of the concrete due to shrinkage.

The calculation of the length  $l_{s,max}$  is as follows:

$$l_{s,max} = k * c + \frac{1}{4} * \frac{f_{ctm}}{\tau_{bms}} * \frac{\emptyset}{\rho_{p,eff}}$$

2-9

The length  $l_{s,max}$  is dependent on the cover, the diameter and the effective reinforcement percentage. The tensile strength and mean bond strength influence this length by the factor between the two values, which can be found in Figure 2-6.

In which:

- $k$  Model code 2010 influence factor of the concrete cover;
- $f_{ctm}$  the mean tensile stress of concrete;
- $\tau_{bms}$  mean bond strength between steel and concrete;
- $\emptyset$  reinforcement bar diameter, (or an equivalent diameter);
- $c$  the cover to the longitudinal reinforcement;
- $\rho_{p,eff}$  effective reinforcement percentage, ratio  $A_s/A_{c,eff}$ .

For the calculation of the crack strain the following expression is applied:

$$\varepsilon_{sm} - \varepsilon_{cm} - \varepsilon_{cs} = \frac{\sigma_s - \beta * \sigma_{sr}}{E_s} - \eta_r * \varepsilon_{sh}$$

2-10

The steel stress is reduced with certain factors. These factors are based on the stress which is formed until cracking of the concrete and the shrinkage of the concrete.

The maximum steel stress in a crack in the crack formation stage is:

$$\sigma_{sr} = \frac{f_{ctm}}{\rho_{p,eff}} * (1 + \alpha_e * \rho_{p,eff})$$

2-11

- $\varepsilon_{sm}$  the average steel strain;
- $\varepsilon_{cm}$  the average concrete strain;
- $\varepsilon_{cs}$  the strain of the concrete due to shrinkage;
- $\sigma_s$  tension stress in the reinforcement;
- $\beta$  Model code 2010 influence factor for the the mean strain over  $l_{s,max}$ ;
- $\sigma_{sr}$  maximum steel stress in a crack in the crack formation stage;
- $\eta_r$  Model code 2010 coefficient for considering the shrinkage contribution;
- $\varepsilon_{sh}$  the shrinkage strain;
- $\alpha_e$  ratio  $E_s/E_{cm}$ ;
- $E_s$  steel young's modulus;
- $E_{cm}$  concrete mean young's modulus.

Values for the mean bond strength ( $\tau_{bms}$ ), the  $\beta$  factor and  $\eta_r$  factor can be taken from Figure 2-6.

	<i>Crack formation stage</i>	<i>Stabilized cracking stage</i>
Short term, instantaneous loading	$\tau_{bms} = 1.8 \cdot f_{ctm}(t)$ $\beta = 0.6$ $\eta_r = 0$	$\tau_{bms} = 1.8 \cdot f_{ctm}(t)$ $\beta = 0.6$ $\eta_r = 0$
Long term, repeated loading	$\tau_{bms} = 1.35 \cdot f_{ctm}(t)$ $\beta = 0.6$ $\eta_r = 0$	$\tau_{bms} = 1.8 \cdot f_{ctm}(t)$ $\beta = 0.4$ $\eta_r = 1$

Figure 2-6; Values for  $\tau_{bms}$ ,  $\beta$  and  $\eta_r$  (International Federation for Structural Concrete, 2013, p. 285)

The values represent the crack width at the level of the reinforcement, when the members are subjected to bending the crack width at the extreme tensile fibre is larger. For this reason the calculated crack width should be multiplied with a factor of  $(h-x)/(d-x)$ .



## 2.3 Other codes

In other countries other codes are used, with these codes a comparison can be made. This gives insight in how other countries approach the crack width criteria. The codes of three countries, which have built the most immersed tunnels, namely the United States, Japan and China, are stated below. The Eurocode 2 (for the Netherlands) is excluded since this is already treated in a previous chapter.

### 2.3.1 AASHTO (US)

The control of flexural crack width in the code of the United States, the AASHTO (American Association of State Highway Transportation Officials, 2012, p. 5.45), is based on the applied reinforcement and this is checked with the following criterion:

$$s \leq \frac{700 * y_e}{\beta_s * f_{ss}} - 2d_e$$

2-12

The distance between the reinforcement bars is checked with the exposure factor, the tensile stress in the reinforcement and the cover.

The influence factor of the tensile stress in the reinforcement  $\beta_s$  can be calculated with:

$$\beta_s = 1 + \frac{d_e}{0.7 * (h - d_e)}$$

2-13

This factor is influenced by the cover and construction height.

In which:

- $s$  spacing of steel reinforcement in the layer closest to the tension face;
- $\gamma_e$  exposure factor of the AASHTO;
- $\beta_s$  AASHTO influence factor of the tensile stress in the reinforcement;
- $d_e$  thickness of concrete cover;
- $f_{ss}$  tensile stress in steel reinforcement at the service limit state;
- $h$  construction height.

In the code it is stated that it is preferable to have many fine cracks instead of a few wide cracks. Cracks can be controlled in a better way when the steel reinforcement is well distributed over the zone of maximum concrete tension. It is better to apply more bars with moderate spacing than applying a few bars with an equivalent area and a larger spacing. The criteria given above are based on a physical crack model where the limitation of bar spacing is used rather than crack width.

The exposure factor  $\gamma_e$  can be modified to make the formula applicable for different allowed crack widths. A factor of one will give a crack width of 0.017 inch, 0.43 mm, a factor of a half can be applied for half of that crack width.

### 2.3.2 JSCE (Japan)

In the Japanese code is stated that crack width is influenced by the cover, the distance between the reinforcement bars, the diameter, the steel stress and the shrinkage of concrete. Furthermore there are influence factors that are based on the surface of the reinforcement, the quality of the concrete, amount of layers.

The examination for flexural cracks in Japanese code (JSCE 2010 concrete committee, 2007, pp. 119-121) is as follows:

$$w_k = 1.1 * j_1 * j_2 * j_3 * (4c + 0.7 * (c_s - \emptyset)) * \left( \frac{\sigma_s}{E_s} + \varepsilon'_{csd} \right)$$

2-14

The factor that takes into account the quality of the concrete is calculated in the following manner:

$$j_2 = \frac{15}{f_{cc} + 20} + 0.7$$

2-15

The factor for the effect of multiple layers of reinforcement is:

$$j_3 = \frac{5 * (n + 2)}{7n + 8}$$

2-16

In which:

- $w_k$  crack width;
- $\sigma_s$  tension stress in the reinforcement;
- $E_s$  steel young's modulus;
- $\emptyset$  reinforcement bar diameter, (or an equivalent diameter);
- $c$  the cover to the longitudinal reinforcement;
- $j_1$  JSCE factor for the effect of reinforcement surface on crack width;
- $j_2$  JSCE constant that takes into account the effect of concrete quality;
- $f_{cc}$  compressive strength of concrete;
- $j_3$  JSCE constant for the effect of multiple layers of tensile reinforcement;
- $n$  number of layers of tensile reinforcement;
- $c_s$  centre-to-centre distance of tensile reinforcement;
- $\varepsilon'_{csd}$  compressive strain due to shrinkage and creep of concrete.

The maximum crack width that is allowed is dependent on the concrete cover:

Type of reinforcement	Environmental conditions for reinforcement corrosion		
	Normal	Corrosive	Severely corrosive
Deformed bars and plain bars	0.005c	0.004c	0.0035c
Prestressing steel	0.004c	----	----

Figure 2-7; Limit value of the crack width (JSCE 2010 concrete committee, 2007)

### 2.3.3 JTG D62 (China)

The calculation of crack width ( $w_k$ ) in the JTG D62 code (China highway planning and design institute of the people's republic of china, 2004) for members in bending is calculated with the following formula:

$$w_k = C_1 * C_2 * C_3 * \frac{\sigma_s}{E_s} \left( \frac{30 + \emptyset}{0.28 + 10\rho} \right)$$

2-17

The Chinese code is dependent on the steel stress, diameter and reinforcement percentage. The influence factors that are applied are taken into account the surface of the reinforcement bars, the effect of duration of loading and the type of stress in this case bending moments.

The stress in the reinforcement is:

$$\sigma_s = \frac{M_s}{0.87 * A_s * h}$$

2-18

The ratio of tension reinforcement:

$$\rho = \frac{A_s}{w * h}$$

2-19

If  $\rho > 0.02$ ,  $\rho = 0.02$  is used; if  $\rho < 0.006$ ,  $\rho = 0.006$  is used.

In which:

- $w_k$             *crack width;*
- $\sigma_s$           *tension stress in the reinforcement;*
- $E_s$             *steel young's modulus;*
- $A_s$             *steel area;*
- $\emptyset$             *reinforcement bar diameter, (or an equivalent diameter);*
- $C_1$             *JTG D62 shape coefficient of surface of rebar, for ribbed rebar;*
- $C_2$             *JTG D62 coefficient influenced by effect of action for long term;*
- $C_3$             *JTG D62 stands for relating coefficient of member stress;*
- $\rho$              *JTG D62 ratio of tension reinforcement;*
- $M_s$             *bending moment;*
- $h$              *construction height;*
- $w$              *width of the structure;*

## 2.4 Differences between the codes

The similarities and differences of the Eurocode 2 and the other codes are explained. All the codes will be compared with the Eurocode 2.

### 2.4.1 Eurocode 2 vs Model code 2010

First the Eurocode 2 is compared with the Model Code 2010.

The two calculations have just a few differences. First the crack spacing is compared:

$$S_{r,max} = k_3 * c + k_1 * k_2 * k_4 \frac{\emptyset}{\rho_{p,eff}}$$

2-20

$$2 * l_{s,max} = 2 * \left( k * c + \frac{1}{4} * \frac{f_{ctm}}{\tau_{bms}} * \frac{\emptyset}{\rho_{p,eff}} \right)$$

2-21

Since  $f_{ctm}$  and  $\tau_{bms}$  are related to each other, the factor between these values can be seen as a constant. When the recommended values are filled in, the following expressions are obtained (short term values are used for both codes)

$$S_{r,max} = 3.4 * c + 0.8 * 0.5 * 0.425 * \frac{\emptyset}{\rho_{p,eff}} = 3.4 * c + 0.17 * \frac{\emptyset}{\rho_{p,eff}}$$

2-22

$$2 * l_{s,max} = 2 * \left( 1 * c + \frac{1}{4} * 0.56 * \frac{\emptyset}{\rho_{p,eff}} \right) = 2 * c + 0.28 * \frac{\emptyset}{\rho_{p,eff}}$$

2-23

In these formulas only the constants differ from each other, these are values that are extracted from experiments and are empiric.

The calculations for the crack strains are:

$$\varepsilon_{sm} - \varepsilon_{cm} = \frac{\sigma_s - k_t * \frac{f_{ct,eff}}{\rho_{p,eff}} (1 + \alpha_e * \rho_{p,eff})}{E_s} \geq 0.6 \frac{\sigma_s}{E_s}$$

2-24

$$\varepsilon_{sm} - \varepsilon_{cm} - \varepsilon_{cs} = \frac{\sigma_s - \beta * \sigma_{sr}}{E_s} - \eta_r * \varepsilon_{sh} = \frac{\sigma_s - \beta * \frac{f_{ctm}}{\rho_{p,eff}} * (1 + \alpha_e * \rho_{p,eff})}{E_s} - \eta_r * \varepsilon_{sh}$$

2-25

The main difference in the strain calculations is the fact that the model code also takes into account shrinkage. In short term calculations this value is zero, because the factor  $\eta_r$  is zero. The factors  $k_t$  and  $\beta$  are the same in the Eurocode 2 and Model code 2010.

For bending members the Model code also includes a correction of  $(h-x)/(d-x)$ , since the calculated crack width is at the height of the reinforcement and the crack width at outer tensile fibre needs to be determined. This factor is not used in the Eurocode 2.

### 2.4.2 Eurocode 2 vs AASHTO

The AASHTO uses a totally different approach for the control of crack width. The spacing between the reinforcement bars is the most important parameter in these calculations. This parameter is not used in the Eurocode 2. The idea behind it is that with smaller spacing between the reinforcement bars the cracks will distribute more evenly, resulting in a larger amount of small cracks instead of a few large cracks. To compare this approach with the Eurocode 2 is quite difficult, since they are very different. The only similarities in the calculations are that both equations contain the cover and the stress in the reinforcement.

### 2.4.3 Eurocode 2 vs JSCE

Next the Eurocode 2 and the Japanese code will be compared, first the Eurocode 2 is fully written out:

$$w_k = S_{r,max} * (\varepsilon_{sm} - \varepsilon_{cm}) = \left( k_3 * c + k_1 * k_2 * k_4 \frac{\phi}{\rho_{p,eff}} \right) * \left( \frac{\sigma_s - k_t * \frac{f_{ct,eff}}{\rho_{p,eff}} (1 + \alpha_e * \rho_{p,eff})}{E_s} \right)$$

2-26

The formula for the crack width of the JSCE is:

$$w_k = 1.1 * j_1 * j_2 * j_3 * (4c + 0.7(c_s - \phi)) * \left( \frac{\sigma_s}{E_s} + \varepsilon'_{csd} \right)$$

2-27

The formulas are relatively similar. The formulas can be split up in a part that calculates the crack spacing and a part that calculates the crack strain. When the parts for the strain and the crack spacing are examined separately the following formulas are obtained:

Crack spacing:

$$3.4 * c + 0.17 * \frac{\phi}{\rho_{p,eff}}$$

2-28

$$1.1 * 1 * 0.972 * 1 * (4c + 0.7(c_s - \phi)) = 4.28 * c + 0.75 * (c_s - \phi)$$

2-29

Both of the formulas used for the crack spacing contain the concrete cover. In the other expression the Eurocode 2 is based on the diameter and the effective tensile concrete area and the JSCE is based on the spacing between the reinforcement bars and the diameter.

It can be concluded that the cover has more influence in the Japanese code, although the difference is smaller than with the Model Code 2010. The second term differ from each other quite much, the only conclusion that can be drawn is that when the diameter gets smaller the second term will be smaller, because spacing between the bars ( $c_s$ ) will be smaller. The spacing between the bars is getting smaller, because when the diameter is smaller more bars must be used. Eventually a smaller diameter will have a positive effect on the crack width.

Crack strain:

$$\frac{\sigma_s - 0.6 * \frac{f_{ct,eff}}{\rho_{p,eff}} (1 + \alpha_e * \rho_{p,eff})}{E_s}$$

2-30

$$\frac{\sigma_s}{E_s} + \varepsilon'_{csd}$$

2-31

Both calculations have the steel strain in them. The difference in the strain calculation is that the JSCE takes the shrinkage and creep into account and the Eurocode 2 a reduction that is based on the tensile strength of concrete.

#### 2.4.4 Eurocode 2 vs JTG D62

Finally, the Chinese code will be compared to the Eurocode, the formulas of the both equations are:

$$w_k = C_1 C_2 C_3 \frac{\sigma_s}{E_s} \left( \frac{30 + \emptyset}{0.28 + 10\rho} \right)$$

2-32

$$w_k = \left( k_3 * c + k_1 * k_2 * k_4 \frac{\emptyset}{\rho_{p,eff}} \right) * \left( \frac{\sigma_s - k_t * \frac{f_{ct,eff}}{\rho_{p,eff}} (1 + \alpha_e * \rho_{p,eff})}{E_s} \right)$$

2-33

It can be concluded that the Chinese code has lesser parameters then the Eurocode 2. Also in the Chinese code calculation, a term for the strain and for the crack spacing can be defined. To be able to see the difference, the two terms are compared with the Eurocode 2 separately.

Crack spacing:

$$\left( \frac{30 + \emptyset}{0.28 + 10\rho} \right)$$

2-34

$$3.4 * c + 0.17 * \frac{\emptyset}{\rho_{p,eff}}$$

2-35

The difference between the two codes is that the Chinese code does not include the cover in the calculation of the crack spacing. The second term of the Eurocode 2 calculation is dependent on almost the same parameters as the Chinese code calculation. For the determination of the reinforcement percentage, the effective tensile area of the concrete is used in the Eurocode 2 instead of the total concrete cross-section that is used in the Chinese code.

Crack strain:

$$C_1 C_2 C_3 \frac{\sigma_s}{E_s}$$

2-36

$$\frac{\sigma_s - 0.6 * \frac{f_{ct,eff}}{\rho_{p,eff}} (1 + \alpha_e * \rho_{p,eff})}{E_s}$$

2-37

The crack strain in the Chinese codes is only dependent on the steel strain and has no reduction like in the calculation of the Eurocode 2.

## 3 Influence height on crack width

In this chapter the calculations of the Eurocode 2 with different heights are made and analysed. First the approach of the calculations is explained, then the parameters are determined. Additionally the influences of the height independent parameters of the Eurocode 2 crack width calculation are discussed and the different codes are compared. These height independent parameters are:

- Cover;
- Reinforcement percentage;
- Tensile strength;
- Reinforcement stress.

### 3.1 Approach calculations

The cover, the reinforcement percentage, the tensile strength and the reinforcement stress are not influenced by the construction height in the Eurocode 2 calculations. When these height independent parameters in the Eurocode 2 crack width calculation are kept constant, the difference in crack width is due to changes in height. The height has an influence on the diameter of the bars, because when the construction height gets larger the diameter of the reinforcement gets larger. Next to the diameter there is an effect of the construction height on the effective height of the tensile zone in the concrete, Figure 2-3. The effect of the construction height on the Eurocode 2 crack width calculation is expected to be small, because the height does not influence the diameter and the effective height of the tensile zone a lot. The reinforcement percentage is not directly used in the Eurocode 2 calculation, but has a relation with the effective reinforcement percentage. The effective reinforcement percentage is dependent on the height, but the reinforcement percentage is not. The ratio between the effective height of the tensile zone and the construction height is the same as the ratio between the reinforcement percentage and the effective reinforcement percentage ( $\rho_{p,eff}$ ) (equation 3-1).

$$effective\ reinforcement\ percentage = \frac{h}{h_{c,eff}} * reinforcement\ percentage$$

3-1

Next to the influence of the height, the influences of the four height independent parameters are analysed. This is done for an additional view on differences in the other codes compared to the Eurocode 2 and for the comparison with the numerical results at the end of this report. In the comparison with the numerical results differences in crack widths, spacing's and strains and the parameter causing this difference can be specified.

There are standard values used for the four parameters named above. These values are:

- Cover of 50 millimetres;
- Concrete tensile strength of 3 N/mm<sup>2</sup>;
- Reinforcement percentage of 1 %;
- Reinforcement steel stress of 400 N/mm<sup>2</sup>.



When the influence of one of these parameters is determined, only the value of that parameter is changed.

Next the presentation of the results is discussed. The results are as follows presented:

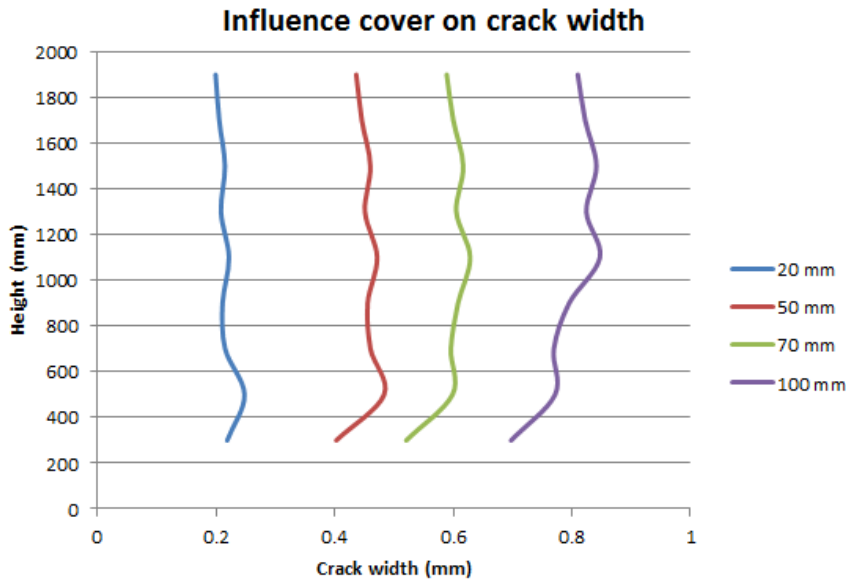


Figure 3-1; example results of influence cover on crack width

In Figure 3-1 the influence of the cover on the crack width is shown. In this figure four lines are given, each of these lines show the influence of the height. The shift between the lines is caused by the influence of the cover. For every height independent parameter the results are presented in this way.

When the effect of the height independent parameter, the cover in this case, is significant an additional graph is given, in which the trend between the height independent parameter and the crack width, spacing or strain is given, see Figure 3-2.

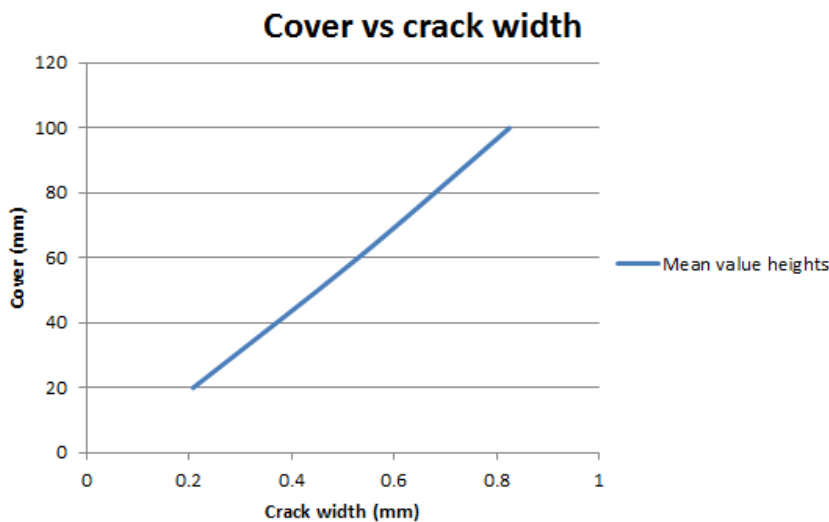


Figure 3-2; example trend between cover and crack width

## 3.2 Input codes

The values of the parameters that are needed in the Eurocode 2 crack width calculation are given below.

### 3.2.1 Geometry

To calculations will be performed on a beam. The dimensions and values are given in Table 3-1. The cross section geometry is presented in Figure 3-3. For the values a range is given, since the influence of these parameters will be investigated or they are adapted to the cross section.

Geometry

Thickness	$h$	300-1900	mm
Width	$w$	$h/2.5$	mm
Bar diameter	$\varnothing$	8-40	mm
Cover	$c$	30-100	mm
Number of bars	$n_b$	2-17	

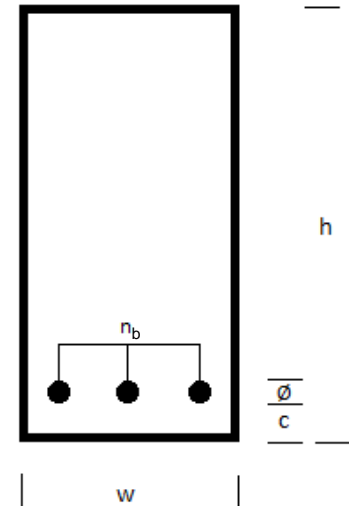


Table 3-1; Geometry beam Eurocode calculations

Figure 3-3; Reinforced concrete beam cross section

### 3.2.2 Materials

The concrete quality that is applied in the calculations is based upon C30, since this is commonly used in civil structures. For the reinforcement the steel quality B500 is applied. The material properties are given in Table 3-2 and Table 3-3. For some values a range is given, since the influence of these parameters will be investigated.

Concrete

Quality	C30		
Tensile strength, flexural	$f_{ctm}$	2-4	$N/mm^2$
Compression strength	$f_{cc}$	30	$N/mm^2$
Youngs modulus	$E_{cm}$	30000	$N/mm^2$

Table 3-2; Concrete material properties

Steel

Quality	B500		
Strength	$f_y$	500	$N/mm^2$
Youngs modulus	$E_s$	200000	$N/mm^2$
Reinforcement percentage		0,5-1,5	%

Table 3-3; Steel material properties

### 3.2.3 Reinforcement percentage

For reinforcement percentage of one percent the following bar diameters and number of bars are used:

Height	Width	$A_c$	$A_{s,1\%}$	$n_b$	$\emptyset$	$A_s$	%
300	120	36000	360	2	16	402	1.12
500	200	100000	1000	2	25	981	0.98
700	280	196000	1960	4	25	1963	1.00
900	360	324000	3240	5	30	3534	1.09
1100	440	484000	4840	5	35	4810	0.99
1300	520	676000	6760	7	35	6734	0.99
1500	600	900000	9000	7	40	8796	0.97
1700	680	1156000	11560	9	40	11309	0.98
1900	760	1444000	14440	11	40	13823	0.96

Table 3-4; Steel area applied for one percent reinforcement

The proposed steel area is calculated by multiplying the proposed reinforcement percentage with the area of the cross section of the concrete beam, columns four and three in Table 3-4. With the number and diameter of the bars the applied steel area can be calculated, see column seven in Table 3-4. The amount and diameter of the bars are definite so that the applied steel area is as close as possible to the proposed steel area; see columns five and six in Table 3-4. Thereafter the used reinforcement percentage is determined; see the last column in Table 3-4.

The influence of the reinforcement percentage is determined with different reinforcement percentages. For each reinforcement percentages a configuration is specified. The configuration for 0.7 percent can be found in Table 3-5 and for 1.5 percent in Table 3-6.

Height	Width	$A_c$	$A_{s,0.7\%}$	$n_b$	$\emptyset$	$A_s$	%
300	120	36000	252	2	12	226	0.63
500	200	100000	700	4	16	804	0.8
700	280	196000	1372	3	25	1472	0.75
900	360	324000	2268	3	30	2120	0.65
1100	440	484000	3388	5	30	3534	0.73
1300	520	676000	4732	5	35	4810	0.71
1500	600	900000	6300	7	35	6734	0.75
1700	680	1156000	8092	8	35	7696	0.67
1900	760	1444000	10108	8	40	10053	0.7

Table 3-5; Configuration 0.7 percent

Height	Width	$A_c$	$A_{s,0.7\%}$	$n_b$	$\emptyset$	$A_s$	%
300	120	36000	540	3	16	603	1.68
500	200	100000	1500	3	25	1472	1.47
700	280	196000	2940	4	30	2827	1.44
900	360	324000	4860	7	30	4948	1.53
1100	440	484000	7260	6	40	7539	1.56
1300	520	676000	10140	8	40	10053	1.49
1500	600	900000	13500	11	40	13823	1.54
1700	680	1156000	17340	14	40	17592	1.52
1900	760	1444000	21660	17	40	21362	1.48

Table 3-6; Configuration 1.5 percent

### 3.2.4 Compression height

For the calculation of the effective height of the tensile zone the compression height is needed. First the maximum normal force is calculated, this is done by multiplying the yield stress of the reinforcement steel with the steel area, equation 3-2.

$$f_y * A_s = N_s \text{ (} F_s \text{ in Figure 34)}$$

3-2

To have horizontal equilibrium, the normal force in the steel should be the same as the normal force in the concrete.

$$N_s = N_c \text{ (} F_s \text{ and } F_c \text{ in Figure 34)}$$

3-3

If the normal force in the concrete is known the compression height of the concrete can be determined. This is done with the Model Code 2010 (International Federation for Structural Concrete, 2013), see Figure 3-4.

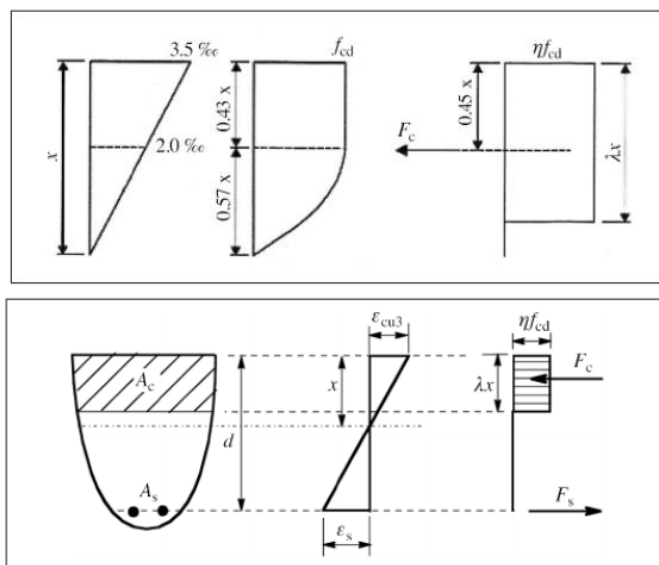


Figure 3-4; Configuration for calculating the compression height of concrete

The formula for the compression force is:

$$N_c = \eta * f_{cc} * \lambda * x * w$$

3-4

When the formula is rearranged the compression height can be calculated;

$$x = \frac{N_c}{\eta * f_{cc} * \lambda * w}$$

3-5

The calculated normal force in the concrete is divided by the compression strength of concrete and the width of the cross section of the beam. The formula used for the compression height is simplified, as can be seen in the top of Figure 3-4; therefore some reduction factors are applied.

The reduction factors  $\lambda$  and  $\eta$  can be found in Figure 3-5.

$$\begin{aligned} \lambda &= 0.8 && \text{for } f_{ck} \leq 50 \text{ MPa} \\ \lambda &= 0.8 - (f_{ck} - 50) / 400 && \text{for } 50 < f_{ck} \leq 100 \text{ MPa} \\ \text{and} \\ \eta &= 1.0 && \text{for } f_{ck} \leq 50 \text{ MPa} \\ \eta &= 1.0 - (f_{ck} - 50) / 200 && \text{for } 50 < f_{ck} \leq 100 \text{ MPa} \end{aligned}$$

Figure 3-5; Values for calculation of the compression height of concrete

Now all the values for the crack width calculation of the Eurocode 2 can be calculated, there are a few other calculations for the other codes. The spacing is an important factor for other codes; this can be calculated in the following manner:

$$s = \frac{w}{(n_b + 1)}$$

3-6

The spacing is calculated by the width divided the number of bars plus one.

### 3.3 Influence cover

First the influence of the cover in the Eurocode 2 is treated. Then for the other codes the influence of the cover is checked.

The cover ( $c$ ) is in the crack spacing term ( $S_{r,max}$ ) of the Eurocode 2 calculation:

$$w_k = S_{r,max} * (\varepsilon_{sm} - \varepsilon_{cm})$$

3-7

$$S_{r,max} = k_3 c + k_1 k_2 k_4 \phi / \rho_{p,eff}$$

3-8

#### 3.3.1 Eurocode 2

To determine the influence of this parameter, different values will be evaluated. These values will be 20, 50, 70 and 100 millimetres.

In Table 3-7 an example is given for a calculation of the crack width with the Eurocode 2, a height of 300 millimetres and a cover of 50 millimetres are used.

Parameter		Value	Unit
Factor for duration	kt	0.6	
Bond properties	k1	0.8	
Distribution of strain	k2	0.5	
Factor influence cover	k3	3.4	
Factor influence diameter	k4	0.425	
Ratio $E_s / E_{cm}$	$\alpha_e$	6.67	
Used reinforcement percentage		1.12	%
Steel area	$A_s$	402	mm <sup>2</sup>
Effective tensile concrete area	$A_{ceff}$	9208	mm <sup>2</sup>
Ratio $A_s / A_{ceff}$	$\rho_{peff}$	0.0437	
Steel stress	$\sigma$	400	N/mm <sup>2</sup>
Crack spacing	$S_{rmax}$	232	mm
Difference between mean strains	$\varepsilon_{sm} - \varepsilon_{cm}$	0.00173	
Crack width	$w_k$	0.403	mm

Table 3-7; Example calculation table (height 300 mm, cover 50 mm)

This calculation has been done for every height with all the different covers. The results can be found in Figure 3-6.

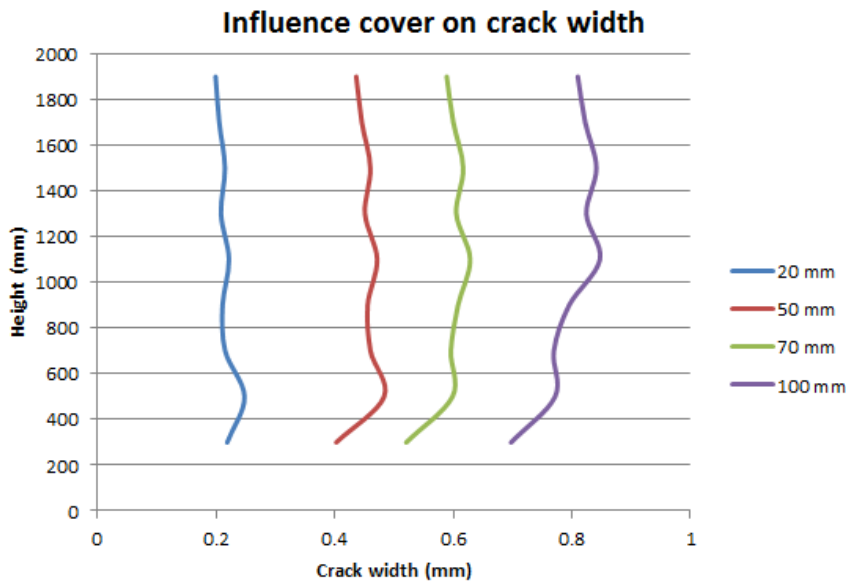


Figure 3-6; Influence of cover on crack width

The crack width increases significantly with increasing cover. The crack width does not change substantially with height; the minor bumps in the lines are caused by the changing diameters. At a height of 500 millimetres the minimum of the calculation of the concrete tensile area changes (Equation 2-5); this is the reason for the slight change in the direction of the trend.

The mean crack width over height is determined for every cover. In this way a trend is found between the crack width and cover, see Figure 3-7. It seems to be a linear process..

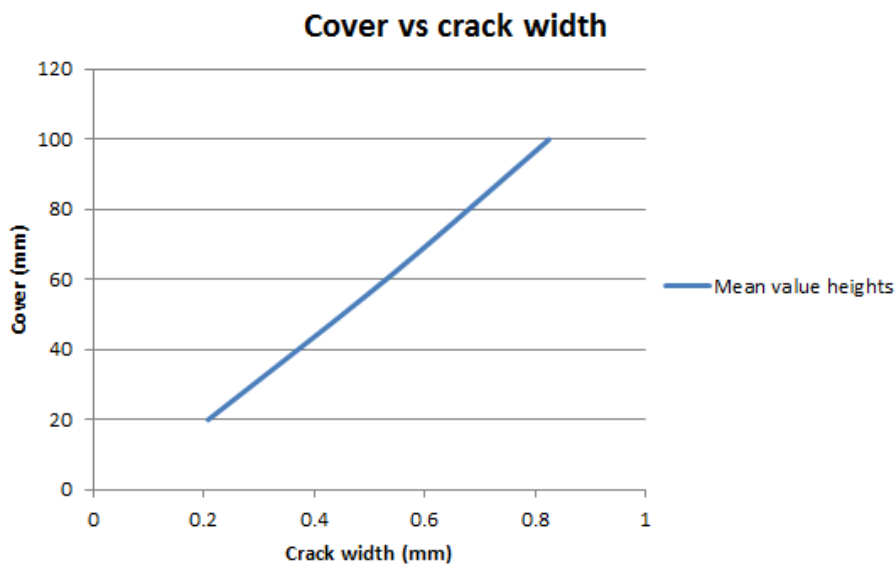


Figure 3-7; Increasing crack width with increasing cover

The cover originates from the crack spacing term. So the influence of the cover on the cracks spacing is also analysed. As expected the same trend is found for the crack spacing as has been found for the crack width, see Figure 3-8.

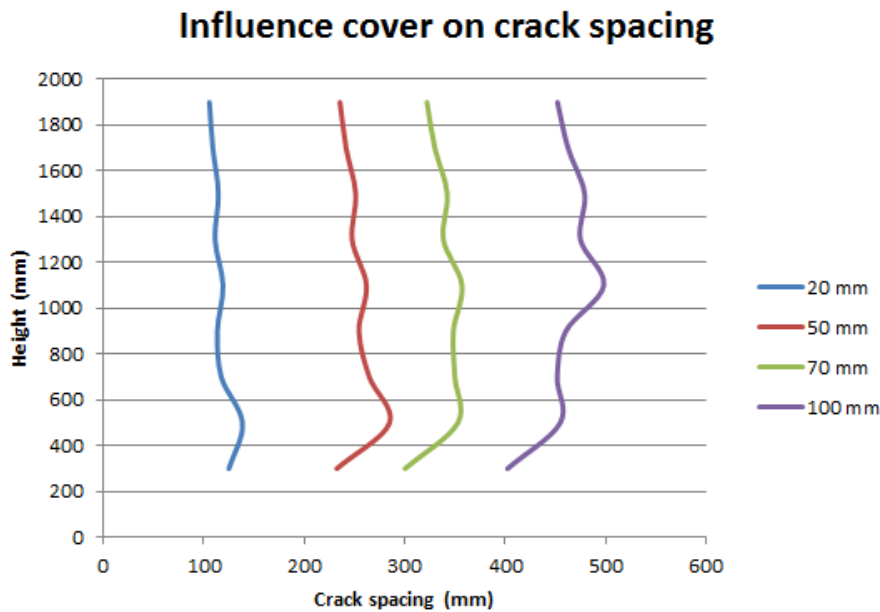


Figure 3-8; Influence of cover on crack spacing

The mean of the crack spacing's over height is determined and set out against the cover, see Figure 3-9.

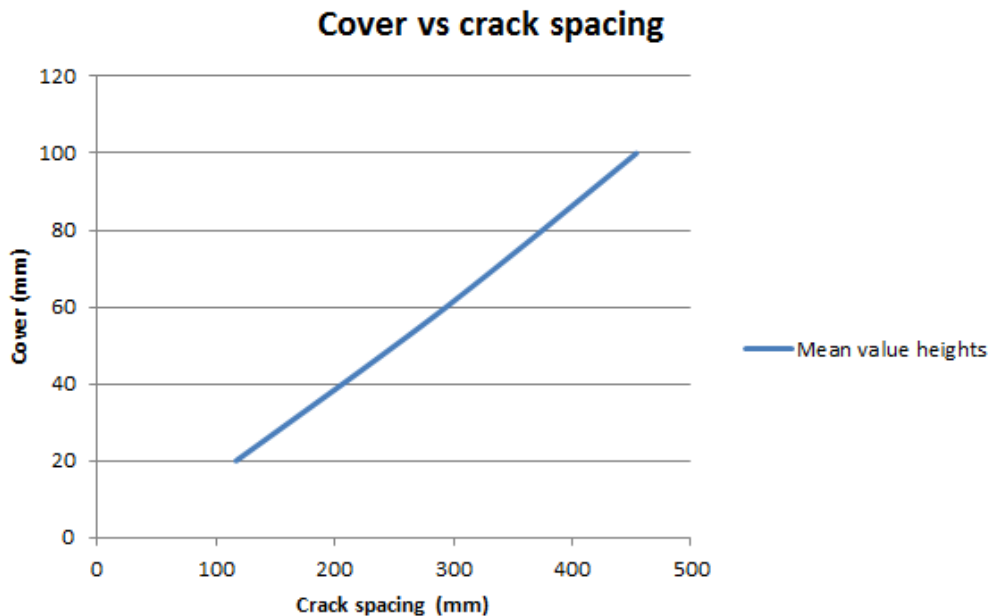


Figure 3-9; Increasing crack spacing with increasing cover

Both the crack width and crack spacing are increasing with increasing cover in a linear manner, because the cover is a linear term in the Eurocode 2.



The cover has also an influence on the effective height of the concrete tensile area and therefore a small influence on the crack strain, see Figure 3-10

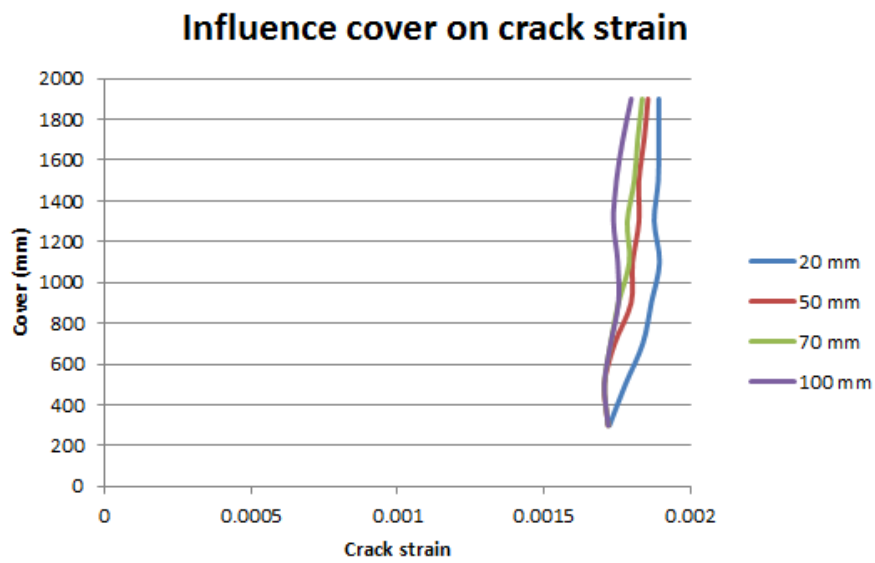


Figure 3-10; Influence of cover on crack strain

There a small decrease of strain with increasing cover, but the difference is negligible.

### 3.3.2 Other codes

Now the influence of the cover is compared with the other codes. For the reason to get some useful information out of the United States codes the stress is reduces from 400 N/mm<sup>2</sup> to 200 N/mm<sup>2</sup>. Since this calculation gives no direct indication of the crack width, but a pass or fail. In this way every calculation of the different codes can be checked with their maximum allowable crack widths, which are taken for severe circumstances. The maximum allowable crack widths are:

Code	Maximum allowable crack width (mm)
Eurocode 2	0.2
Model code 2010	0.2
AASHTO (US)	Based upon 0.2
JSCE (Japan)	0.175 / 0.245
JTG D62 (China)	0.2

Table 3-8; Maximum allowable crack width in the different codes

The maximum allowable crack width of the JSCE is dependent on the cover, so the check is done with two different maximum crack widths. In Figure 3-11, the differences between the codes are shown.

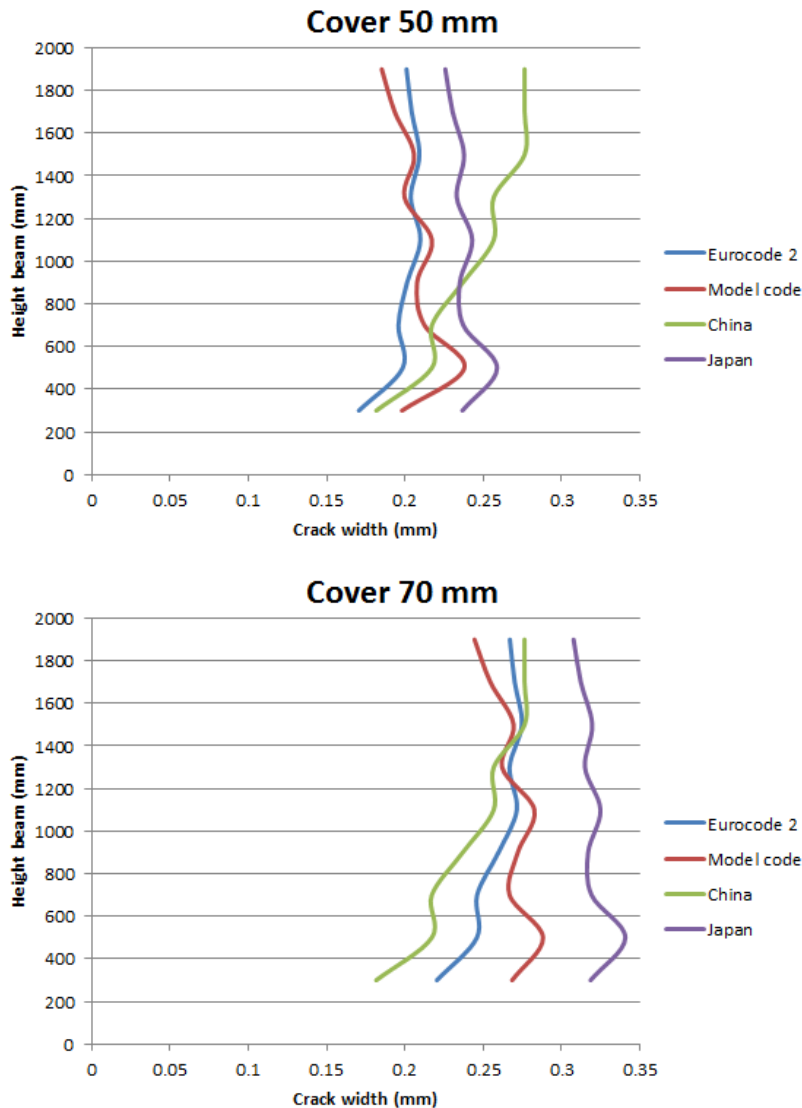


Figure 3-11; Influence of cover in different codes

All the codes give an increase of crack width with increase of cover, except the JTG D62 code from China. In the code of Japan the influence of the cover is the biggest, though the maximum allowable crack width also increases with a bigger cover.

When a cover of 50 millimetre is applied the Eurocode 2 and at higher heights the Model code 2010 are in range of the maximum allowable crack width. At a cover of 70 millimetres the crack widths are above the maximum allowable crack width. The code from the United States is satisfying the maximum crack width quite easily for both covers. Since this code is based on the spacing between the bars and the bar spacing is relatively small in these calculations.

### 3.4 Influence reinforcement percentage

Secondly the influence of the reinforcement percentage in the Eurocode 2 is treated. Thereafter the influence of the reinforcement percentage in the other codes is checked.

The reinforcement percentage ( $\rho_{p,eff}$ ) is in the crack spacing ( $S_{r,max}$ ) and strain term ( $\epsilon_{sm} - \epsilon_{cm}$ ) of the Eurocode 2 calculation:

$$w_k = S_{r,max} * (\epsilon_{sm} - \epsilon_{cm})$$

3-9

$$S_{r,max} = k_3c + k_1k_2k_4\phi/\rho_{p,eff}$$

3-10

$$\epsilon_{sm} - \epsilon_{cm} = \frac{\sigma_s - k_t * \frac{f_{ct,eff}}{\rho_{p,eff}} (1 + \alpha_e * \rho_{p,eff})}{E_s} \geq 0.6 \frac{\sigma_s}{E_s}$$

3-11

#### 3.4.1 Eurocode 2

A percentage of 0.7 and 1.5 will be used next to the standard parameter of one percent. In Figure 3-12 the results are presented.

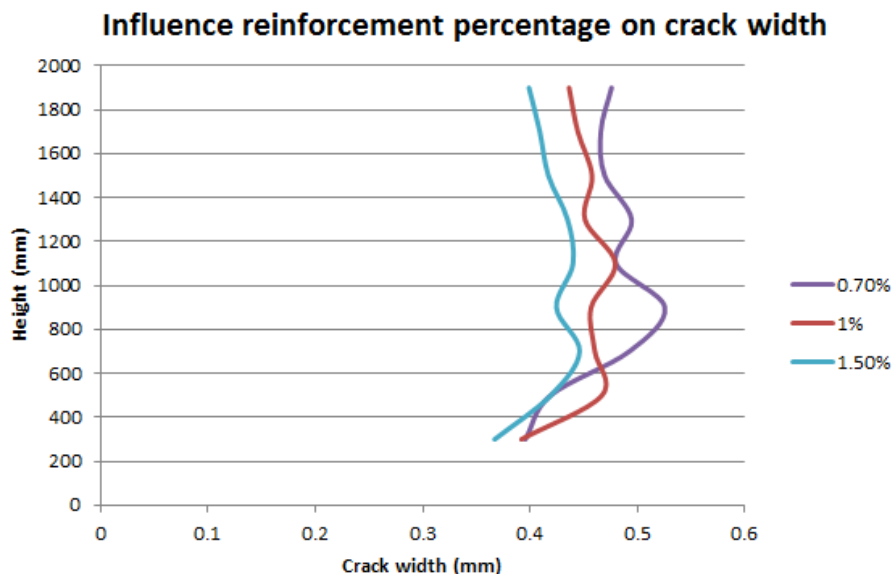


Figure 3-12; Influence reinforcement percentage on crack width

It can be concluded that with increasing reinforcement percentage the crack width gets slightly smaller. Though, there is no significant difference in crack width between the different percentages. At lower heights and middle heights the lines cross and touch each other, this is because of the different diameters in each of the reinforcement percentages. The construction height does not have a great effect on the crack width.

Since the difference between the lines is not substantial, a graph of the crack width over reinforcement percentage will not give much information and is therefore left out.

The results for the crack spacing are presented in Figure 3-13. The same trend as in the crack width results can be observed. So for the crack spacing no graph is made of the crack spacing over reinforcement percentage.

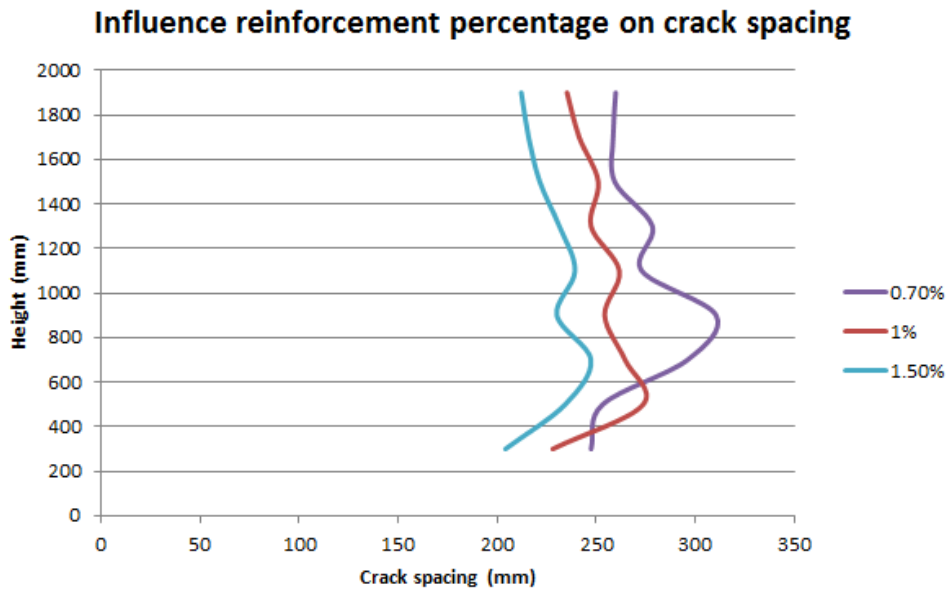


Figure 3-13; Influence reinforcement percentage on crack spacing

Next the crack strain is analysed since the reinforcement percentage influence the crack strain as well, Figure 3-14 shows the results.

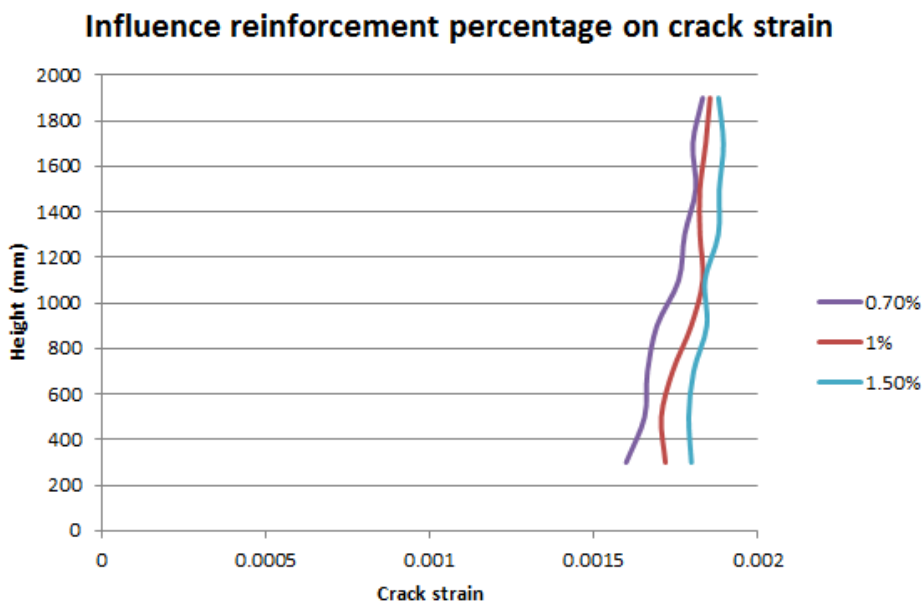


Figure 3-14; Influence reinforcement percentage on strain

The strain increases with increasing reinforcement percentage, but the effect is minimal. The crack spacing shows that there is a decrease in crack spacing with increasing reinforcement percentage. These two effects counter each other; the influence of the crack spacing is bigger, so this is dominantly present in the crack width. Like the crack width and spacing, the increasing of height does not show significant changes in crack strain.

### 3.4.2 Other codes

Now the influence of the reinforcement percentage is compared with the other codes. For the reason to get some useful information out of the United States codes the stress is reduced from 400 N/mm<sup>2</sup> to 200 N/mm<sup>2</sup>. Since this calculation gives no direct indication of the crack width, but a pass or fail. In this way every calculation of the different codes can be checked with their maximum allowable crack widths, which are taken for severe circumstances. The maximum allowable crack widths can be found in Table 3-8. In Figure 3-15, the differences between the codes are shown.

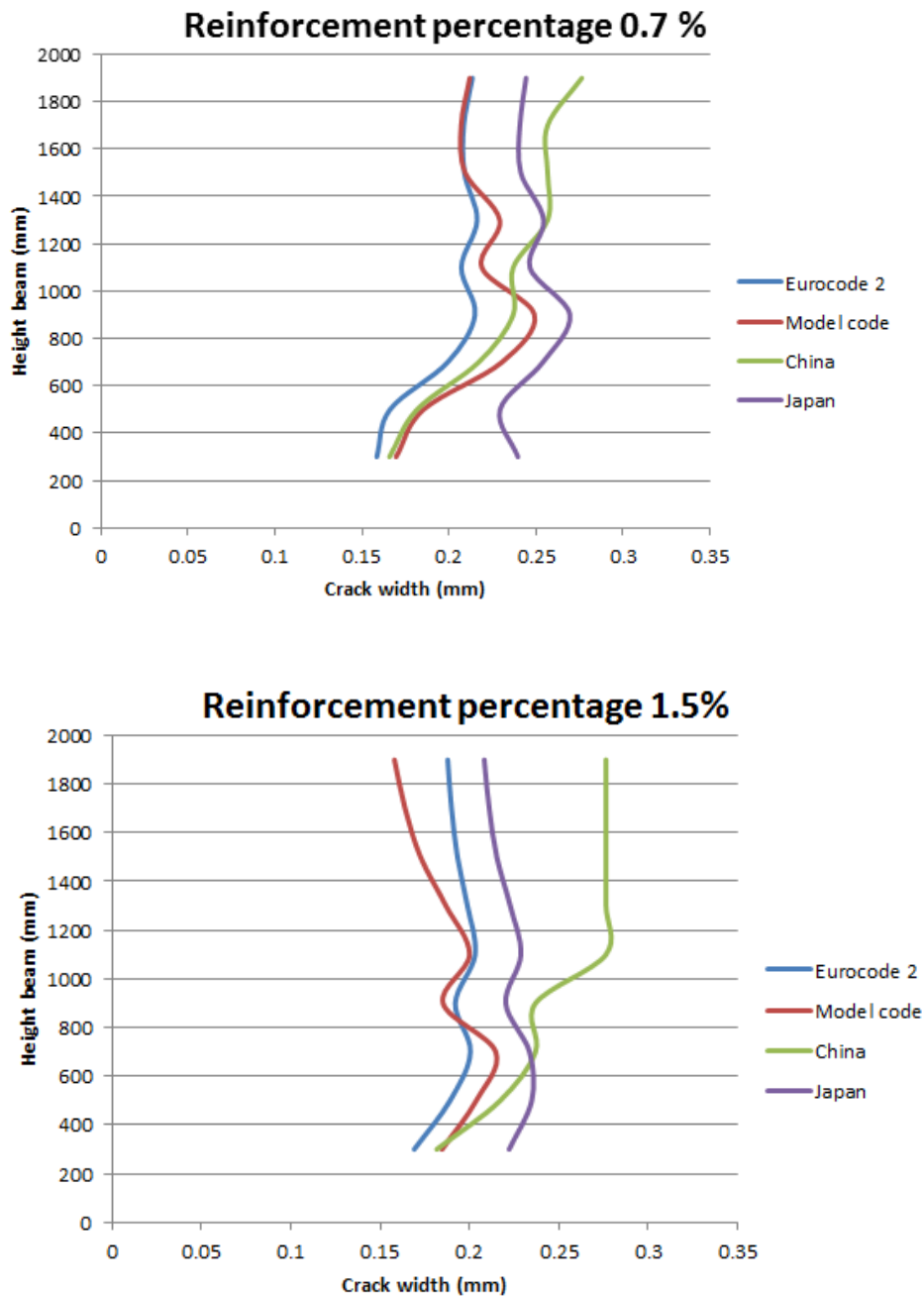


Figure 3-15; Influence of reinforcement percentage is different codes

There are some clear differences notable. At low construction heights the results do not change much when the reinforcement percentage is increased. At the larger construction heights the Chinese code increases with increasing reinforcement percentage, the Japanese code, the Model code and the Eurocode 2 in a lesser manner have a decrease with increasing percentage.

For the reinforcement percentage of 0.7%, the crack width results at smaller heights meet the maximum allowable crack widths. At larger construction heights the lines are on or over the 0.2 millimetre mark. At the reinforcement percentages of 1.5% the Eurocode 2 and Model code are below the maximum allowable crack width. The Chinese and Japanese are over the maximum. The United States code passes at every height for both reinforcement percentages.

## 3.5 Influence concrete tensile strength

Next the influence of the concrete tensile strength in the Eurocode 2 is treated. Then the influence of the concrete tensile strength in the other codes is checked.

The concrete tensile strength ( $f_{ct,eff}$ ) is in the crack strain term ( $\varepsilon_{sm} - \varepsilon_{cm}$ ) of the Eurocode 2 calculation:

$$w_k = S_{r,max} * (\varepsilon_{sm} - \varepsilon_{cm})$$

3-12

$$\varepsilon_{sm} - \varepsilon_{cm} = \frac{\sigma_s - k_t * \frac{f_{ct,eff}}{\rho_{p,eff}} (1 + \alpha_e * \rho_{p,eff})}{E_s} \geq 0.6 \frac{\sigma_s}{E_s}$$

3-13

### 3.5.1 Eurocode 2

To investigate the influence of the concrete tensile strength there are three different values used, the standard parameter of the concrete tensile strength of 3 N/mm<sup>2</sup> and the values 2 and 4 N/mm<sup>2</sup>.

The results for the crack widths can be found in Figure 3-16.

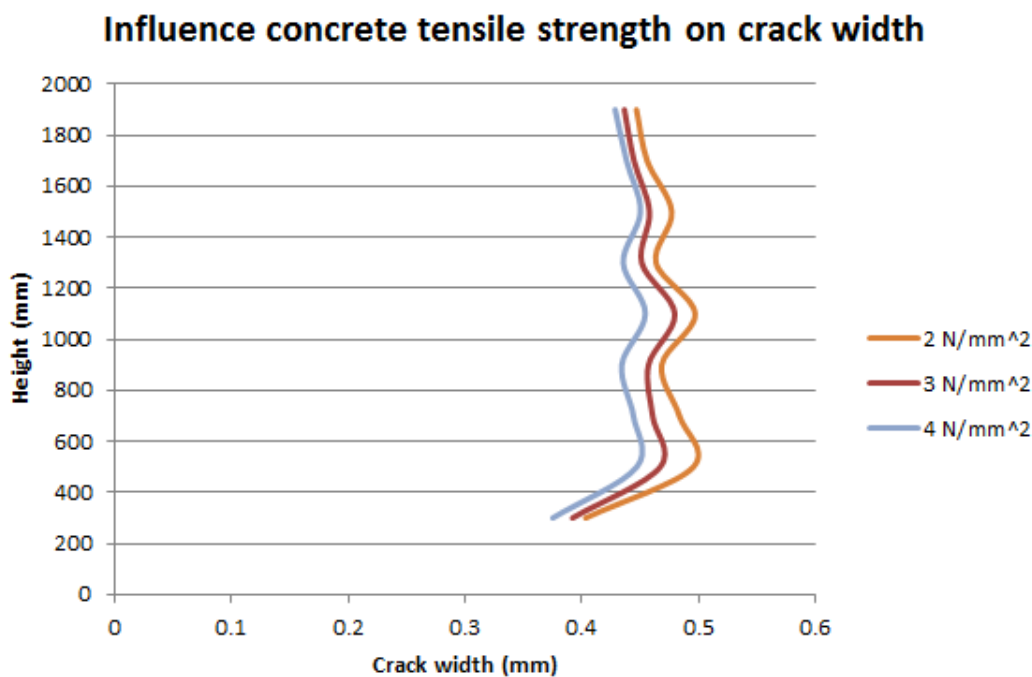


Figure 3-16; Influence of concrete tensile strength on crack width

The increase of tensile strength will cause some decrease of crack width, but it does not have a substantial influence. The tensile strength has no influence on the crack width in terms of height; the crack width stays stable with increasing height.

Since the influence is not significant the graph of crack width over tensile strength will not give much information and is therefore left out.



Logically the crack spacing will not change with changing concrete tensile stress, since this value is not in the crack spacing term.

The tensile strength is in the crack strain term; the results of the crack stain are presented in Figure 3-17.

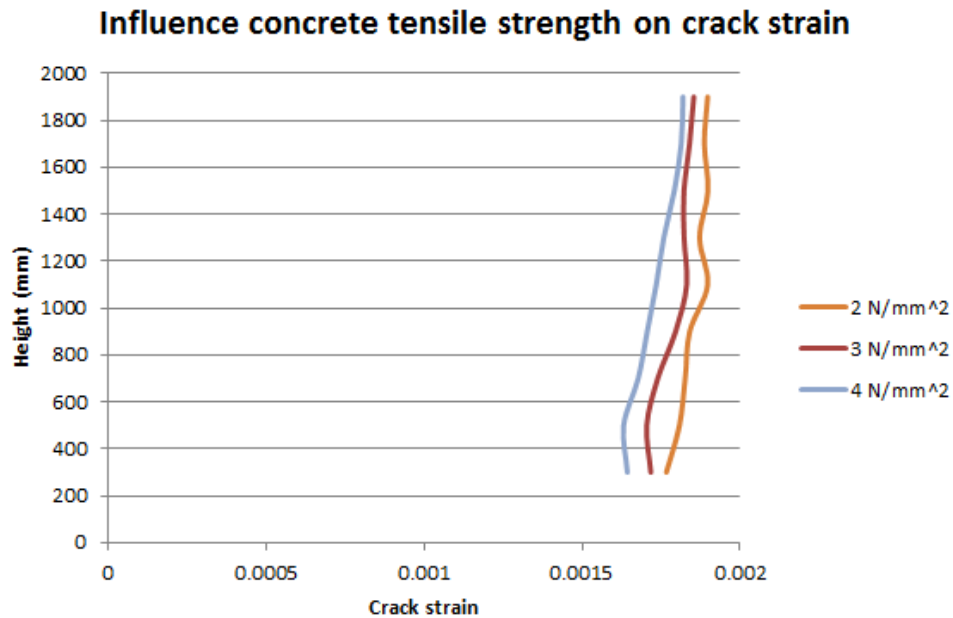


Figure 3-17; Influence concrete tensile strength on crack strain

Since the crack spacing is not changing the crack strain has the same relative increase as the crack width. There is almost no influence of construction height on the strain.

### 3.5.2 Other codes

Now the influence of the concrete tensile strength is compared with the other codes. For the reason to get some useful information out of the United States codes the stress is reduced from  $400 \text{ N/mm}^2$  to  $200 \text{ N/mm}^2$ . Since this calculation gives no direct indication of the crack width, but a pass or fail. In this way every calculation of the different codes can be checked with their maximum allowable crack widths, which are taken for severe circumstances. The maximum allowable crack widths can be found in Table 3-8. In Figure 3-18 Figure 3-15, the differences between the codes are shown.

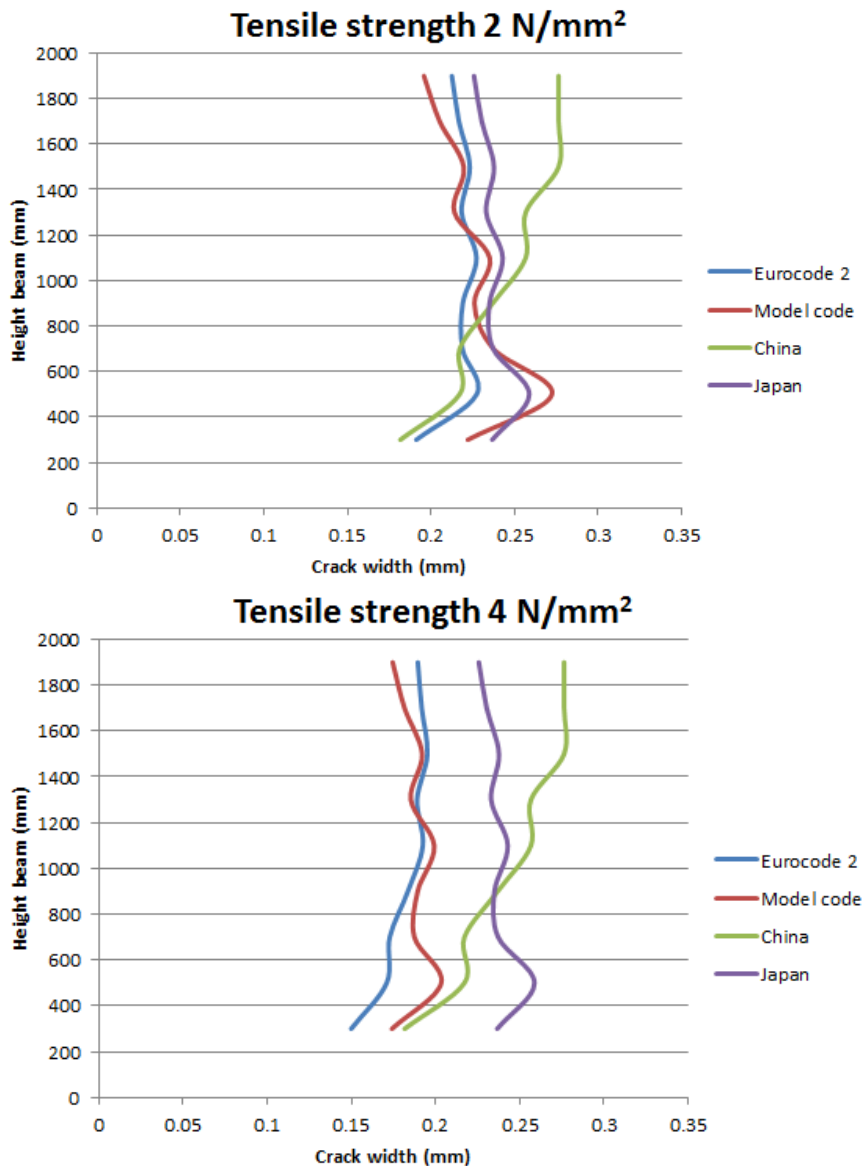


Figure 3-18; Influence of concrete tensile strength in different codes

In the results of the different codes only the Eurocode 2 and Model code are influenced by the concrete tensile strength. The increase of tensile strength results in a decrease of crack width. This effect is greater at smaller heights than at larger heights. At higher tensile strengths the Eurocode 2 and the Model code are under the maximum allowable crack width, the Japanese and Chinese codes are not. The tensile strength has no effect in the code of the United States.

## 3.6 Influence reinforcement stress

Next the influence of the reinforcement stress in the Eurocode 2 is treated. Then the influence of the reinforcement stress in the other codes is checked.

The reinforcement stress ( $\sigma_s$ ) is in the crack strain term ( $\varepsilon_{sm} - \varepsilon_{cm}$ ) of the Eurocode 2 calculation:

$$w_k = S_{r,max} * (\varepsilon_{sm} - \varepsilon_{cm})$$

3-14

$$\varepsilon_{sm} - \varepsilon_{cm} = \frac{\sigma_s - k_t * \frac{f_{ct,eff}}{\rho_{p,eff}} (1 + \alpha_e * \rho_{p,eff})}{E_s} \geq 0.6 \frac{\sigma_s}{E_s}$$

3-15

### 3.6.1 Eurocode 2

Four different values are used to determine the influence of the reinforcement stress on the crack width, which are 100, 200, 300 and 400 N/mm<sup>2</sup>. In Figure 3-19, the different stresses are shown.

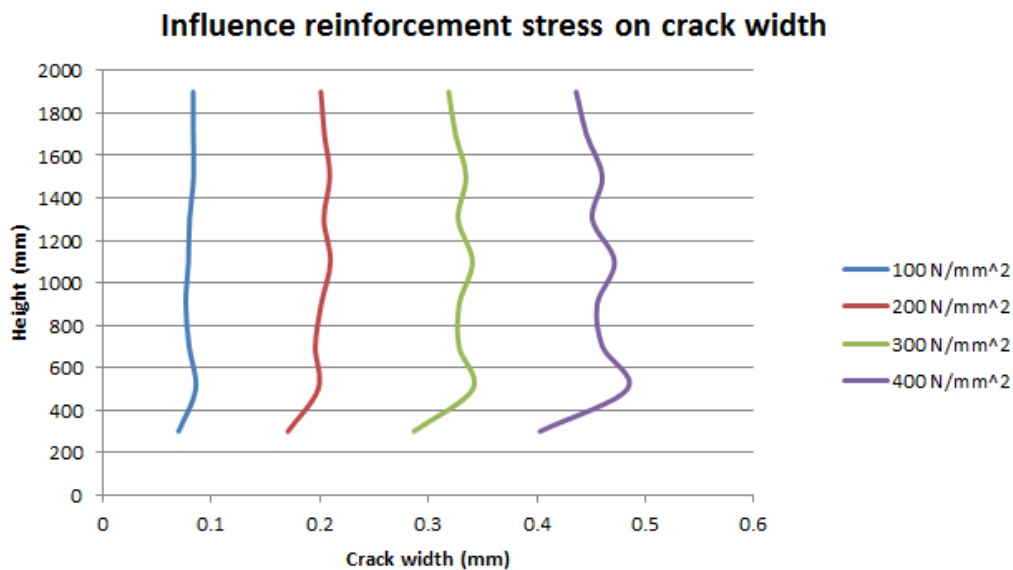


Figure 3-19; Influence of reinforcement stress on crack width

It is clear that with increasing steel stress the crack width increases. In Figure 3-20, the trend between the reinforcement stress and crack width is presented. In the beginning the cracks grow slower than at higher end of the stress stages. There is a small kink at around 90 N/mm<sup>2</sup>; this is the result of equation 2-2. The height does not influence the crack width.

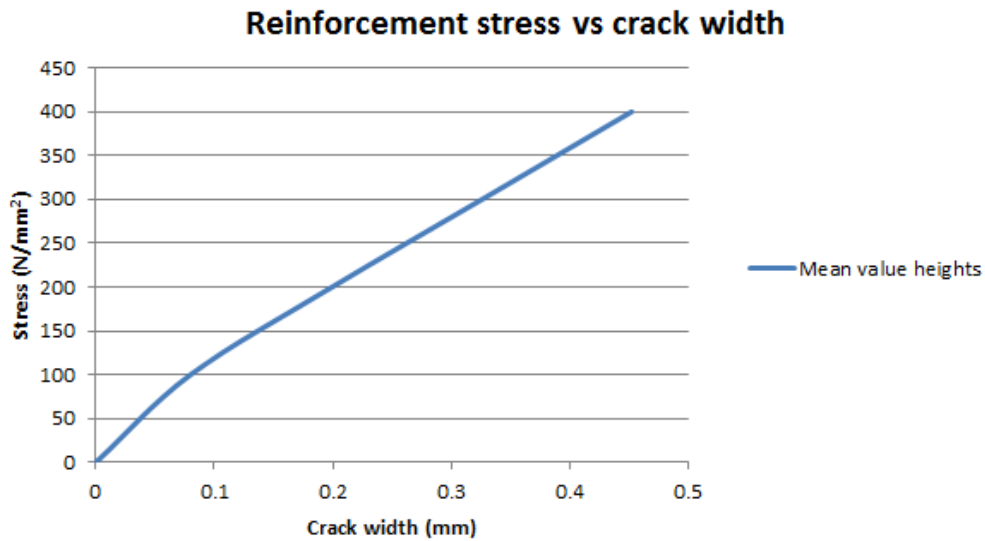


Figure 3-20; Reinforcement stress over crack width

Since the stress is only in the strain term of the Eurocode 2; the crack spacing does not change. It is the same as the result of the cover of 50 millimetres, which can be found in Figure 3-8. The crack strain is investigated and is presented in Figure 3-21.

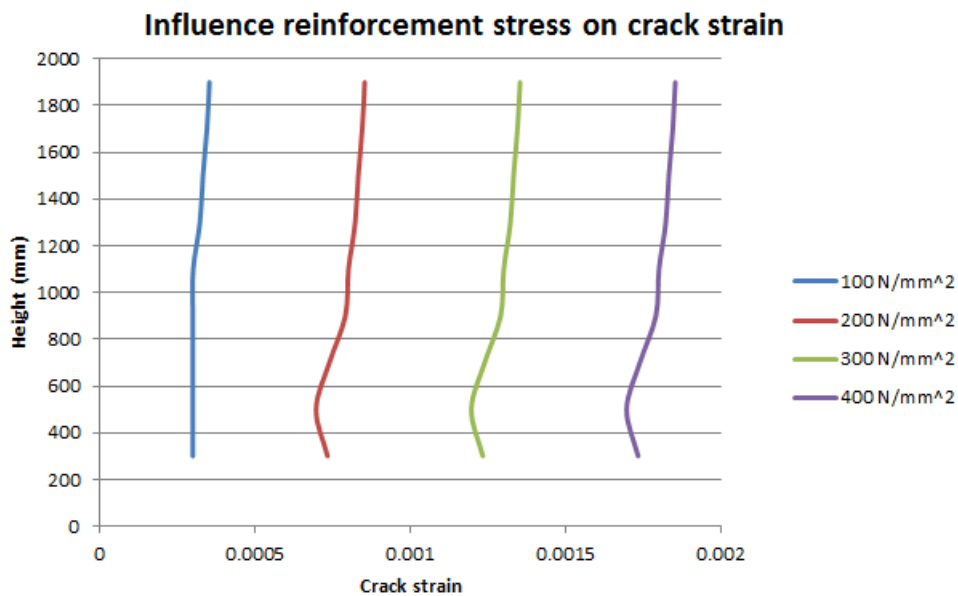


Figure 3-21; Influence of reinforcement stress on crack strain

The same relative increase with increasing reinforcement stress as the crack width can be found. This increase is visualized in Figure 3-22.

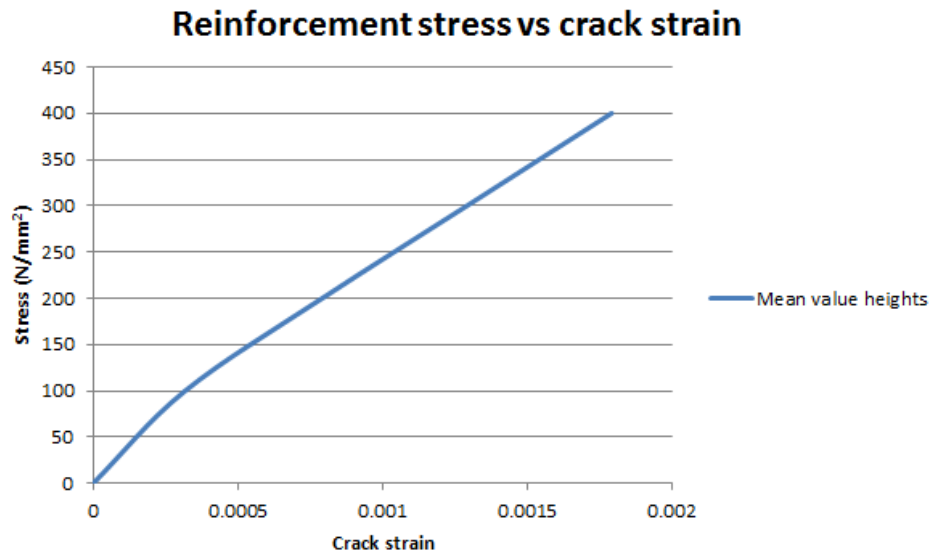


Figure 3-22; Reinforcement stress over crack strain

This line is, because of the constant crack spacing, relatively the same as the influence of the reinforcement stress on the crack width.

### 3.6.2 Other codes

Now the influence of the reinforcement stress is compared with the other codes. The maximum allowable crack widths can be found in Table 3-8. The maximum allowable crack widths can be found in Table 3-8. The results for 100 N/mm<sup>2</sup> and 300 N/mm<sup>2</sup> are given in Figure 3-23.

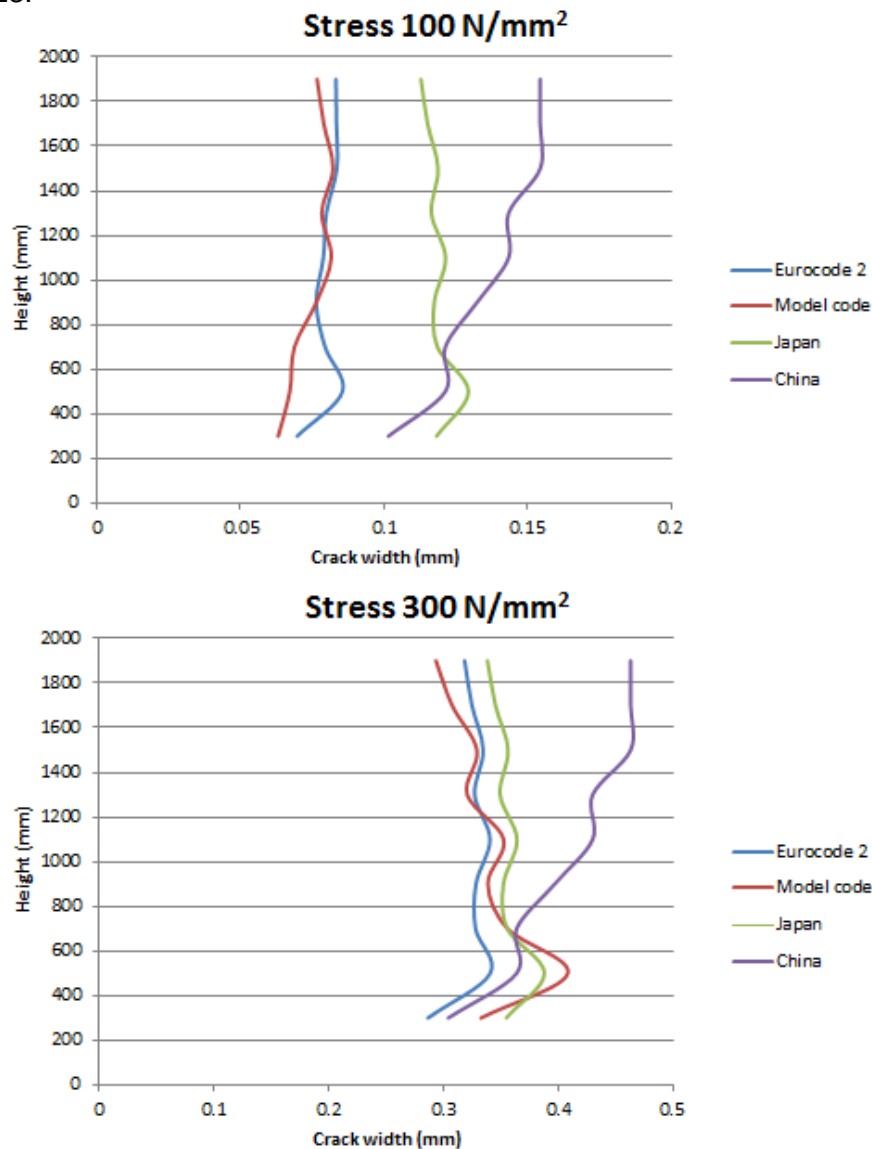


Figure 3-23; Influence of reinforcement stress in different codes

In every code the crack width increases with increasing stress. This is quite trivial. Though, the increase of crack width is not the same. The Eurocode 2 and Model code have lower crack width values at a reinforcement stress of 100 N/mm<sup>2</sup>, but when the stress is increased to 300 N/mm<sup>2</sup> the Eurocode 2 and Model code are getting in range of the crack widths calculated with the Japanese and Chinese code. There have been shown in Figure 3-11 (cover 50 mm) that the codes are around or just above the maximum allowable crack width with a reinforcement stress of 200 N/mm<sup>2</sup>. In Figure 3-23 the crack widths are all below the maximum allowable crack width for 100 N/mm<sup>2</sup> and all above for 300 N/mm<sup>2</sup>. Around 290 N/mm<sup>2</sup> the United States code gives failure for every height; this is quite higher than the other codes. If the spacing between the bars would be bigger the code would give a failure at lower stresses.

## 3.7 Conclusions

### 3.7.1 Cover

The influence of the cover is quite significant in the Eurocode 2; there is a large increase of crack width and crack spacing with increasing cover. When the influence of changing cover is investigated with the other codes, it can be concluded that in the Japanese code the crack width changes the most with changing cover. The change of crack width in Model code is comparable with the change in the Eurocode 2. In the Chinese code the cover is not included so it does not have any effect. No failures have been seen in the results of the United States code when the cover increases, were all the other codes mostly fail with a cover of 70 millimetres.

### 3.7.2 Reinforcement percentage

The influence of the reinforcement percentage in the Eurocode 2 is less significant, though a slight decrease of crack width and crack spacing with increasing reinforcement percentage has been seen. The crack strain reacts in an opposite manner, the strain increases with increasing reinforcement percentage. The differences in the other codes is that all the crack widths decrease with increasing reinforcement percentage, except the Chinese code here a slight increase is noticeable. In the United States codes there is again no failure.

### 3.7.3 Concrete tensile strength

The influence of the concrete tensile strength is small; there is a small decrease of crack width with increasing concrete tensile strength. The same relative change is seen in the crack strain results, this is logical since the concrete tensile strength is only in the crack strain term of the crack width calculation in the Eurocode 2. When the other codes are compared, only a shift in crack width in the Eurocode 2 and Model code 2010 are visible.

### 3.7.4 Reinforcement stress

The influence of the reinforcement steel stress is next to the cover a significant factor in the Eurocode 2 calculation. A great increase of crack width is the results of an increase of reinforcement stress. The source of this increase of crack width can be found in the crack strain, because the crack strain also increases significantly with increasing reinforcement stress. When the Eurocode 2 is compared with other codes, the conclusion is that all the crack widths increase with increasing reinforcement stress. Though, at lower steel stresses the Eurocode 2 and Model code 2010 have lower crack widths, at higher steel stresses the codes are closer to each other. The United States code gives failures at higher steel stresses.

### 3.7.5 General conclusion

All together the most important factors in the Eurocode 2 are the cover and reinforcement steel stress. When the Eurocode 2 is compared with the other codes it seems not to be conservative. The influence of increasing construction height is in all the results of the Eurocode 2 negligible, there is no substantial change with increasing construction height. This was expected, since the height does not have a great influence on the parameters used in the Eurocode 2 crack width calculation. The effect of the construction height is in the other codes negligible as well, since the crack widths do not change significantly with increasing height.

## II Numerical calculations

In this section the numerical calculations are covered; these will be done with the Finite Element program DIANA, version 10.1. First the material models and elements in DIANA that are of importance are explained. Thereafter the DIANA model will be verified with experiments, eventually there are several of beams with different heights calculated in DIANA and the crack widths are presented.



## 4 DIANA

In this chapter a general description of DIANA is given. Thereafter the material models and elements that are of interest are discussed.

### 4.1 General description

DIANA is a on the Displacement Method based finite element code, DIANA stands for DIsplacement method ANALyser. It is developed by the 'Nederlandse Organisatie voor toegepaste-natuurwetenschappelijk onderzoek' (TNO).

DIANA is a finite element program with extensive material, element and procedure libraries and pre and postprocessors for building the model in a graphical environment. Since the program is developed by civil engineers, DIANA is one of the best programs to use for calculations with concrete and soil. All over the world engineers use DIANA for bridges, dams, offshore platforms, tunnelling and oil and gas applications.

Notably are the constitutive models for smeared and discrete cracking, and for reduction of prestress due to special effects. (DIANA FEA BV, 2016)

### 4.2 Material models

Material aspects such as cracking of concrete, plastic yielding of steel, creep and shrinkage, aging and ambient influences can be considered in DIANA. The material models that can be used for cracking are the smeared and discrete cracking models. To apply discrete cracking the places, where the concrete is going to crack, have to be known. This is not needed in a smeared cracking model; a smeared cracking model is therefore the better choice for the purpose of this thesis. Within smeared cracking there are different kinds of models, the two that are commonly used are:

- Total strain crack model
- Multi directional fixed crack model

#### 4.2.1 Total strain crack model

'In the Total Strain crack model the user defines the uniaxial stress-strain curve and the principal stresses and strains are evaluated against this curve. The Total Strain crack model can be used with fixed, rotating or rotating to fixed crack orientation.' (DIANA FEA BV, 2016, p. Getting started 1.1.4).

#### 4.2.2 Multi directional fixed crack model

'For temperature and maturity dependent cracking the multi-directional fixed crack model can be used. This crack model is based on strain decomposition, with the total strain consisting of an elastic, crack and plastic strain component. The multi-directional fixed crack model can be used in combination with plasticity models for crushing and shearing failure.' (DIANA FEA BV, 2016, p. Getting started 1.1.4).

### 4.2.3 Tensile behaviour of concrete

Concrete behaves very differently in tension than in compression. In concrete the tension behaviour can be seen as linear, until it reaches the crack strain / stress. After this point the relation between the stress and strain show softening of the material, see Figure 4-1. This means that at higher strains the material can bear less stress.

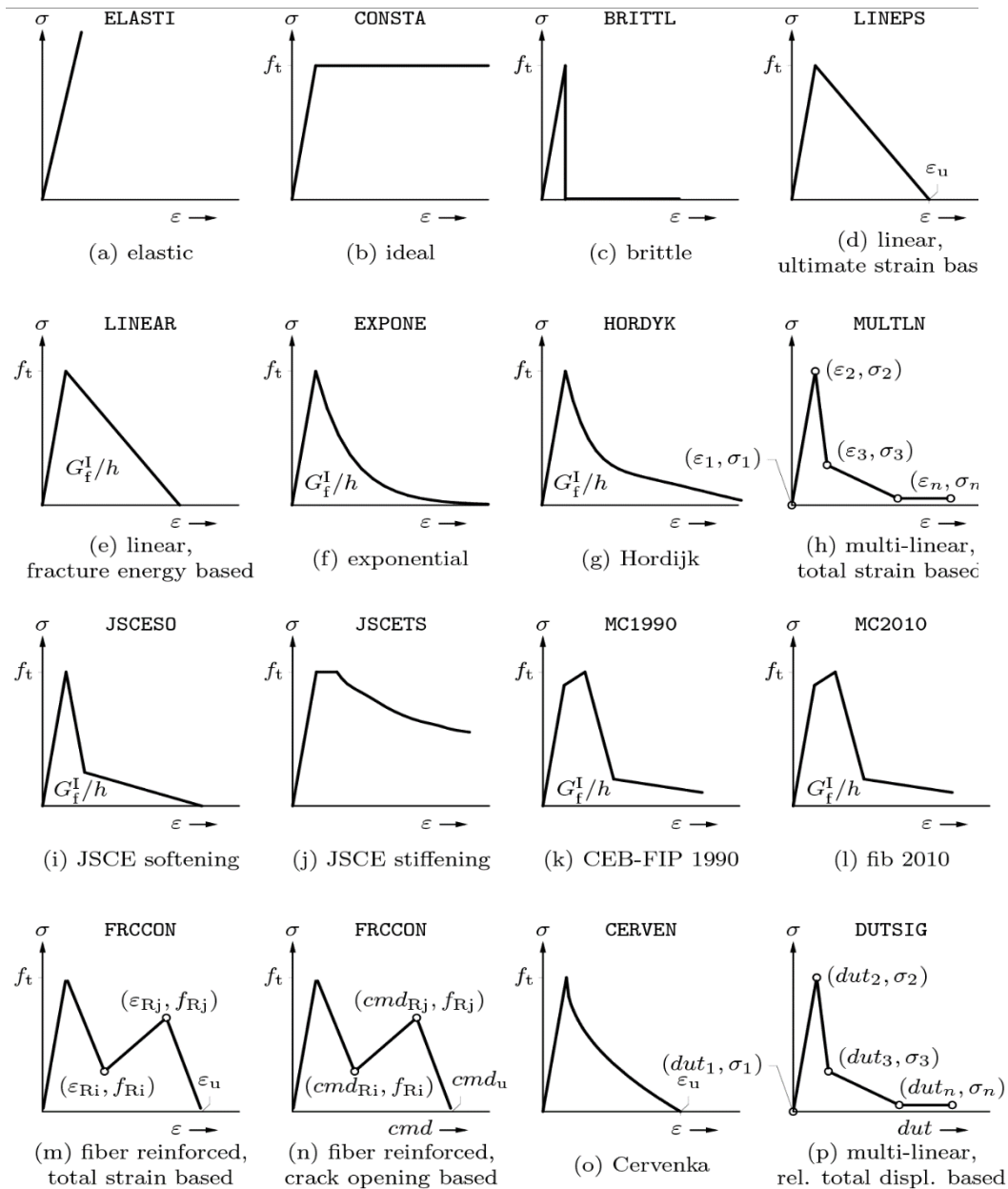


Figure 4-1; Predefined tension softening (DIANA FEA BV, 2016, p. Material library 6.2.2)

### 4.2.4 Compressive behaviour of concrete

In DIANA there are different forms of stress strain relations that represent the compressive behaviour of concrete, see Figure 4-2. Most of them have an ultimate compression strength, when this strength is reached softening of the material appears.

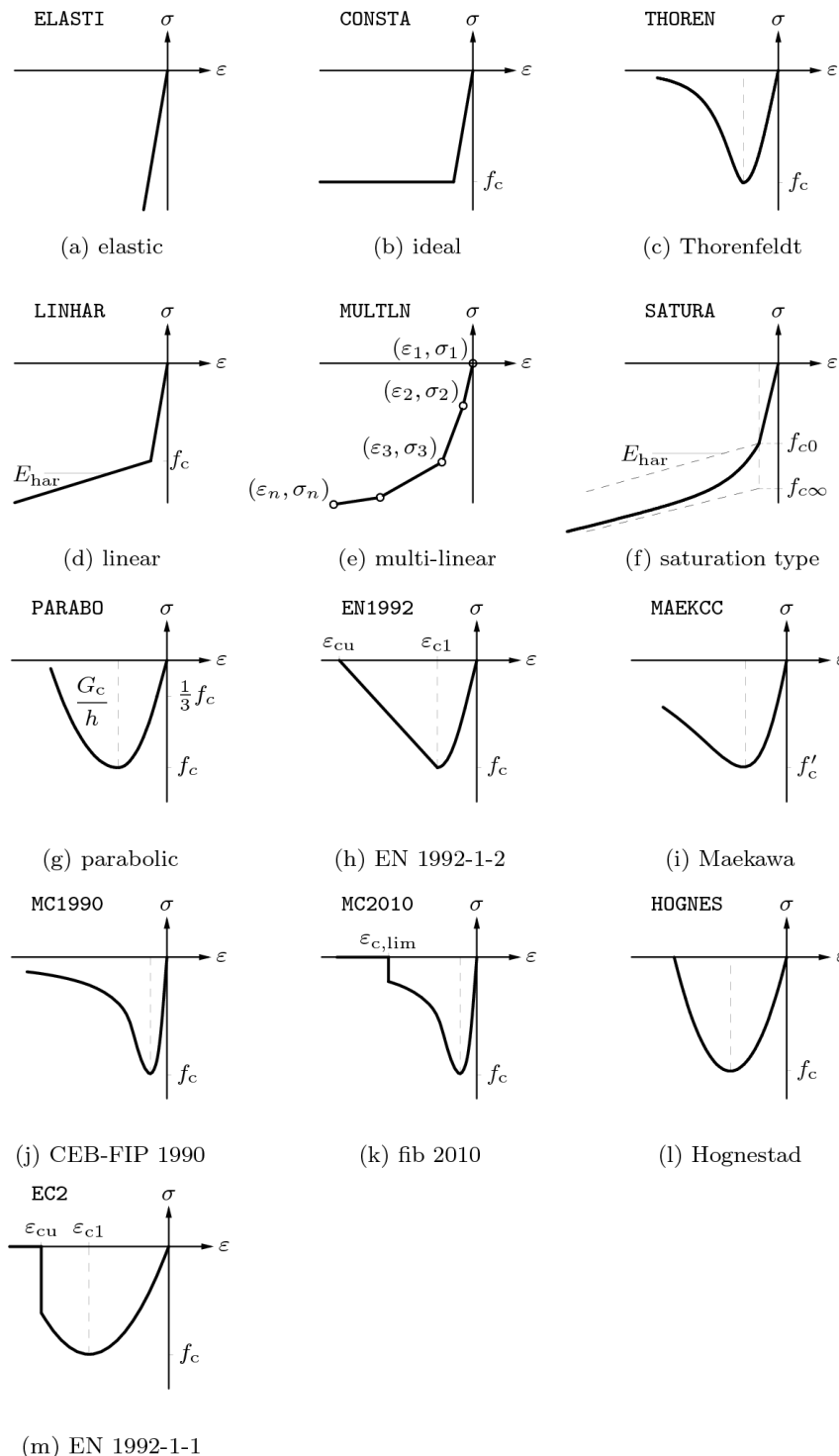


Figure 4-2; Predefined compressive softening (DIANA FEA BV, 2016, p. Material library 6.2.3)

### 4.2.5 Bond-slip

The interaction between concrete and reinforcement is a complex process, but it is an imported parameter in determining crack width. In DIANA this behaviour can be modelled with a bond slip mechanism, in which the relative slip between the reinforcement and the concrete is described. In the model an interface element around the reinforcement with a thickness of zero is used to describe the mechanical behaviour.

The following constitutive laws for bond slip are proposed in DIANA:

- Cubic function according to Dörr;
- Power law relations proposed by Noakowski;
- Bond-slip relations proposed by Shima et al;
- Bond-slip-strain relation proposed by Shima et al;
- User defined multi linear diagram.

The laws are mostly based on a total deformation theory; this means that it expresses the traction as a function of the total relative displacement. The curves of these laws are presented in Figure 4-3.

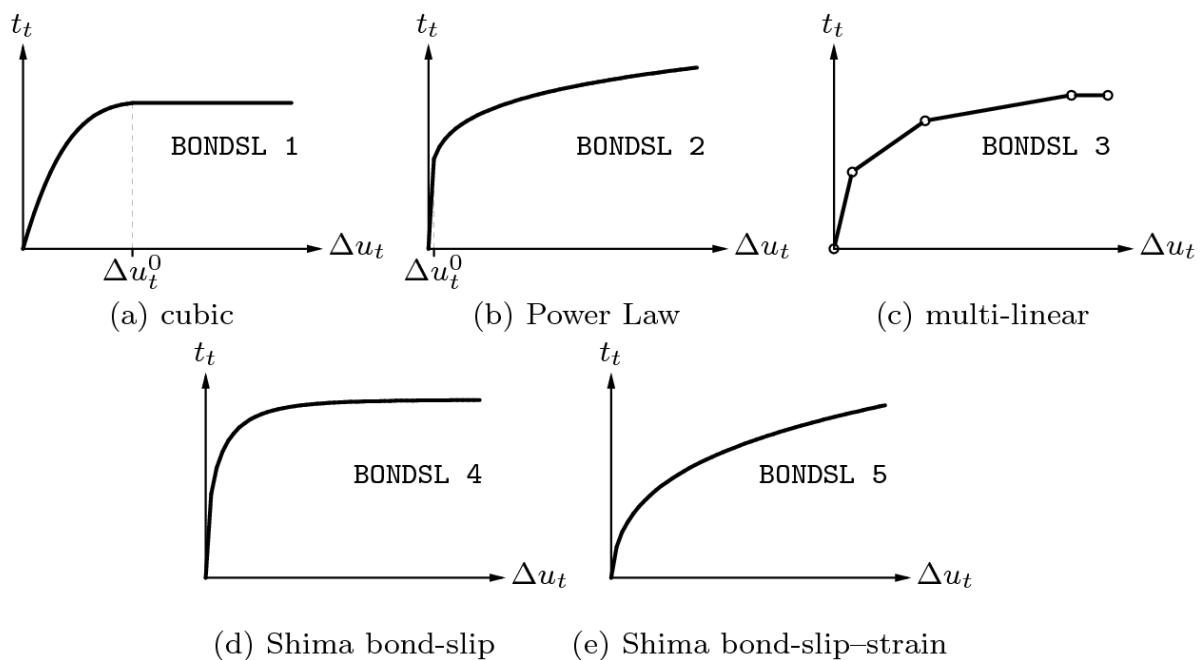


Figure 4-3; Bond shear traction slip curves, (DIANA FEA BV, 2016, p. Material library 9.3)

## 4.3 Elements

After meshing the geometry will be divided in different kind of elements, for an example see Figure 4-4.

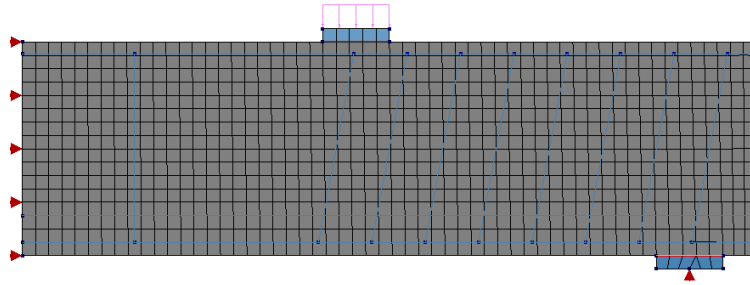


Figure 4-4; Example mesh

These elements are called structural elements. Within the structural elements there are categories: truss elements, beam elements, plane stress elements, etc. For concrete in a two dimensional model often plane stress elements are used. The element that is used in this thesis is CQ16M, which is a quadrilateral element with eight nodes and each node has two degrees of freedom see Figure 4-5.

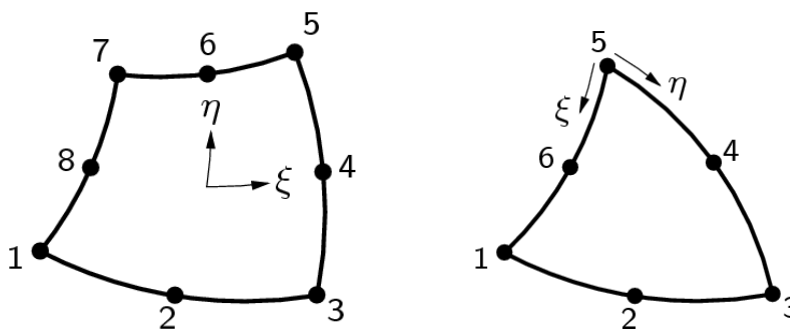


Figure 4-5; CQ16M and CT12M (DIANA FEA BV, 2016, p. Element library 5.7.4)

Sometimes DIANA uses also triangle elements in the mesh; these have six nodes with each 2 degrees of freedom. The code of these elements is CT12M see Figure 4-5.

Next to plane stress elements, structural interface elements are used. These are applied between the load and support structure and the concrete beam. The reason that these are applied is for a proper introduction of the load on the beam. The code of these elements is CL12I, and is shown in Figure 4-6.

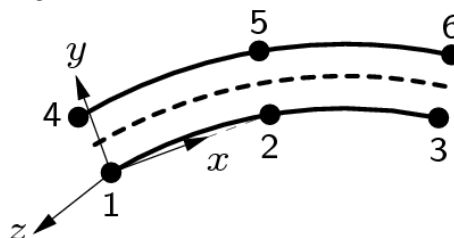


Figure 4-6; CL12I (DIANA FEA BV, 2016, p. Element library 12)

For the bond slip reinforcement truss elements are used, which can only bear a normal force. These elements are implemented in the concrete beam and have no own code.

## 5 Verification

In this chapter the DIANA verification is discussed. First the general input of the DIANA model is given. To ensure that the results that the DIANA model calculates are reliable, the model has to be verified. The verification will be done with experimental results, there are three different experiments used in the verification:

- Braam (Braam, 1990);
- E3 (Leonhardt & Walther, 1962);
- VS-C3 (Vecchio & Shim, 2004).

For every experiment the input in DIANA is discussed, and then the results of the experiments are compared with results of the corresponding DIANA model. The results that will be compared are:

- Force-Displacement diagram;
- Crack patterns;
- Crack widths.

### 5.1 Input DIANA

The parameters and material models that are used in the modelling of the concrete beams in DIANA are for each validation the same. The values for the different materials are given below.

#### 5.1.1 Concrete

The used parameters and models for the concrete are given in Table 5-1:

Name	Value
Material class	Concrete and masonry
Material model	Total strain based crack model
4Color	grey
Young's modulus	<u>Variable</u> N/mm <sup>2</sup>
Poisson's ratio	0.2
Crack orientation	Rotating
Crack bandwidth specification	Rots
Tensile curve	Hordijk

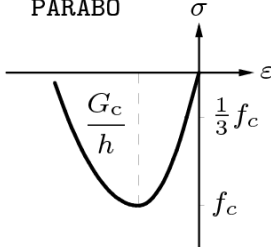
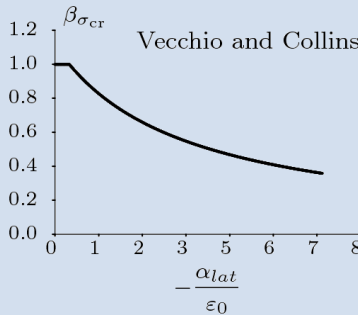
Tensile strength	<u>Variable</u> N/mm <sup>2</sup>
Mode-I tensile fracture energy	<u>Variable</u> N/mm
Reduction model	No reduction
Compression curve	Parabolic
	
Compressive strength	<u>Variable</u> N/mm <sup>2</sup>
Compressive fracture energy	<u>Variable</u> N/mm
Reduction model	Vecchio and Collins 1993
	
Lower bound reduction curve	0.6
Confinement model	No increase

Table 5-1; Parameters and models for the concrete

The values for the Young's modulus, strength and the fracture energy are experiment dependent. These values are taken from the experiment input.

The total strain based crack model is used, with a rotating crack orientation. This model is used, because the stress-strain relations are known for the linear parts, and for the non-linear parts they are adjusted to the quality of the results. Next to that there is no temperature or maturity dependent cracking investigated for which the multi directional fixed crack model is mostly used.

The rotating crack orientation is used, since it gives a better crack pattern.

The tensile curve of Hordijk and the Parabolic compressive curve are used, because the best crack patterns/crack widths are generated with these curves.

The compressive strength of the concrete reduces when the concrete is cracked, because of the large tensile strains perpendicular to the principal compressive direction, the reduction model of Vecchio and Collins 1993 takes this into account.

### 5.1.2 Reinforcement steel

The values for the steel, which are used for the reinforcement, are given in the table below:

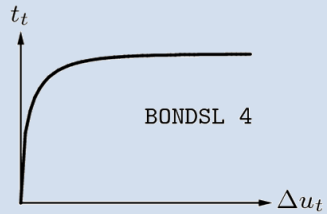
Name	Value
Material class	Reinforcements and pile foundations
Material model	Bond-slip reinforcement
Color	slateblue
Young's modulus	200000 N/mm <sup>2</sup>
Plasticity model	Von Mises plasticity
Yield	VMISES
Hardening function	No hardening
Yield stress	<i>Variable</i> N/mm <sup>2</sup>
Normal stiffness modulus	1000 N/mm <sup>3</sup>
Shear stiffness modulus	1000 N/mm <sup>3</sup>
Bond-slip interface failure model	Shima bondslip function
 <p>(d) Shima bond-slip</p>	
Bondsl	4
Compressive strength	<i>Variable</i> N/mm <sup>2</sup>
Diameter per bar	<i>Variable</i> mm
Factor to shear-stress	1
Reset state parameters on material change	F

Table 5-2; Parameters and models for the reinforcement

The steel must be able to yield, so Von Mises plasticity is used.

Hardening is only used when the default hardening does not suffice. When the default hardening in DIANA is applied, the young's modulus will reduce by a factor of thousand after the yield stress is reached.

Bond-slip is only applied in the main tension reinforcement. The normal and shear stiffness modulus are elastic stiffness's of the slip interface, with unloading and reloading these values are used. For the bond-slip interface failure model the Shima bondslip function is used, because a better force displacement curve and crack widths are found.



### 5.1.3 Steel plates

To transfer the load to the beam and from the beam to the support a linear elastic steel element is used.

Name	Value
Material class	Steel
Material model	Linear elastic isotropic
Young's modulus	200000 N/mm <sup>2</sup>
Poisson's ratio	0.3

Table 5-3; Parameters and models for modeling elements

Since the stresses and strains in these elements are not of interest, a simple linear elastic and isotropic material model is used.

### 5.1.4 Interfaces

Name	Value
Material class	Interface elements
Material model	Nonlinear elasticity
Color	silver
Type	2D line interface
Normal stiffness modulus-y	1000000 N/mm <sup>3</sup>
Shear stiffness modulus-x	0.1 N/mm <sup>3</sup>
No-tension or diagram	No-tension with shear stiffness reduction
Tension reduction parameters	0.001 0 mm
Shear stiffness reduction parameters	0.001 0 mm

Between the steel plates and the concrete beam an interface is applied, this carries the purpose of transferring the load between the steel plate and the concrete beam without any numerical errors. In normal direction the stiffness is large, because the load is in this direction and no large deformation should appear in the interface. In shear direction the stiffness is small, since loads in this direction are minimal.

## 5.2 Experiment Braam

The parameters of the materials that are used in the experiment of Braam are given in the table below:

Name	Value
Young's modulus concrete	31800 N/mm <sup>2</sup>
Tensile strength concrete	4.08 N/mm <sup>2</sup>
Tensile fracture energy concrete	0.15 N/mm
Compressive strength concrete	55,9 N/mm <sup>2</sup>
Compressive fracture energy concrete	30 N/mm
Yield stress main reinforcement	570 N/mm <sup>2</sup>
Yield stress stirrups and rest	550 N/mm <sup>2</sup>
Diameter first layer	20 mm
Diameter second layer	10 mm

Table 5-4; Parameters for the experiment of Braam

### 5.2.1 Geometry

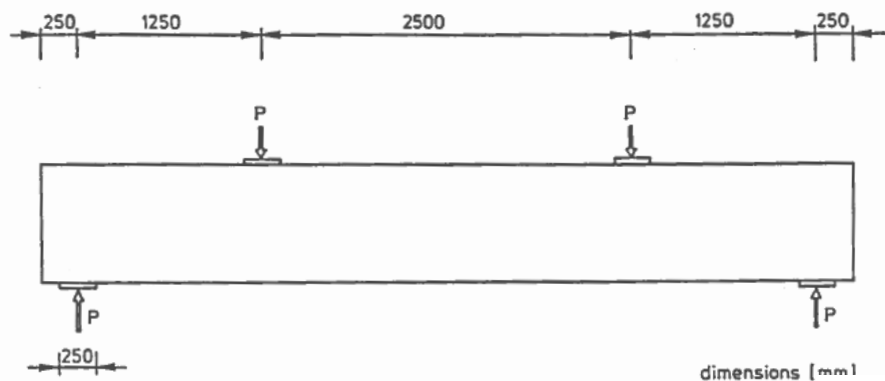


Figure 5-1; Geometry of the beam of the experiment of Braam

The beam has a length of 5,5 metres, the distance between the centres of the supports is 5 meter and the distance between the centres of the loads is 2,5 metres.

The height of the beam is 0,8 meters and the width is 0,3 meters.

The main tensile reinforcement consists of four bars with each a diameter of 20 millimetres and above those four bars there are two bars with a diameter of 10 millimetres. The stirrups and the compressive reinforcement have a diameter of 10 millimetres.

The cover is 40 millimetres.

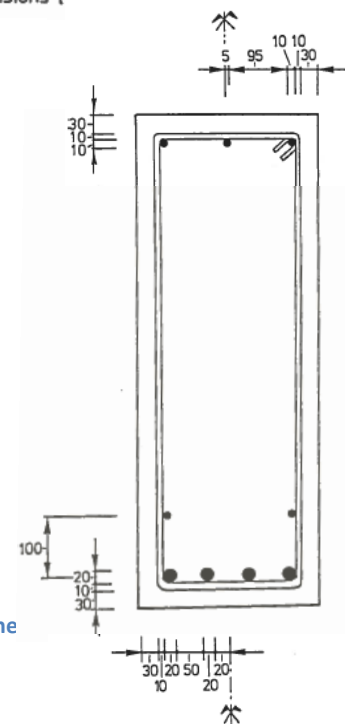


Figure 5-2; Cross-section of the experiment of Braam

In DIANA only half of the beam is modelled, because the geometry of the beam and the loading is symmetric. The computing time is due to the smaller model significantly less. At half of the height a composed line is added, this line is not attributing to the strength of the structure, but gives some integrated results.

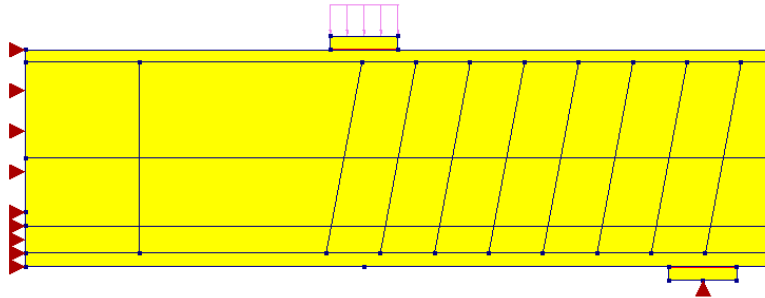


Figure 5-3; Geometry DIANA model experiment Braam

Figure 5-3 shows the concrete, the reinforcement and the load and support configuration. There are eight stirrups used between the load and support point and one between the middle point and the load point.

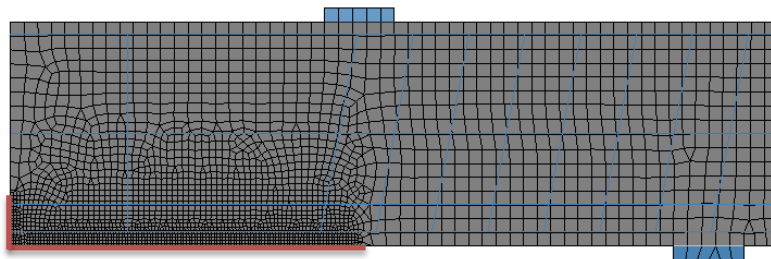


Figure 5-4; Mesh of the DIANA model of the experiment of Braam

For the general mesh an element size of 50 mm is used. Along the red indication line in Figure 5-4 an element size of 10 mm is applied to have a good localization of the cracks.

There are four load stages during the experiments, 218 kN, 368 kN, 468 kN and 668 kN. For each of these load stages the cracks between the loading points are recorded in the experiment, see Figure 5-5 (red box). All of these crack patterns have been compared with the results in the DIANA model.

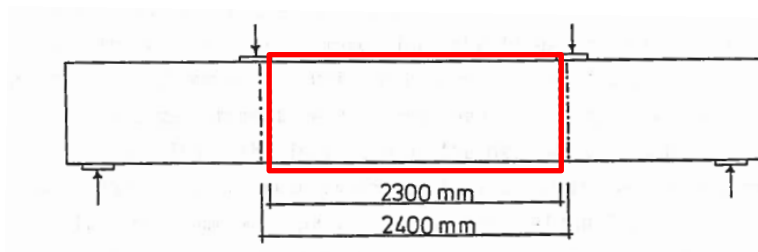


Figure 5-5; Part of the beam where crack patterns are recorded

## 5.2.2 Force-Displacement

The first check is the force-displacement diagram. Half of the beam is used in the DIANA model, so also half of the load, is used. The force-displacement diagram is presented in Figure 5-6.

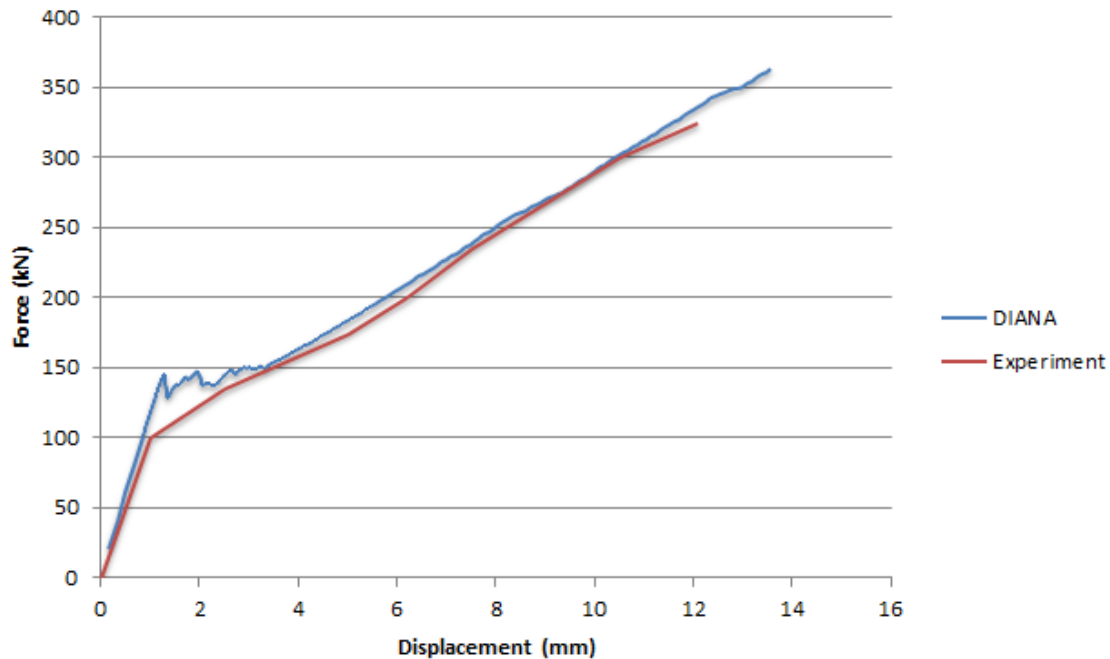


Figure 5-6; Force-displacement diagram

The force-displacement diagram of the DIANA has a good fit with the diagram of the experiment of Braam, the difference between the lines is mostly less than five percent. After the linear part, there is a small difference between the lines. This difference is the result of the tension softening model of Hordijk. This tension softening model is used, because it gives the best results for the crack pattern and width.

### 5.2.3 Crack pattern

The third of the four load stages is reviewed, since at this stage a clear crack pattern has been formed in both the experiment and the DIANA results and therefore a good comparison can be made. For the other load stages see Appendix C. This load stage has a load of 468 kN, so a load of 234 kN each load point.

The crack pattern of the experiment:

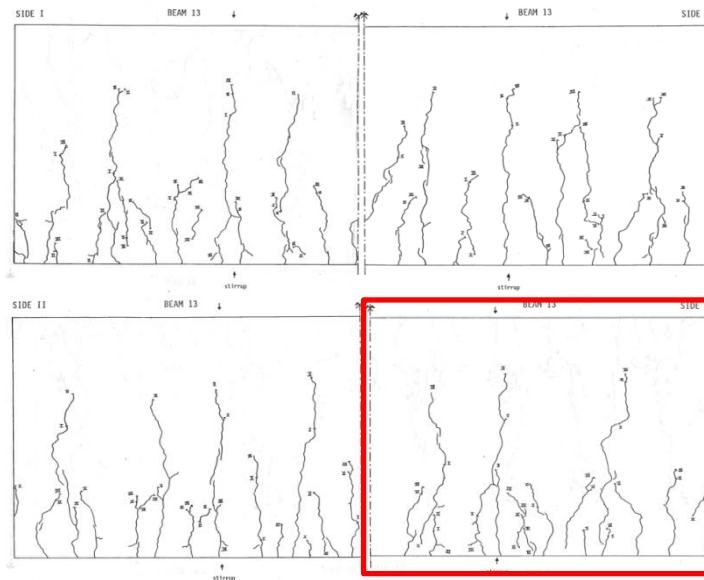


Figure 5-7; Crack pattern beam 468 kN

The crack pattern in DIANA:

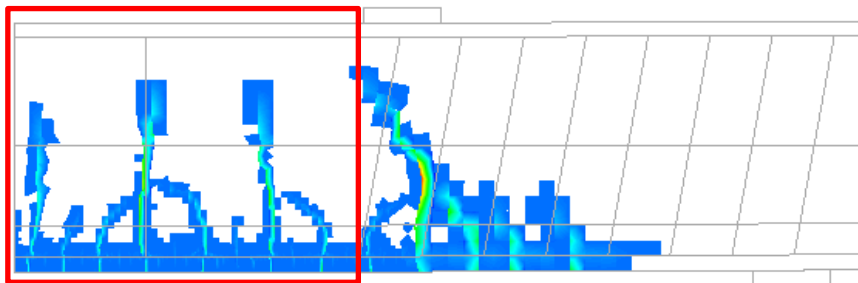


Figure 5-8; Crack pattern beam DIANA results 468 kN

The red outlined area in the result of the DIANA model (Figure 5-8) should be compared with half of the two patterns of the experiment (Figure 5-7). The red outlined area in the figure of the experiment results gives one of the four possibilities for the comparison.

There are differences notable when the four crack patterns of the experiment, each half of the two beams in Figure 5-7, are compared with each other. The reason for this phenomenon is that concrete is an anisotropic material, and the cracks will sooner appear in the weaker points of the material. These weaker points can appear at random locations, and so differences in crack patterns are noticeable. Therefore the comparison between experiment and DIANA is also not expected to be perfect overlapping.

The conclusion is that in the end the crack pattern of the DIANA results has a good comparison with the crack pattern of the experiment.

### 5.2.4 Crack width

After the crack pattern the crack widths are checked. The crack width is determined with the differences in displacement in x-direction ( $dx$ ) over the complete crack spacing. In Figure 5-9 is shown between which points, indicated with the red dots, the displacement is measured. Because the difference in x-direction is taken over the whole crack spacing, there can be argued that the linear concrete behaviour within this area is also taken into account. Though, this effect is negligible.

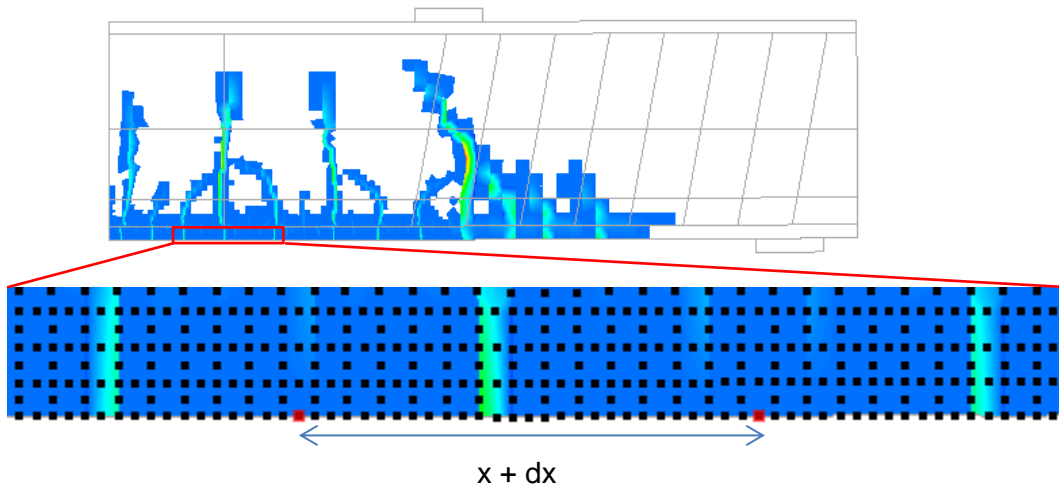


Figure 5-9; Check of crack widths (close view of bottom edge)

In the DIANA results there are seven cracks that can be clearly indicated, these are between the red indication lines in Figure 5-10. The distance between these lines is the crack spacing. So for the crack spacing and the crack width, the distance between red lines and difference in displacement in x-direction of the red lines are determined.

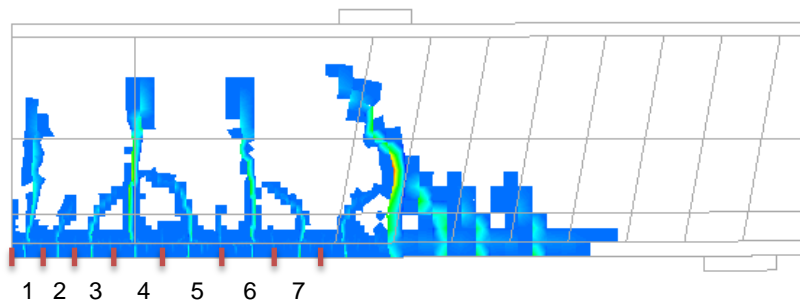


Figure 5-10; Crack width and crack spacing

In the experiment the crack width is analysed at every load stage. This has been done at several of heights, see Figure 5-11. The two measures closest to the outer fibre have been used for the comparison of the crack width, since the cracks at the surface are of interest.

An example of an overview of the experiment results is given in Figure 5-12; these are the results of loading stage three. The red indicated numbers are used in the comparison with the result of DIANA. The maximum crack width is used, since the small cracks, which have been taken into account in the mean of the experiment, are not visible in the DIANA results. Therefore it is expected that the crack widths of DIANA will be closer to the maximum crack width of the experiment.

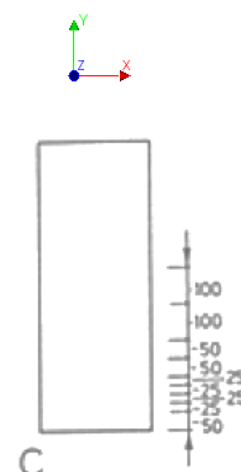


Figure 5-11; Measure heights of the crack widths

loading stage	line no.	$l_m$ [mm]	$w_{min}$ [mm]	$w_{max}$ [mm]	$w_m$ [mm]	c.v. [-]	$w_k$ [mm]	$w_k/w_m$ [-]	$w_{max}/w_m$ [-]	
3	1	52	88	0.01	0.22	0.103	0.51	0.19	1.83	2.14
	2	51	90	0.01	0.24	0.104	0.47	0.18	1.77	2.31
	3	47	98	0.01	0.23	0.117	0.44	0.20	1.73	1.97
	4	47	98	0.01	0.24	0.101	0.56	0.19	1.92	2.38
	5	49	94	0.01	0.25	0.089	0.67	0.19	2.10	2.82
	6	43	107	0.01	0.25	0.086	0.88	0.21	2.45	2.90
	7	25	184	0.01	0.31	0.126	0.75	0.28	2.24	2.45
	8	17	271	0.01	0.28	0.149	0.51	0.27	1.84	1.88
	9	16	288	0.01	0.16	0.083	0.49	0.15	1.80	1.94

Figure 5-12; Results of crack width experiment Braam

The results of the crack widths at the different loads are presented in Figure 5-13.

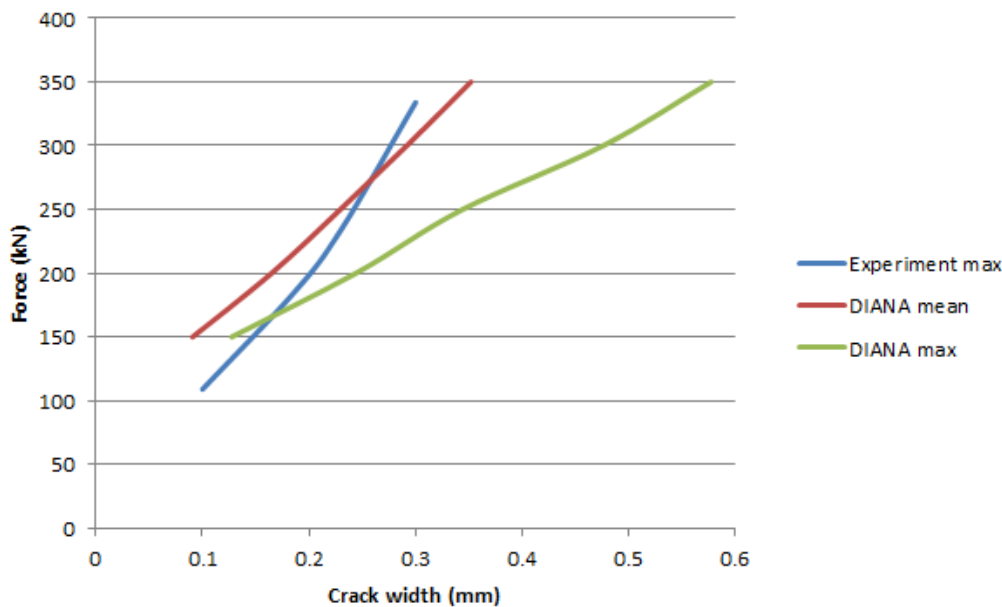


Figure 5-13; Crack width comparison experiment Braam

The DIANA result overestimates the crack width especially at higher loads. An explanation for this conclusion is that the small secondary cracks that appear around the bigger primary cracks in the experiments, do not appear in the DIANA results. Additionally, the differences in the crack widths of the DIANA results and the experiment results can be explained by the same reason there were differences in the force displacement comparison. Because of the tension softening the cracks appeared at a higher load than was seen in the experiments. Nevertheless, it can be concluded that the mean of the DIANA result is comparable with the maximum of the experiments; for 150 kN the difference between the crack widths is forty percent, for loads above 200 kN the difference between the crack widths is maximum fifteen percent. The fact that the crack widths in DIANA would be closer to the maximum crack width was expected, but that it would be comparable was not anticipated.

In Appendix C a more detailed review of the experiment Braam can be found. The other experiments are also checked in more detail, in a similar way as the more detailed version of the experiment of Braam.

## 5.3 Experiment E3

The parameters of the materials that are used in the experiment of E3 are given in the table below:

Name	Value
Young's modulus	22483 N/mm <sup>2</sup>
Tensile strength	2.26 N/mm <sup>2</sup>
Tensile fracture energy	0.1506 N/mm
Compressive strength	28,74 N/mm <sup>2</sup>
Compressive fracture energy	33.5 N/mm
Yield stress tensile reinforcement	433 N/mm <sup>2</sup>
Yield stress stirrups	465 N/mm <sup>2</sup>
Yield stress compressive reinforcement	430 N/mm <sup>2</sup>
Diameter first layer	18 mm
Diameter second layer	16 mm

Table 5-5; Parameters for the experiment of E3

### 5.3.1 Geometry

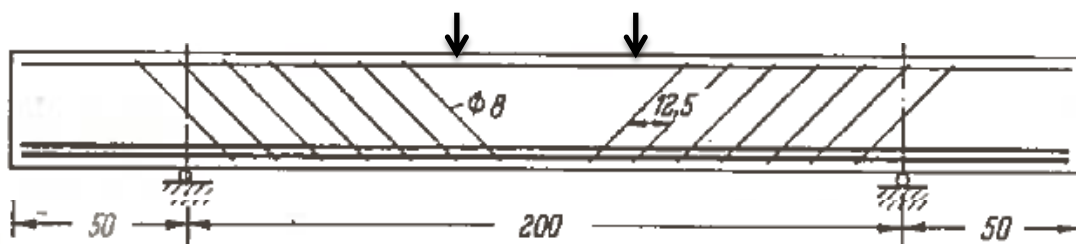


Figure 5-14; Geometry of the beam of experiment E3

The beam is 3 metres long, of which 2 metres between the supports. The distance between the support and the closest load point is 0,75 metres and the distance between the load points is 0,5 metres. There are seven stirrups used on both sides with each a distance between them of 0,125 metres.

The beam has a height of 0,32 metres and a width of 0,19 metres. The main tensile reinforcement consists of two bars with a diameter of 20 millimetres and three bars with a diameter of 16 millimetres. The stirrups have a diameter of 8 millimetres. The top reinforcement consists of 2 bars with a diameter of 10 millimetres.

The cover that is applied at the bottom part is 31 millimetres.

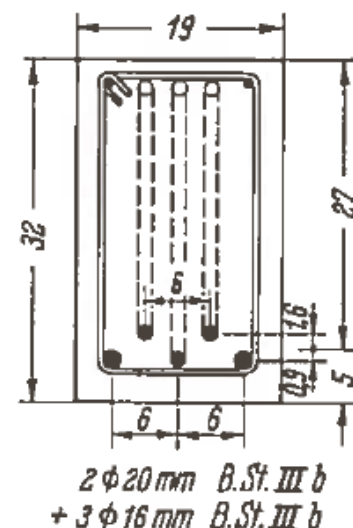


Figure 5-15; Cross-section of the beam of experiment E3



In DIANA only half of the beam is modelled, because the geometry of the beam and the loading is symmetric. The computing time is due to the smaller model significantly less. At half of the height a composed line is added, this line is not attributing to the strength of the structure, but gives some integrated results.

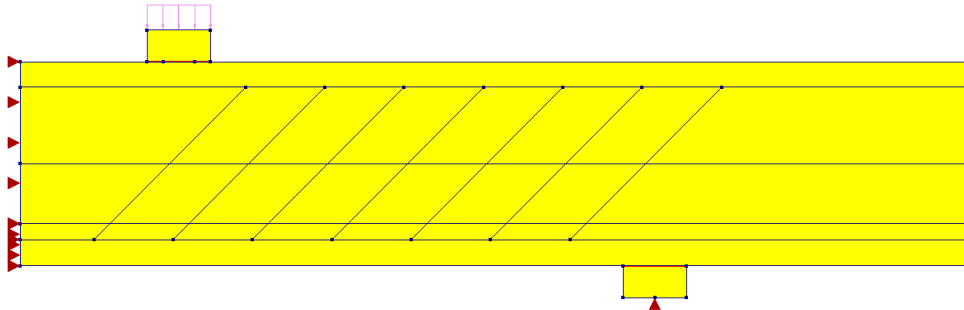


Figure 5-16; Geometry DIANA model experiment E3 half beam

This figure shows the concrete, the reinforcement and the load and support configuration. There are seven stirrups at an angle used between the load and support point.

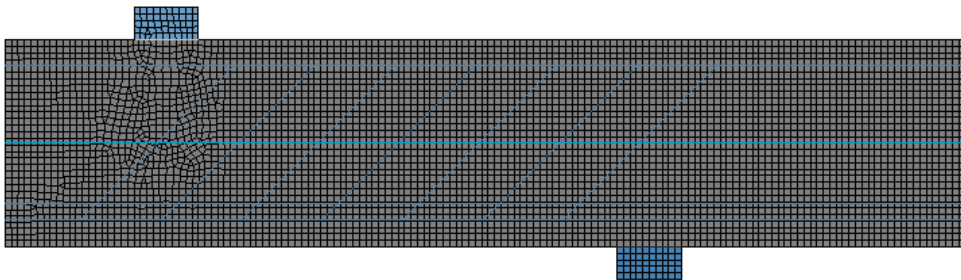


Figure 5-17; Mesh DIANA model experiment E3 half beam

For the mesh an element size of 10 millimetres is used.

In the DIANA model a small amount of hardening in the reinforcement is added, this has been done for improvement of the force displacement comparison after the yield stress is reached.

### 5.3.2 Force-Displacement

The force-displacement diagram of the experiment and the DIANA results are compared.

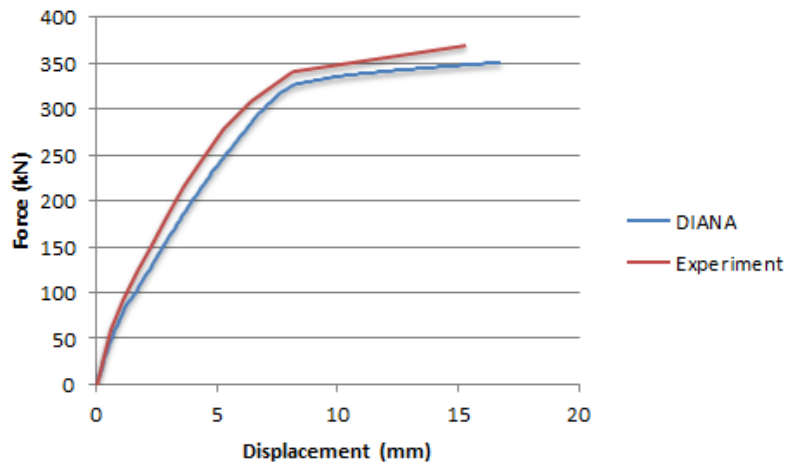


Figure 5-18; Force displacement diagram of Experiment E3 and DIANA results

In the force-displacement diagram, the DIANA results slightly underestimate the stiffness and strength. At an force of 250 kN the biggest difference between the displacements is found and is around twenty percent. Between the forces at which the reinforcement is starting to yield there is a difference of less than five percent.

### 5.3.3 Crack pattern

Next the crack pattern is compared. Of the experiment only the crack pattern at failure is known so this pattern will be compared with the crack pattern from DIANA. There are no cracks outside the supports; therefore it is left out in figures.

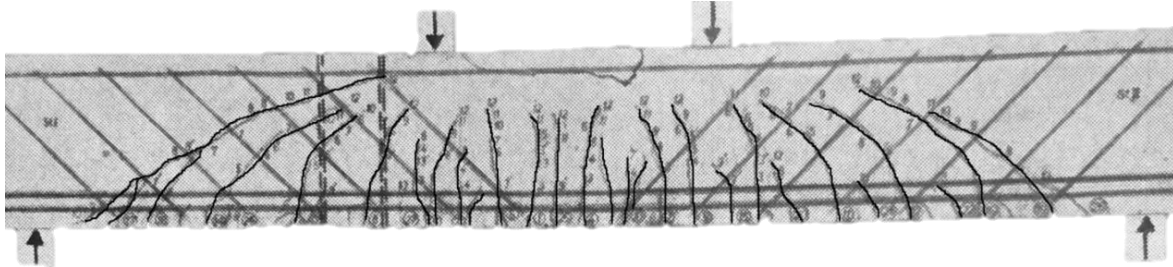


Figure 5-19; Failure crack pattern beam experiment E3

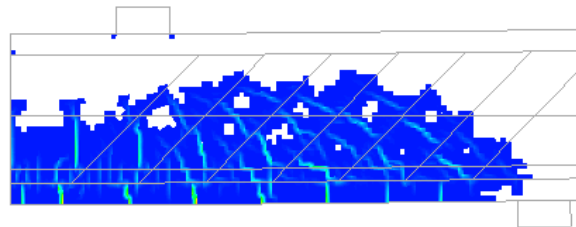


Figure 5-20; Failure crack pattern DIANA results E3

The crack patterns are quite similar, what is noticeable is that most of the cracks start at the tip of the stirrups in both the experiments as in the DIANA results. In the experiment there are some small cracks between the bigger cracks. These small cracks aren't visible in the crack pattern of the DIANA results. In the DIANA results of the experiment of Braam these smaller cracks weren't visible either.

### 5.3.4 Crack width

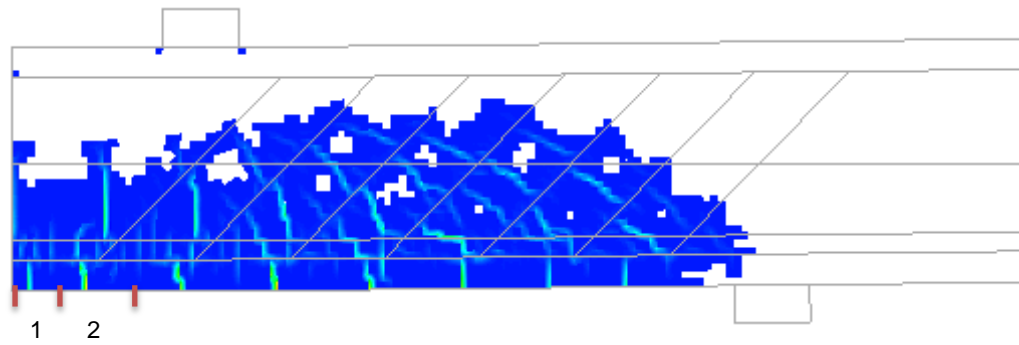


Figure 5-21; Crack width determination, failure crack pattern

The approach for determining the crack width that is used in the experiment of Braam, see chapter 5.2.4, is applied. There are only two cracks appearing in the area where there is a constant moment, see Figure 5-21. An extended version is made of the experiment to be able to examine more cracks and getting a better reading of the crack width, see Figure 5-22.

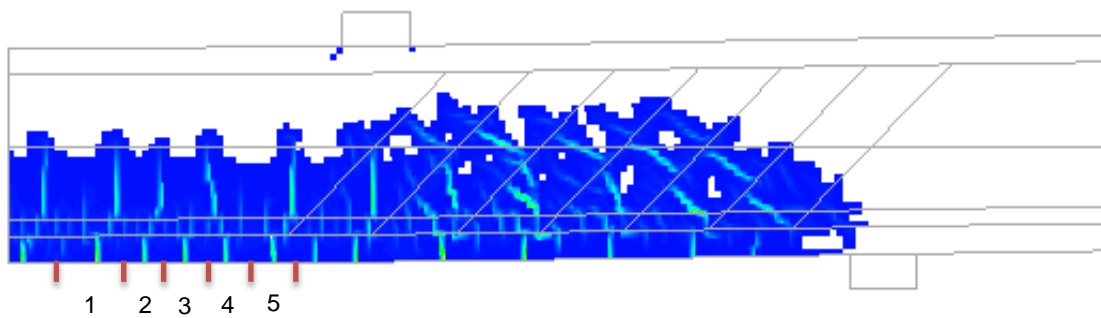


Figure 5-22; Extended version crack width determination, failure crack pattern

In the experiment the mean crack width and the maximum crack width with increasing load are given, see Figure 5-23.

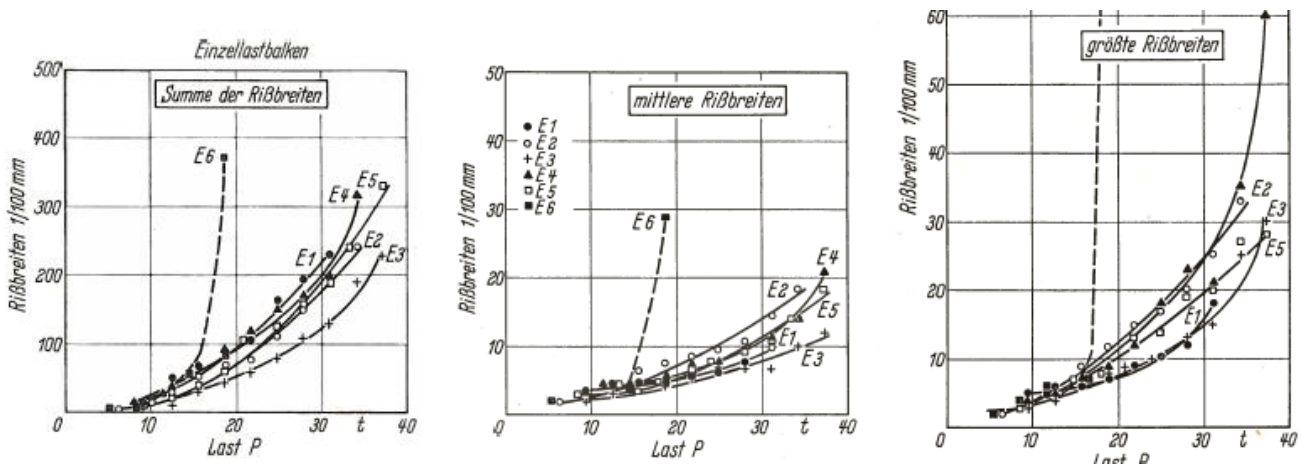


Figure 5-23; Crack widths experiment E3

The maximum crack width of the experiment and the mean and maximum value of the DIANA results are presented in Figure 5-24.

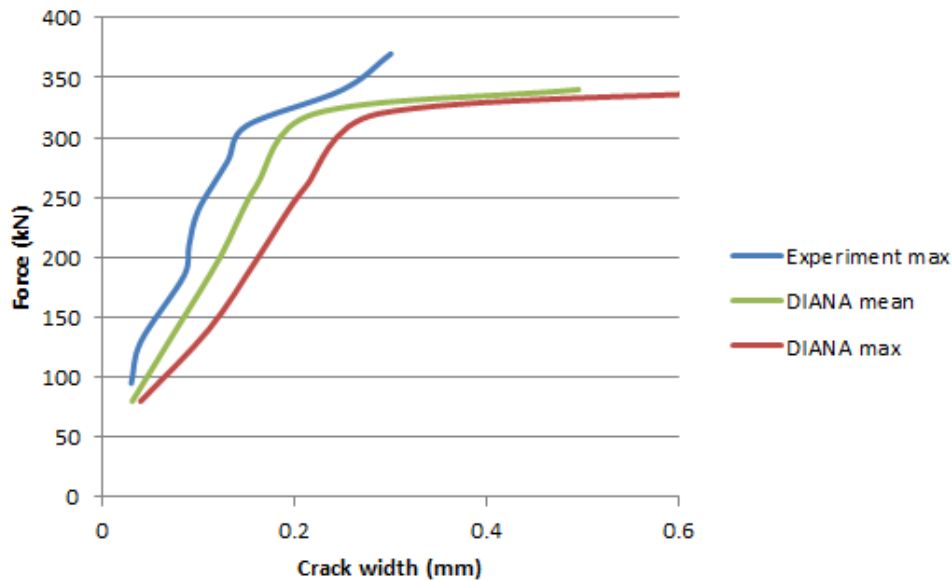


Figure 5-24; Crack width comparison experiment E3

It can be concluded that the cracks widths in DIANA are bigger than the maximal crack widths in the experiment. The mean crack width of the DIANA results is about forty percent higher than the maximum crack width of the experiment. The force displacement line was underestimating the stiffness and strength. This can be a reason for the fact that the crack widths are over estimated. The fact that the smaller cracks between the bigger cracks did not appear can also attribute to the outcome. Though, the mean of the DIANA model has a similar progression as the maximum of the experiment.

## 5.4 Experiment VS-C3

The parameters of the materials that are used in the experiment VS-C3 are given in the table below:

Name	Value
Young's modulus	34300 N/mm <sup>2</sup>
Tensile strength	3.13 N/mm <sup>2</sup>
Tensile fracture energy	0.1439 N/mm
Compressive strength	43.5 N/mm <sup>2</sup>
Compressive fracture energy	35.975 N/mm
Yield stress tension reinforcement M30	436 N/mm <sup>2</sup>
Yield stress tension reinforcement M25	445 N/mm <sup>2</sup>
Yield stress compression reinforcement	315 N/mm <sup>2</sup>
Yield stress stirrups	600 N/mm <sup>2</sup>
Diameter first layer	30 mm
Diameter second layer	25 mm

Table 5-6; Parameters for the experiment VS-C3

### 5.4.1 Geometry

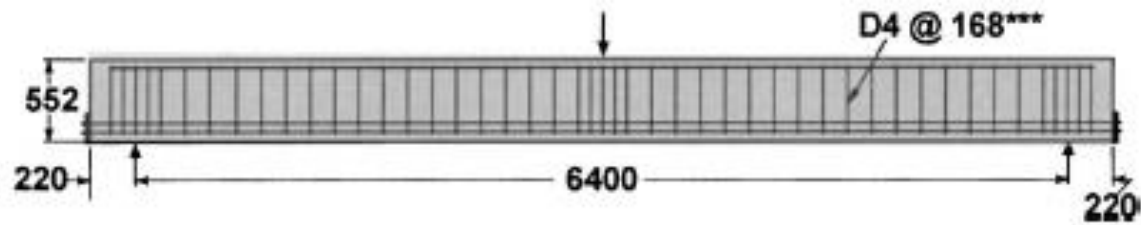


Figure 5-25; Geometry of the beam of the experiment VS-C3

The beam has a length of 6,84 metres, the distance between the centres of the supports is 6,4 metres. The load is located in the centre of the beam.

The height of the beam is 0,552 meters and the width is 0,155 meters.

The main reinforcement consists of four bars. The bottom two bars are M30 bars, which have a diameter of 29.9 millimetres. Above these two bars there are two M25 bars, which have a diameter of 25.2 millimetres. The reinforcement in the top of the beam, M10 bars, have a diameter of 11.3 millimetres. The stirrups are D4 bars, these have a diameter of 3.7 millimetres.

The cover is 49 millimetres

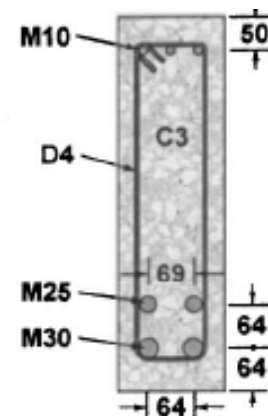


Figure 5-26; Cross-section of the experiment VS-C3

In DIANA only half of the beam is modelled, because the geometry of the beam and the loading is symmetric. The computing time is due to the smaller model significantly less. At half of the height a composed line is added, this line is not attributing to the strength of the structure, but gives some integrated results.

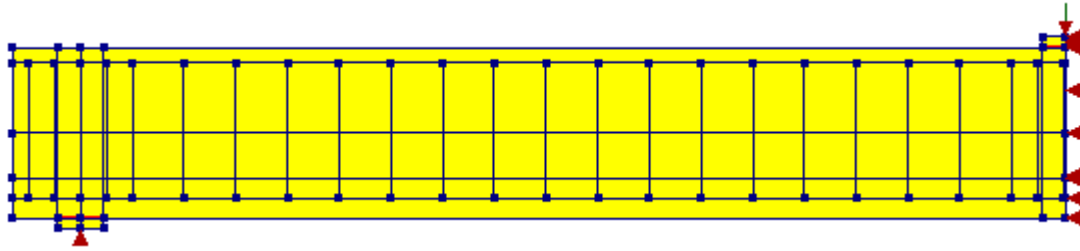


Figure 5-27; Geometry DIANA model experiment VS-C3

This figure shows the concrete, the reinforcement and the load and support configuration.

In Figure 5-28 the mesh is presented. For the mesh an element size of 25 mm is used. This element size is larger than that is applied (at the edge of the beam) in the other two experiments. Though, it turned out that this element size was sufficient for the verification of this experiment.

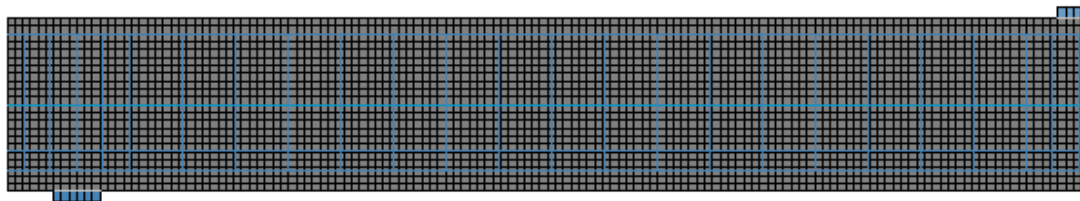


Figure 5-28; Mesh of the DIANA model of the experiment VS-C3

### 5.4.2 Force-Displacement

The force-displacement diagram of the experiment and the DIANA results are compared.

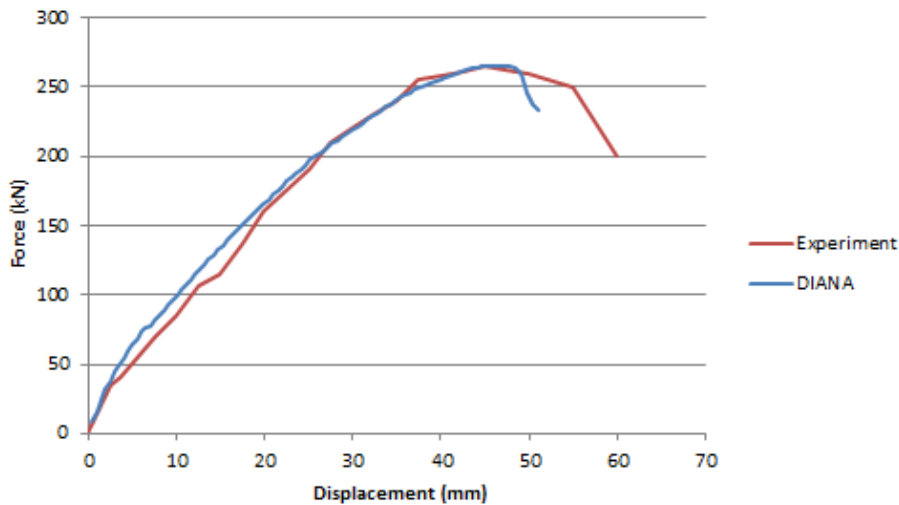


Figure 5-29; Force displacement diagram of with result of experiment VS-C3 and DIANA

The graphs are comparable, after the linear part the DIANA results somewhat over estimates the strength, but in the end the lines come together again. The same effect has been seen in the experiment of Braam, chapter 5.2.2. The difference between the force-displacement diagrams is in the lower range of the forces (100 kN) around fifteen percent, above the 150 kN the difference is less than five percent. Failure is in both the experiment and the DIANA results around 265 kN.



### 5.4.3 Crack pattern

The crack pattern that is known of this experiment is at failure, see Figure 5-30.

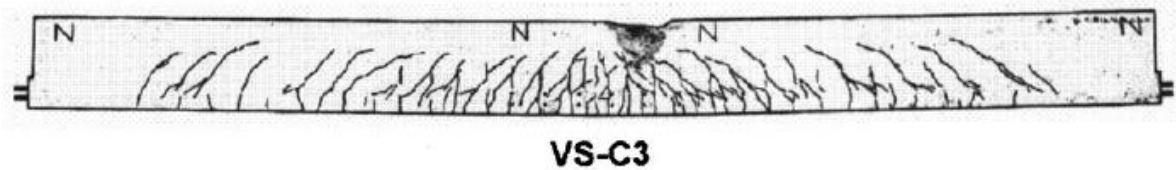


Figure 5-30; Crack pattern experiment VS-C3

The right part of the beam is compared with the result of the DIANA model, see Figure 5-31 and Figure 5-32.



Figure 5-31; Right part of the crack pattern of experiment VS-C3

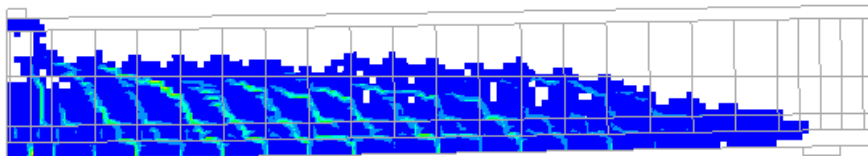


Figure 5-32; Crack pattern of the DIANA results

The crack patterns are similar, so the DIANA results gives a good approximation for the crack pattern.

### 5.4.4 Crack width

There is little information of the crack widths in the beam, only the maximum values for the crack width at failure. This is 0.9 millimetre in this experiment. The largest crack in the DIANA results is in the middle and is around 0.8 millimetre.

## 5.5 Conclusion

### 5.5.1 Force displacement

The force displacement diagrams of the DIANA results are quite similar to the results of the experiments.

In the experiment of Braam there is a deviation right after the concrete reaches its tensile strength, but overall the difference between the displacements is within 5 percent.

The differences in displacement between the results in the verification with experiment E3 are below the twenty percent. The difference in force at failure is below the five percent.

The differences seen in experiment VS-C3 are similar to the experiment of Braam. Directly after the tensile strength of the concrete is reached, the difference between the displacements is around fifteen percent. At higher loads the difference shrinks to a difference less than five percent. The failure loads are almost identical in the verification with experiment VS-C3.

Therefore the global behaviour of the DIANA model appears to be acting properly.

### 5.5.2 Crack pattern

The crack patterns are also quite comparable. The primary cracks are showing similar patterns. Though, the smaller secondary cracks that appear in the experiments are not always visible in the DIANA results. For example the crack patterns in experiment E3; the cracks appear at the tip of the stirrups in both the experiment results and DIANA results, but in the experiment there are also cracks between these cracks and in the DIANA they are not.

### 5.5.3 Crack width

The total amount of cracks is larger in the experiments, because of the fact that there are more secondary cracks. This results in a lower mean value of the crack width for the experiments. The maximum value of the experiment is therefore used for the comparison with the DIANA results. It seemed that the values of the DIANA results were higher, when the maximum values of the experiments are compared with the maximum values of the DIANA results. The difference between them runs up to a factor of two. So the DIANA model overestimates the crack width. The difference between the mean value of the DIANA results and the maximum value of the experiments are more comparable. Though, there are still differences that are around forty percent. In experiment E3 the DIANA values were higher, in the experiment of Braam the two trends run through each other. Eventually the mean crack width of the DIANA will be used for the comparison with the Eurocode 2, since the mean crack width is closer to the maximum crack width of the experiment results. And when a relatively high reinforcement stress (high load) is used the mean crack widths of the DIANA model are higher than the maximum crack width of the experiments (see Figure 5-13 above 300 kN and Figure 5-23). It could be stated that the Eurocode 2 is conservative, when the Eurocode 2 result is higher than the DIANA result. Because in DIANA calculated values are higher than the values of the experiments, when a relatively high reinforcement stress is used.

## 6 Influence height on crack width

In this chapter the influence of the height and other parameters on the crack width in DIANA will be investigated. First the inputs for the DIANA calculations are discussed. Thereafter the influences of the different parameters are evaluated.

### 6.1 DIANA input

Eventually the DIANA results will be compared with the Eurocode 2. Therefore the same approach as have been used in the Eurocode 2 calculations will be used in the DIANA calculations. The reason for using this approach and how the results are presented are explained in chapter 3.1.

To be able to specify what the influence is of the height and what the influence is of other factors, the influence of the height independent parameters of the Eurocode 2 are also analysed. These parameters are:

- Cover;
- Reinforcement percentage;
- Concrete tensile strength;
- Reinforcement stress.

The heights that are investigated are from 300 millimetres till 1900 millimetres. Values used for the cover are 20, 50, 70 and 100 millimetres. For the reinforcement percentage values of 0.5%, 1% and 1.5% are applied. The concrete strength values are 2 N/mm<sup>2</sup>, 3 N/mm<sup>2</sup> and 4 N/mm<sup>2</sup>. And the stress in the reinforcement will be reviewed from 0 N/mm<sup>2</sup> until 400 N/mm<sup>2</sup>.

For the determination of the crack width, cracks are needed. In DIANA these are simulated in a comparable beam model as is used in the verification of the experiment of Braam, chapter 5.2.1. A standard configuration for the beam is made. The dimensions are a factor of the height. So for every height the beam geometry is the same, except the scaling. The reason for this approach is a proper introduction of the moment. The geometry of the standard beam is as presented in Figure 6-1.

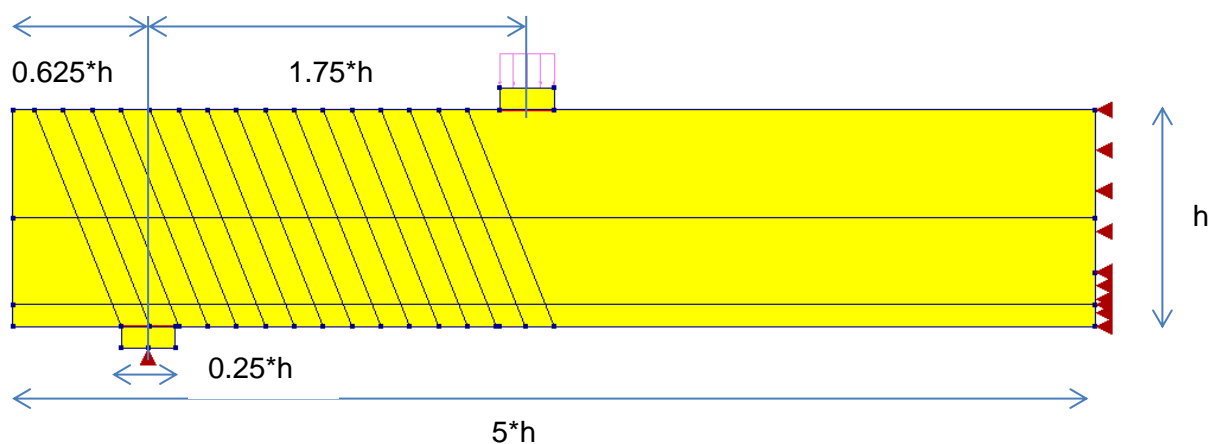


Figure 6-1; Geometry standard beam

Symmetry is used in these models, since half of the beam is modelled. This is applied for decreasing the calculation time.

The model is meshed, see Figure 6-2.

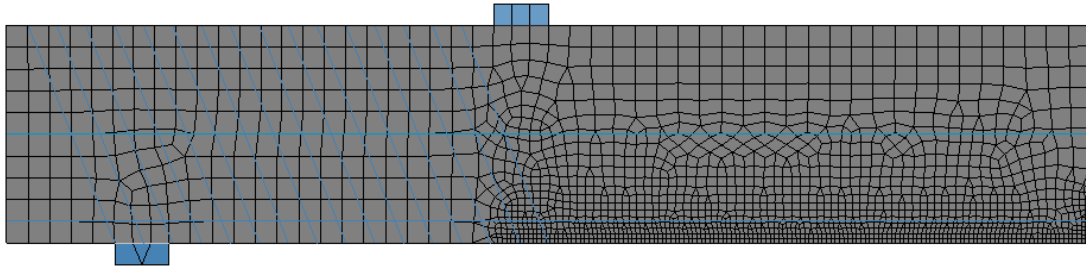


Figure 6-2; Mesh standard beam

The general mesh is dependent of the height ( $0.1 \cdot \text{height}$ ). In the area in which the cracks of interest are formed, the bottom at the right side of the load, a mesh with an element size of 10 mm is applied. The size is so small, because the cracks than localize well in one integration point. This approach of meshing has also been applied in the validation of the experiment of Braam, chapter 5.2.1.

The dimensions of the cross section used in the analytical calculation, chapter 3.2, also have been used for the numerical one.

Height (mm)	Width (mm)	$A_c$ (mm <sup>2</sup> )	$A_{s1\%}$ (mm <sup>2</sup> )	$n_b$	$\emptyset$ (mm)	$A_{s, \text{applied}}$ (mm <sup>2</sup> )	%
300	120	36000	360	2	16	402	1.12
500	200	100000	1000	2	25	981	0.98
700	280	196000	1960	4	25	1963	1.00
900	360	324000	3240	5	30	3534	1.09
1100	440	484000	4840	5	35	4810	0.99
1300	520	676000	6760	7	35	6734	0.99
1500	600	900000	9000	7	40	8796	0.97
1700	680	1156000	11560	9	40	11309	0.98
1900	760	1444000	14440	11	40	13823	0.96

Table 6-1; Steel area applied for one percent reinforcement

For the input of the reinforcement a bar diameter, steel area and perimeter is needed. The perimeter is calculated by the perimeter of one bar and that multiplied with the total of bars. Next the capacity of the force is needed. With the values of Table 6-1 a good estimation can be made of the capacity of the beam. Given that it won't fail on compression.

The estimation is:

$$\text{Moment capacity} = M_r = 0.9 \cdot (h - c) \cdot \sigma_s \cdot A_s$$

6-1

If the moment capacity is divided by the distance between the load and support point the maximum force can be calculated, this distance is dependent on the height.

$$\text{Force capacity} = \frac{M_r}{h * 1.75}$$

6-2

The force capacity is used as an indication for the load that is applied on the beam. The steps in DIANA are taken such that the total load factor is above the 1.0. This should cause the beam to fail, in this way there is checked whether the beam reacts as expected.

The input for every height is given in Table 6-2.

Height (mm)	Width (mm)	$A_c$ (mm <sup>2</sup> )	$A_{s1\%}$ (mm <sup>2</sup> )	$n_b$	$\emptyset$ (mm)	$A_{s,applied}$ (mm <sup>2</sup> )	Perimeter (mm)	Force capacity (kN)
300	120	36000	360	2	16	402.1	100.5	86.2
500	200	100000	1000	2	25	981.8	157.1	227.2
700	280	196000	1960	4	25	1963.4	314.1	468.8
900	360	324000	3240	5	30	3534.2	471.2	858.3
1100	440	484000	4840	5	35	4810.6	549.8	1180.8
1300	520	676000	6760	7	35	6734.8	769.7	1665.2
1500	600	900000	9000	7	40	8796.4	879.6	2186.5
1700	680	1156000	11560	9	40	11309.7	1131.0	2822.7
1900	760	1444000	14440	11	40	13823.0	1382.3	3461.0

Table 6-2; Input parameters for the different heights

The configuration of the cross section is different for the reinforcement percentages of 0,7% and 1.5%. These are presented in Table 6-3 and Table 6-4.

Height (mm)	Width (mm)	$A_c$ (mm <sup>2</sup> )	$A_{s0.7\%}$ (mm <sup>2</sup> )	$n_b$	$\emptyset$ (mm)	$A_{s,applied}$ (mm <sup>2</sup> )	Perimeter (mm)	Force capacity (kN)
300	120	36000	252	2	12	226	75	49
500	200	100000	700	4	16	804	201	186
700	280	196000	1372	3	25	1473	236	352
900	360	324000	2268	3	30	2121	283	515
1100	440	484000	3388	5	30	3534	471	868
1300	520	676000	4732	5	35	4811	550	1190
1500	600	900000	6300	7	35	6735	770	1674
1700	680	1156000	8092	8	35	7697	880	1921
1900	760	1444000	10108	8	40	10053	1005	2517

Table 6-3; Input parameters for 0.7 % reinforcement percentage

Height (mm)	Width (mm)	$A_c$ (mm <sup>2</sup> )	$A_{s1.5\%}$ (mm <sup>2</sup> )	$n_b$	$\emptyset$ (mm)	$A_{s,applied}$ (mm <sup>2</sup> )	Perimeter (mm)	Force capacity (kN)
300	120	36000	540	3	16	603	151	129
500	200	100000	1500	3	25	1473	236	341
700	280	196000	2940	4	30	2827	377	675
900	360	324000	4860	7	30	4948	660	1202
1100	440	484000	7260	6	40	7540	754	1851
1300	520	676000	10140	8	40	10053	1005	2486
1500	600	900000	13500	11	40	13823	1382	3436
1700	680	1156000	17340	14	40	17593	1759	4391
1900	760	1444000	21660	17	40	21363	2136	5349

Table 6-4; Input parameters for 1.5% reinforcement percentage

Python is the underlying code of DIANA. Since there are a lot of variations in the models a python script is made. In this script a loop is made which runs the code to build and calculate the DIANA model with the different parameters. An example of this python script can be found in appendix D.

The mean value of the crack widths is used to present the DIANA results. Since in the Eurocode 2 a maximum value is calculated for the crack width, and the mean value of the DIANA results was in range of the maximum results of the experiments. The values of results are sometimes fluctuating with increasing height. These fluctuations are caused by the number of small cracks that appear in the DIANA model. Small cracks have an impact on the mean value, because they lower the mean value. When there is a difference in the number of small cracks the mean value is influenced.

## 6.2 Influence cover

First the influence of the cover is analysed with DIANA. This is done with the covers 20 mm, 50 mm, 70 mm and 100 mm.

The influence of increasing cover on the crack width is presented in Figure 6-3.

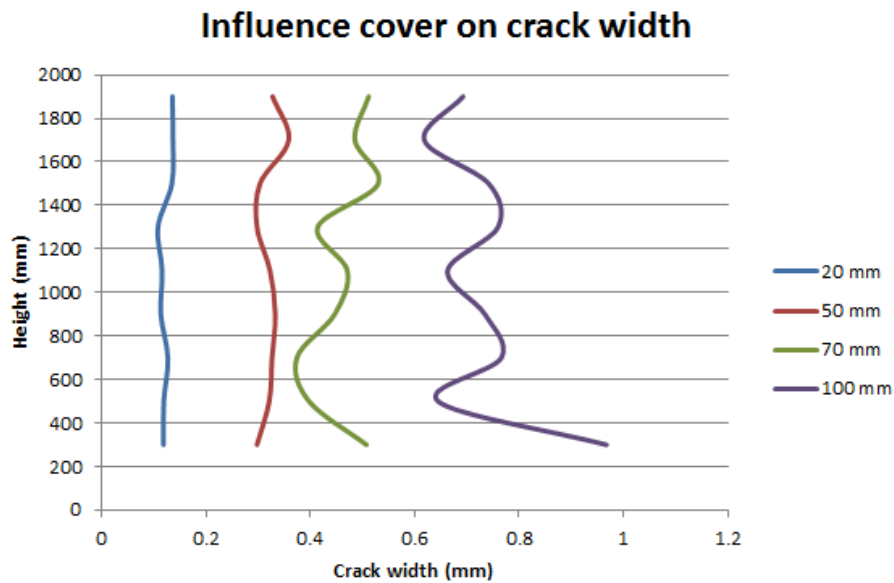


Figure 6-3; Influence of cover on crack width

With increasing height the crack width stays relatively similar. The results of the 70 and 100 millimetres show fluctuating crack widths at increasing height. This can be the result of the fact that there are sometimes small cracks (0.1-0.2 mm) appearing in these models, which combined with the lower amount of cracks results in a mean that fluctuates more. A high cover height ratio (height of 300 millimetres and cover of 100 millimetres) also causes problems, but these are not realistic and therefore not of interest.

The mean crack width over height is determined for every cover. With these values a graph can be made of the influence of cover on the crack width, see Figure 6-4.

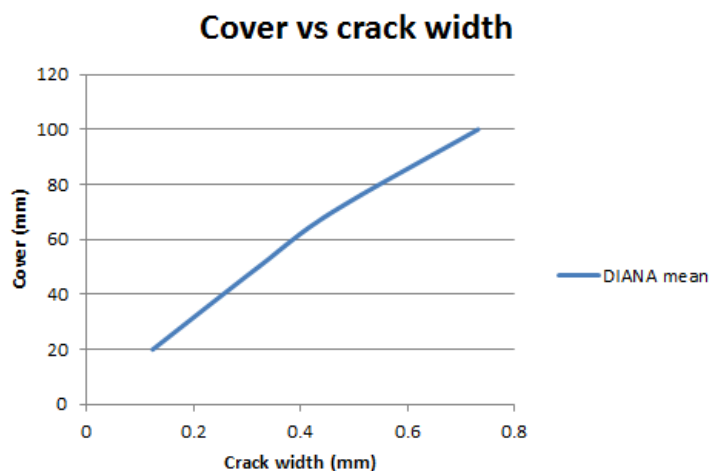


Figure 6-4; Cover over crack width

When the cover increases the crack width also increases. This process has a linear trend.

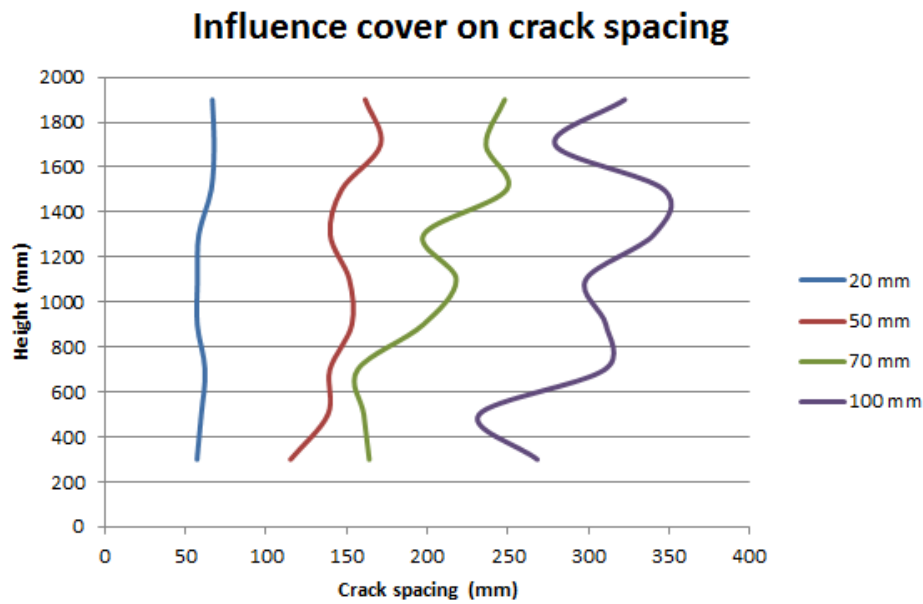


Figure 6-5; Influence of cover on crack spacing

In the crack spacing graph, see Figure 6-5, the construction height has not a significant impact on the crack spacing. The influence of the cover on the crack spacing is substantial. A large increase of crack spacing with increasing cover can be concluded out of Figure 6-5.

The mean crack spacing over height is determined for every cover. This is done to see what the result is on the crack spacing if the cover changes, see Figure 6-6. The line seems to be linear increasing.

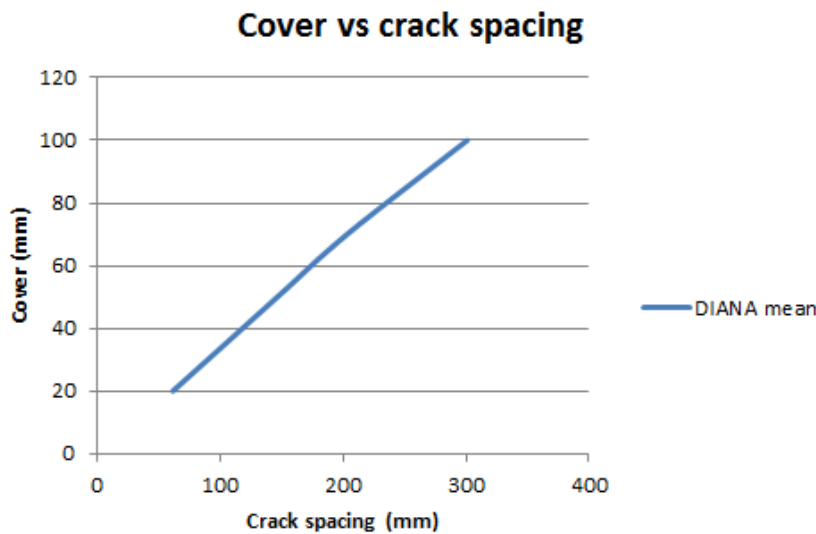


Figure 6-6; Cover over crack spacing

A reason for this influence of the cover on the crack spacing is that the concrete has more area in tension with larger covers. When a crack has appeared all the tensile force in the crack is in the reinforcement. Due to the bonding between the reinforcement and concrete the stress in the concrete is slowly increasing with increasing distance of the crack. A larger area in tension results into more tensile resistance of the concrete, which means that the bonding between the reinforcement and concrete needs a longer distance to transfer the required stress for a new crack to appear in the concrete



The graph of the influence of the cover on the crack strain is given in Figure 6-7.

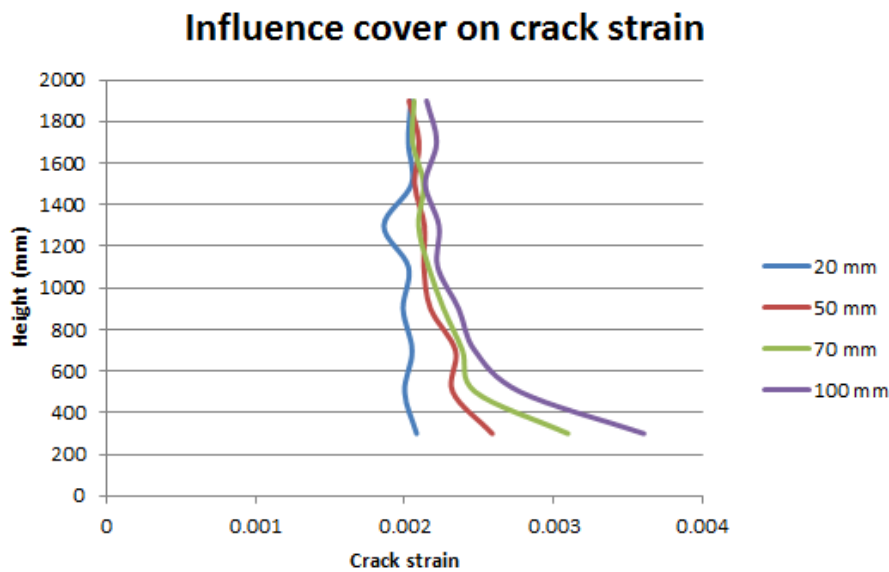


Figure 6-7; Influence of cover on cracks strain

The construction height has an effect in the lower range of heights. There is a significant decrease of strain with increasing height when large covers are applied. This effect is the result of a bending moment load. The crack strain is dependent on the strain of the reinforcement, when the cover changes the strain of the reinforcement is almost unaffected. But because of the cover and the rotation in the structure the strain at outer fibre is larger than at reinforcement height. The crack strain at outer fibre is therefore dependent on the height-cover ratio.

This effect of the rotation and therefore the bending moment load is also visible in a single crack, see Figure 6-8. The crack width reduces with decreasing distance to the reinforcement, see Table 6-5.

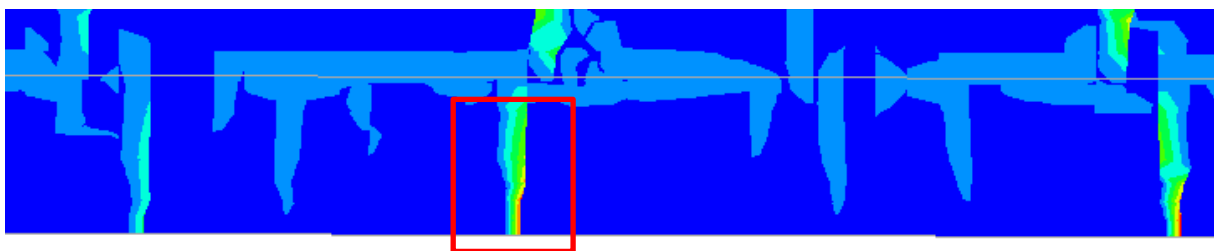


Figure 6-8; Single crack DIANA model, height 900 mm, cover 100 mm

Distance to reinforcement	Crack width
100	0.75
90	0.7
78	0.65
66	0.6
54	0.54
38	0.47

Table 6-5; Crack width with distance to reinforcement

### 6.3 Influence reinforcement percentage

After the cover the influence of the reinforcement percentage will be investigated. The values 0.7%, 1% and 1.5% are used in this investigation.

The influence of increasing reinforcement percentage is presented in Figure 6-9.

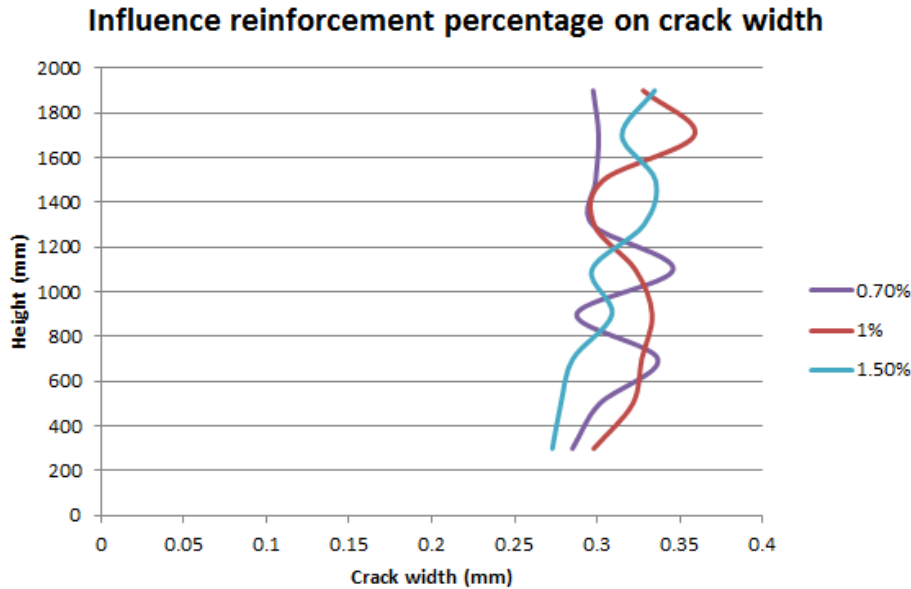


Figure 6-9; Influence reinforcement percentage on crack width

The results give no clear indication of an increase or decrease of the crack width with increasing reinforcement percentage, since with increasing height the lines cross each other multiple times.

The same trend is visible in the crack spacing graph, Figure 6-10, as was in the crack width graph.

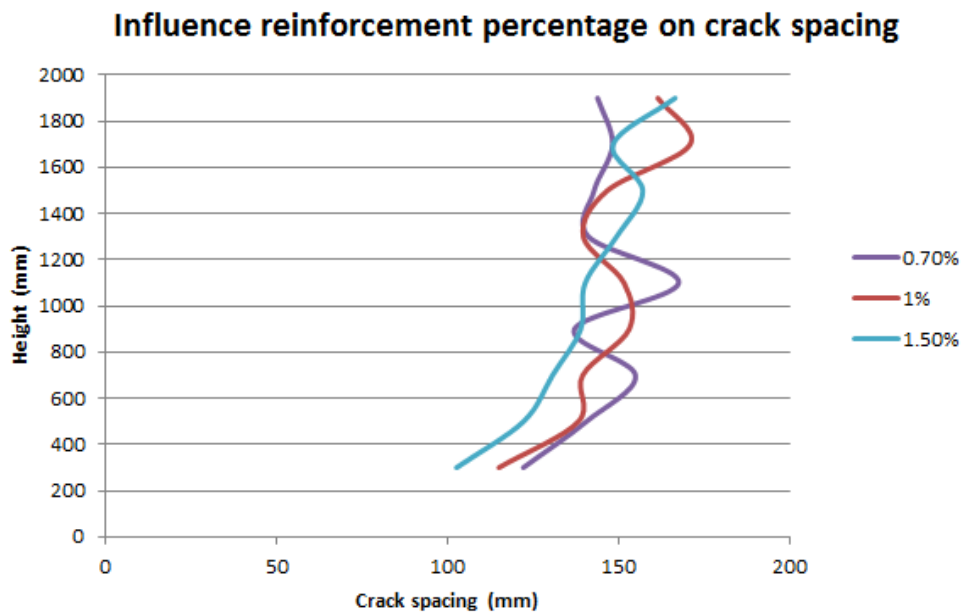


Figure 6-10; Influence reinforcement percentage on crack spacing

Since the reinforcement percentage also has an influence on the crack strain in the Eurocode 2 calculations; this is also investigated. The crack strain is calculated by deviding the crack widths with the crack spacing. Figure 6-11 shows the results.

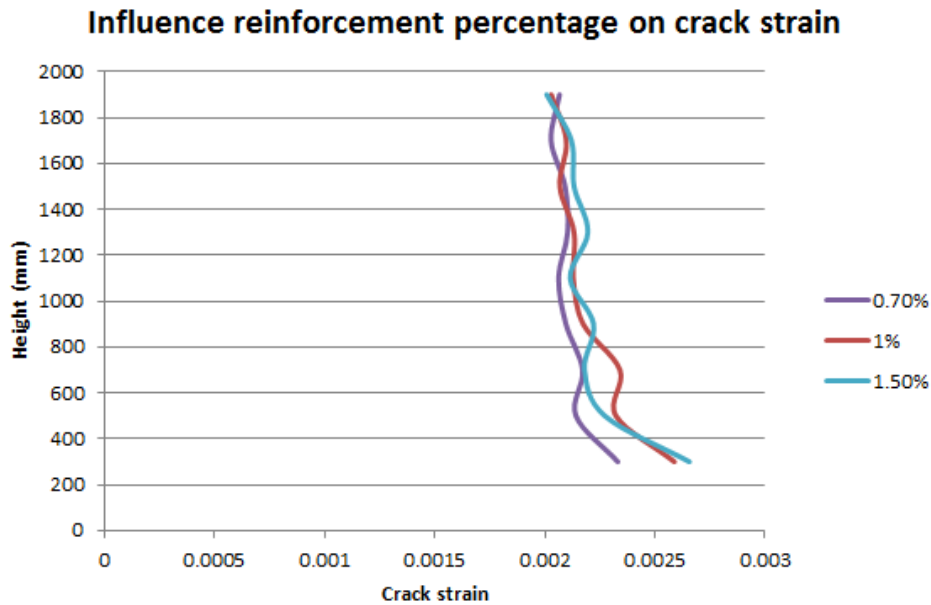


Figure 6-11; Influence reinforcement percentage on strain

The differences between the crack strains are so small that the effect is negligible. So the reinforcement percentage has no significant influence on the crack strain.

## 6.4 Influence concrete tensile strength

Next the influence of the tensile strength of concrete is checked. This is done with the values of 2, 3 and 4 N/mm<sup>2</sup>. The result of the influence on the crack width can be found in Figure 6-12.

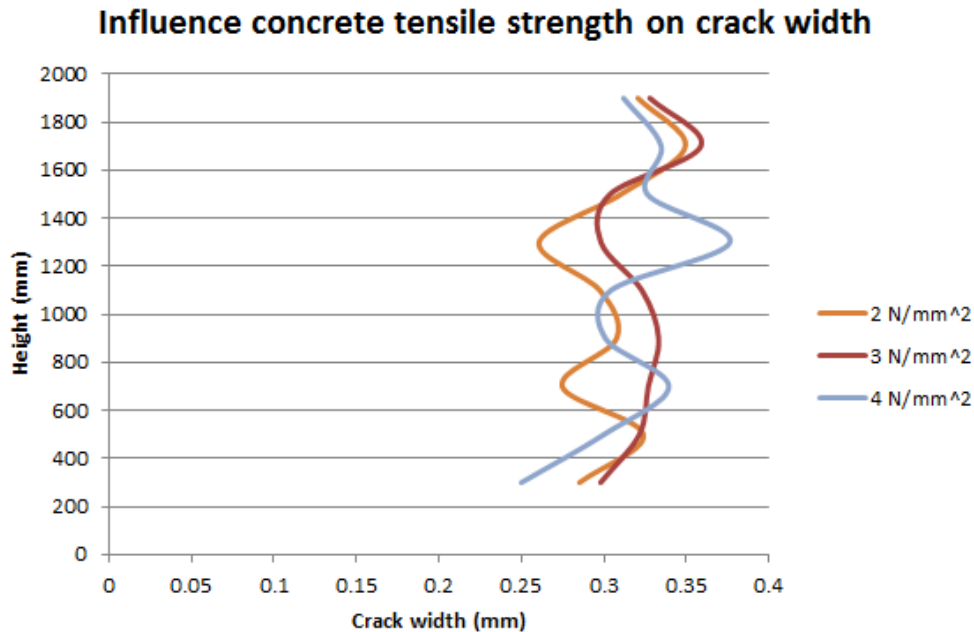


Figure 6-12; Influence concrete tensile strength on crack width

The influence of the concrete tensile strength on the crack width is hard to define, since the graphs overlap each other. So there is no clear trend to discover.

The crack spacing is presented in Figure 6-13, also here there is no logical sequence to discover.

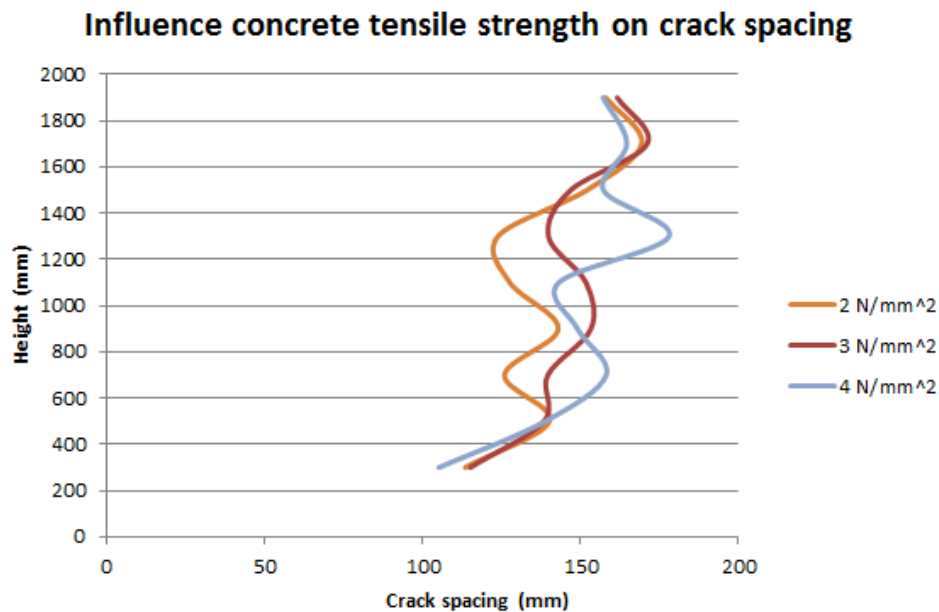


Figure 6-13; Influence concrete tensile strength on crack spacing

Since the concrete tensile strength is in the crack strain term in the Eurocode 2; the crack strain is also calculated and presented in Figure 6-14. This crack strain is calculated by dividing the crack width by the crack spacing.

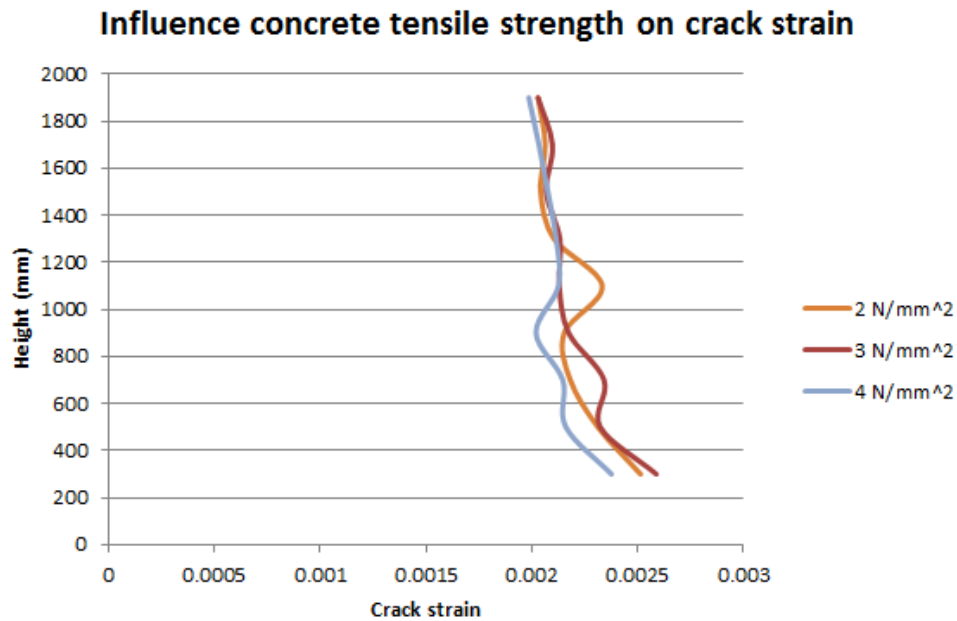


Figure 6-14; Influence concrete tensile strength on crack strain

Here can be concluded that the strain does almost not change with changing concrete tensile strength and construction height.

## 6.5 Influence reinforcement stress

Last the reinforcement steel stress in treated. The values that are used to determine the influence of the reinforcement stress are 100 N/mm<sup>2</sup>, 200 N/mm<sup>2</sup>, 300 N/mm<sup>2</sup> and 400 N/mm<sup>2</sup>. The results are given in Figure 6-15.

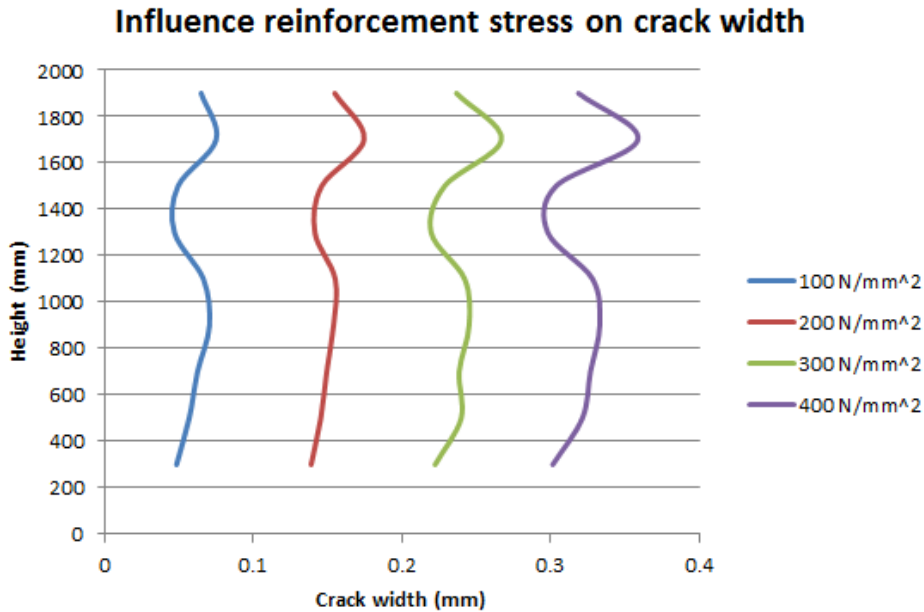


Figure 6-15; Influence reinforcement stress on crack width

It can be concluded that the reinforcement stress has a significant influence on the crack width. The amount of increase of crack width with increasing stress is in Figure 6-16 visualized.

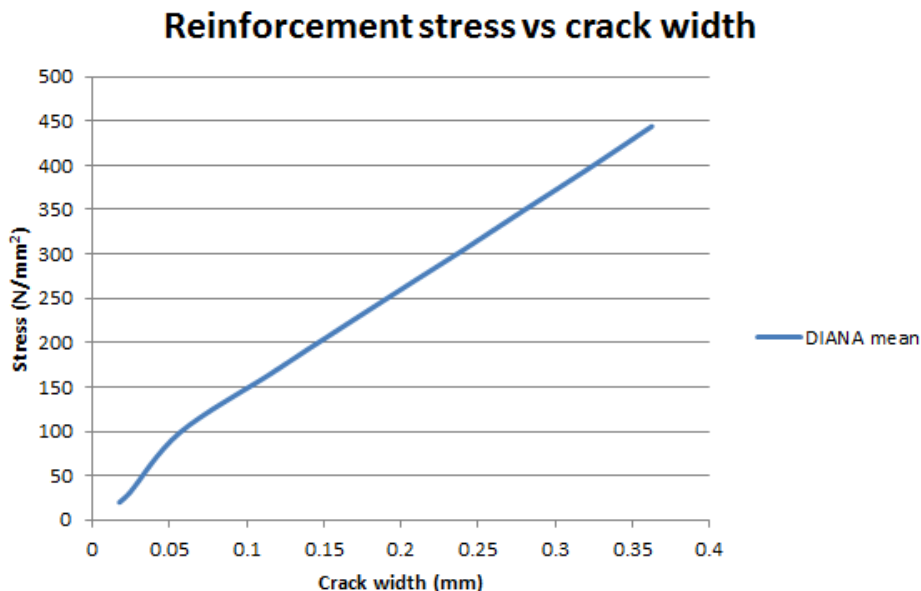


Figure 6-16; Reinforcement stress over crack width

It is not a completely linear line, but after a stress of 100 N/mm<sup>2</sup> it becomes linear. This behaviour was expected.

The reinforcement steel stress is a factor in the crack strain term in the Eurocode 2 and therefore the influence of the reinforcement stress on the crack strain is analysed. The crack width is divided by the crack spacing (Figure 6-5, cover of 50 mm) to obtain the crack strain. In Figure 6-17 the results are shown.

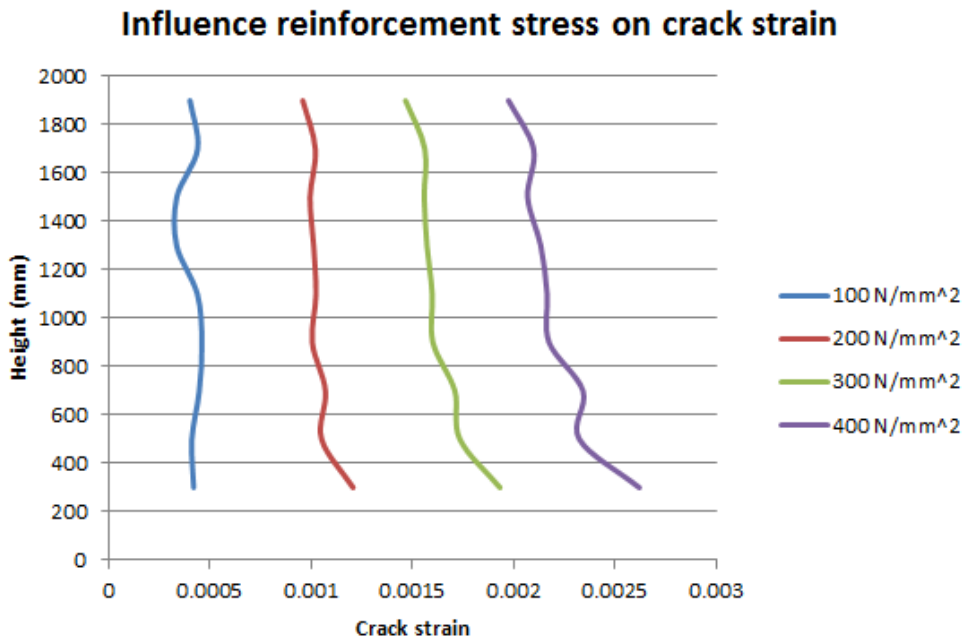


Figure 6-17; Influence reinforcement stress on crack strain

The strain clearly increases with increasing reinforcement stress, see Figure 6-18. The trend of the increase is about the same as the trend of the crack width.

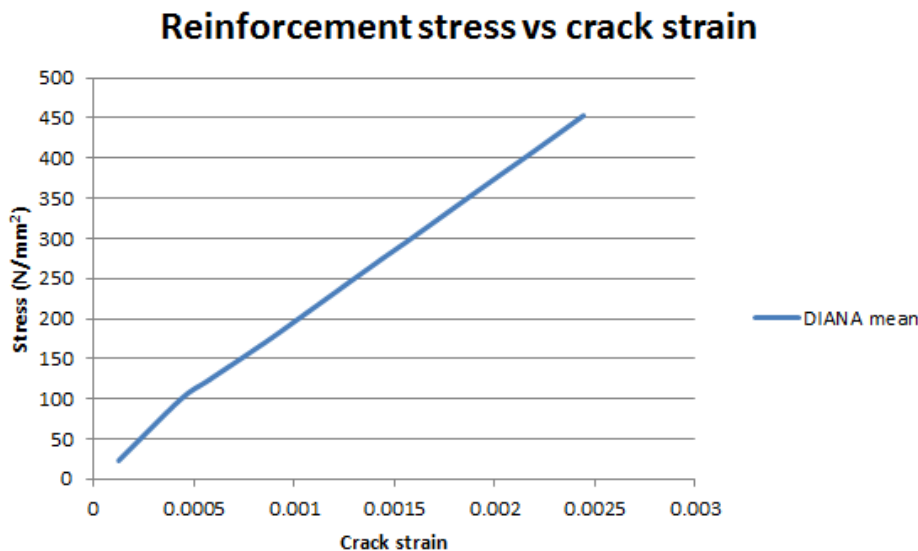


Figure 6-18; Reinforcement stress over crack strain

It is quite trivial that the crack strain, which is dependent on the strain of the reinforcement, is increasing with increasing reinforcement stress.

## 6.6 Conclusions

### 6.6.1 Cover

The cover has quite a significant influence on the crack width; this is dominantly seen in the crack spacing term. The crack strain is also influence by the cover; this effect was caused by the rotation in the structure which is the result of the bending moment load.

### 6.6.2 Reinforcement percentage

The influence of the reinforcement percentage seemed to be small; no substantial influence could be detected in the crack width, the crack spacing and the crack strain.

### 6.6.3 Concrete tensile strength

The DIANA model reacts about the same on the influence of the concrete tensile strength as it did on the reinforcement percentage, so there is no significant influence.

### 6.6.4 Reinforcement stress

The reinforcement steel stress has a great impact on the crack width; there is a strong increase of crack width with increasing reinforcement stress. Since the crack spacing does not change, the increase of crack strain is relatively the same as the crack width.

### 6.6.5 General conclusion

All together most important factors are the cover and reinforcement steel stress in the DIANA results. The cover has a great impact on the crack spacing and the reinforcement stress is important for the crack strain. The influence of the height has been limited in the DIANA results. Only in the analysis of the influence of the cover a significant change in crack strain has been seen due to the construction height, especially when a large cover is applied. This effect is the result of the rotation in the structure that is caused by the bending moment.



# III Comparison, Conclusions and Recommendations

In this section a comparison between the analytical and numerical calculation will be carried out. And eventually the conclusions and recommendations will be given.

## 7 Comparison Analytical and Numerical

In this chapter the results that have been found in the analytical calculations and the numerical calculations will be compared. This includes the influences of height and the influence of the height independent parameters in the Eurocode 2 calculation.

The comparison will be between the mean of the DIANA results and the Eurocode 2 results. Since in the Eurocode 2 a maximum value is calculated for the crack width, and the mean value of the DIANA results was in range of the maximum results of the experiments.

## 7.1 Influence cover

First the influence of the cover is compared; the Eurocode 2 and the DIANA crack width results are shown in Figure 7-1.

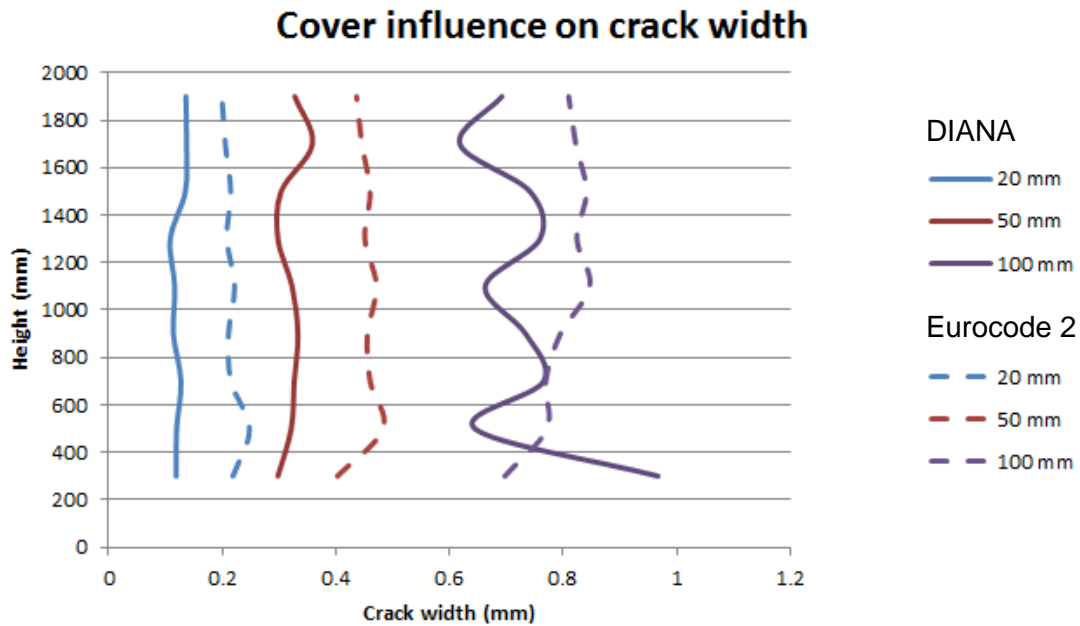


Figure 7-1; Influence cover on crack width

There can be concluded that the cover in both the Eurocode 2 and the DIANA model has a significant influence on the crack width. When the Eurocode 2 and the DIANA results are compared it is clear that the Eurocode 2 has larger crack widths than the DIANA results. With increasing construction height no important differences are visible.

The cover over crack width graphs (Figure 3-7 and Figure 6-4) are combined and presented in Figure 7-2.

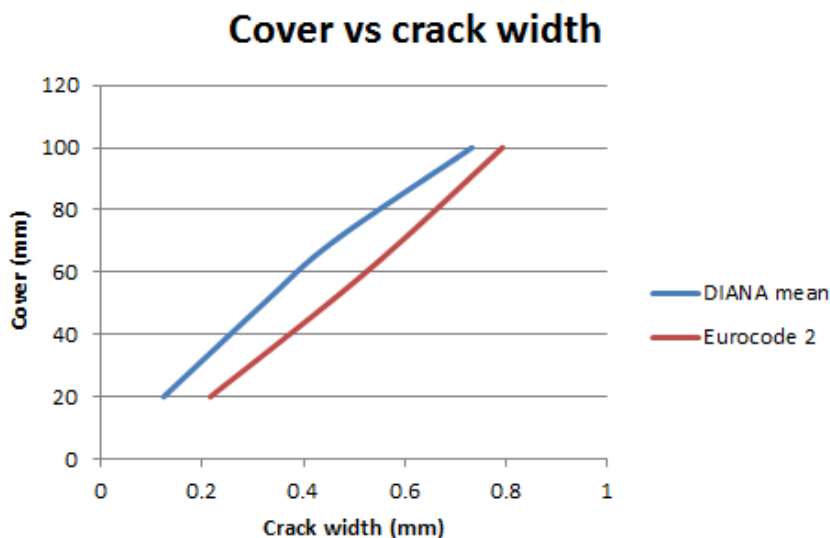


Figure 7-2; Comparison cover over crack width

There is a shift visible in the graph; the crack width calculated in the Eurocode 2 is around 0.1 millimetres bigger for every cover.

Next to the crack width, the crack spacing is investigated for the cover term. The results of the Eurocode 2 and the DIANA model can be found in Figure 7-3.

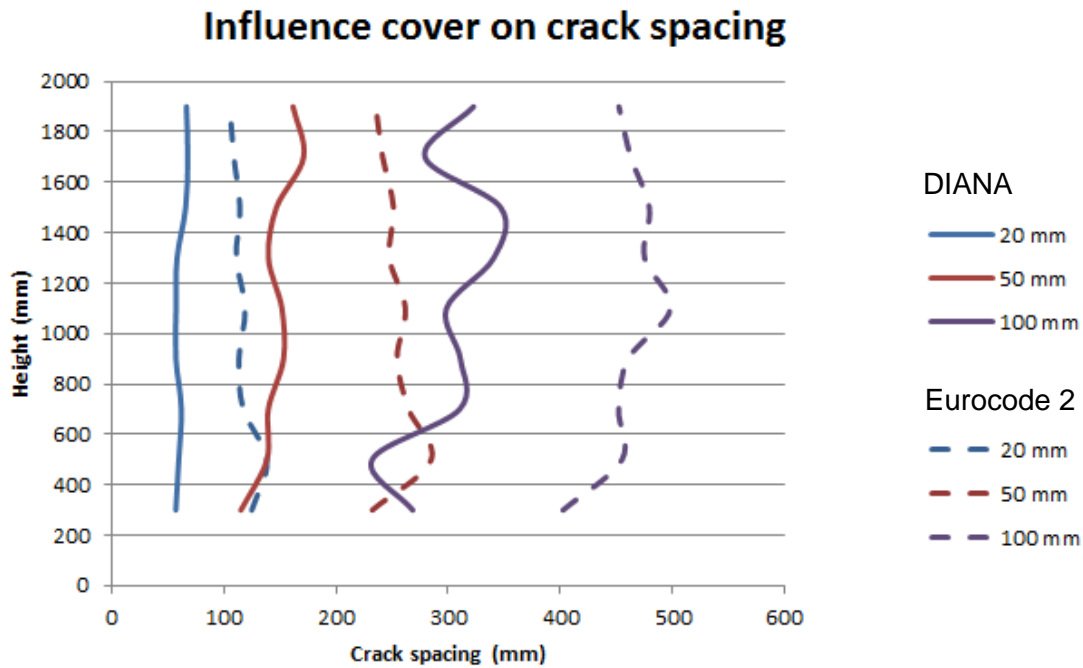


Figure 7-3; Influence cover on crack spacing

In the graph there is a clear increase of crack spacing with increasing cover noticeable. When the Eurocode 2 and the DIANA results are compared the crack spacing is larger in the Eurocode 2. And there are no significant changes with changing height. When the graph of the cover over crack spacing of both the Eurocode 2 (Figure 3-9) and DIANA model (Figure 6-6) are combined the following graph can be made (Figure 7-4).

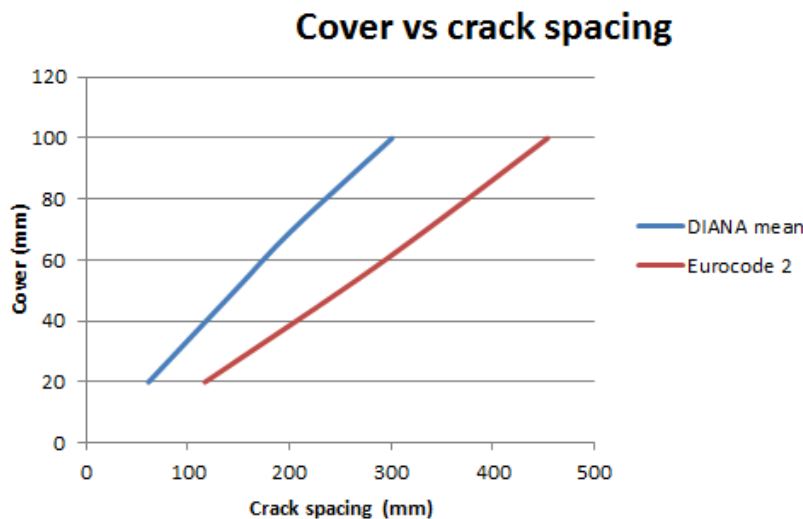


Figure 7-4; Comparison cover over crack spacing

In this graph there is a factor of 1.5 between the values with a cover of 20 millimetres and 1.9 between the two lines at a cover of 100 millimetres. The results that are presented in Figure 7-4, should have about the same trend as the results of Figure 7-2, because the Eurocode 2

states that the crack strain is just slightly influenced by the cover (concrete tensile area). Though, this is not the case. Therefore the strain is also investigated.

The crack strains of the Eurocode 2 and the DIANA results are presented in Figure 7-5.

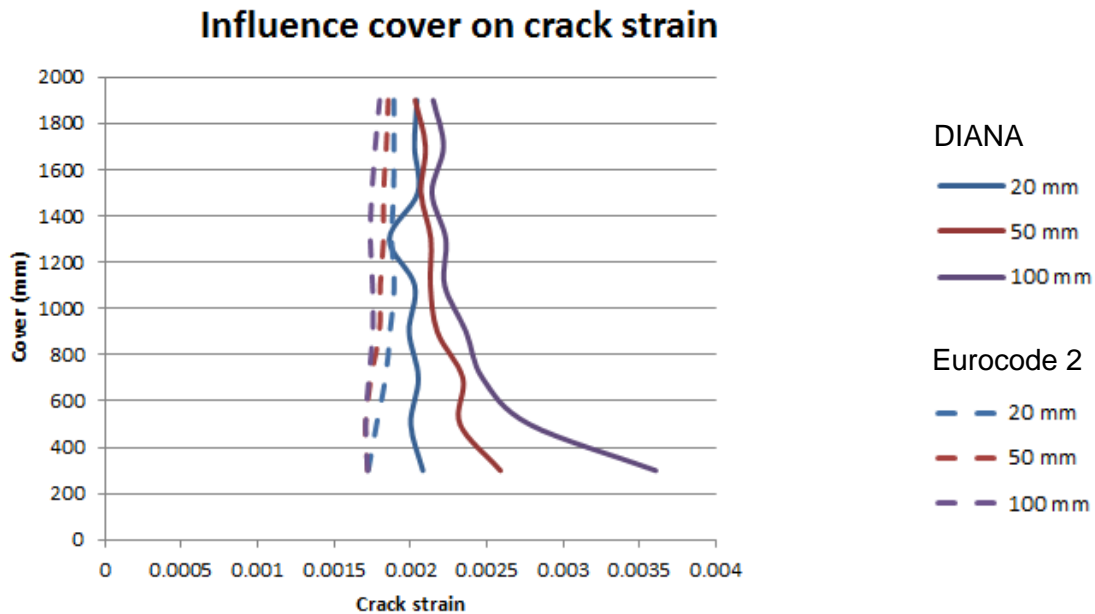


Figure 7-5; Influence cover on crack strain

Here the minor influence of the cover in the Eurocode is visible. In the DIANA results the influence is also minor, but where the crack strain of the Eurocode 2 is around 0.0018 and has a small decrease with increasing cover, the DIANA model results has a crack strain of around 0.0022 and is slightly increasing with increasing cover. The results of high covers with small construction heights give deviant results. This kind of configuration is not realistic, but reveals the fact that there is a bending moment load, and that the strain at the outer fibre is bigger than at reinforcement height (which is calculated in the Eurocode 2). A high construction height over cover ratio causes the bending influence to disappear.

So the crack width is smaller in the DIANA model. The crack spacing is relatively even smaller; therefore the crack strain is larger in the DIANA model. When a large cover is applied the strain decrease with increasing height in the DIANA model, this is not seen in the Eurocode 2.

The height has no significant influence on the crack width and crack spacing. Just a slight influence on the crack spacing in the DIANA results. This is seen in all further results.

## 7.2 Influence reinforcement percentage

Next the influence of the reinforcement percentage will be compared. The results of the crack width of the Eurocode 2 and DIANA model are in Figure 7-6.

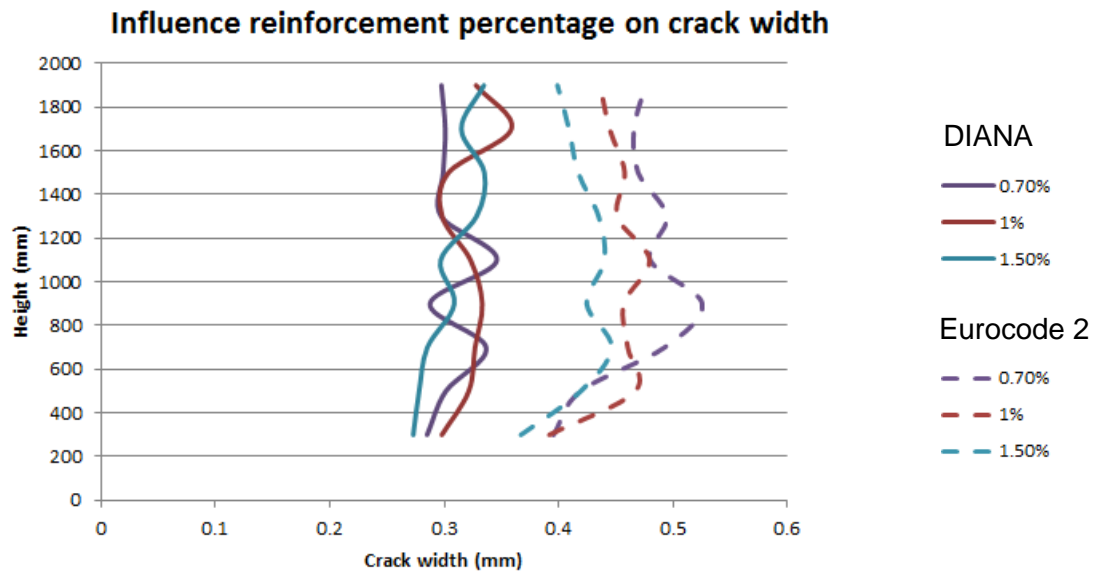


Figure 7-6; Influence reinforcement percentage on crack width

The biggest difference between the Eurocode 2 and the DIANA model in these results is the difference in the average crack width, which already has been seen in the influence of the cover. Also a slight decrease of crack width with increasing reinforcement percentage is noticeable in the Eurocode 2 results; this effect is not seen in the DIANA model results. The DIANA model results scatter. Eventually the total influence of the reinforcement percentage on the crack width is in both calculations small.

In the Eurocode 2 the reinforcement percentage has an influence on the crack spacing and crack strain. Therefore the crack spacing's and strains are compared. The crack spacing's results of the Eurocode 2 and the DIANA model are in Figure 7-7.

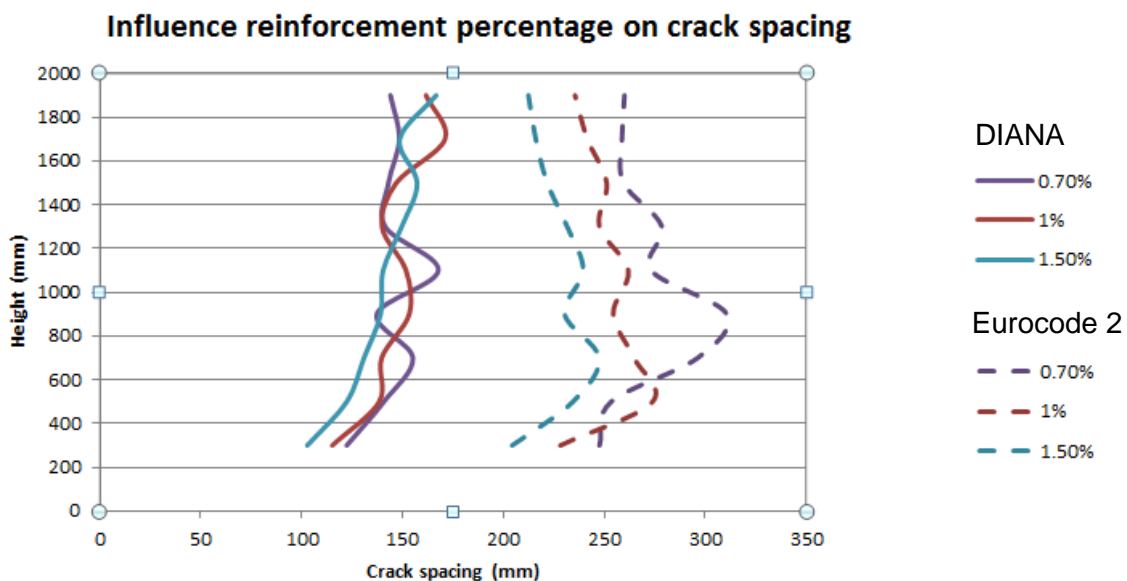


Figure 7-7; Influence reinforcement percentage on crack spacing

The same trend with the same conclusions can be found in the crack spacing results as have been found in the crack width results.

The theory behind the Eurocode 2 results is that when the reinforcement percentage increases the surface area of the steel increases, because more bars or larger diameters are applied. In a crack the steel takes all the tensile force. The steel is loading the concrete with increasing distance of the crack by the bond between these two materials, in Figure 2-5 this effect is shown. With more surface area there is a shorter distance needed to load the concrete till the tensile strength. After the tensile strength is reached a new crack will appear. And so the distance between the two cracks, the crack spacing, is shorter. This effect is not clearly seen in the DIANA results.

The crack strain results of the Eurocode 2 and DIANA model are presented in Figure 7-8.

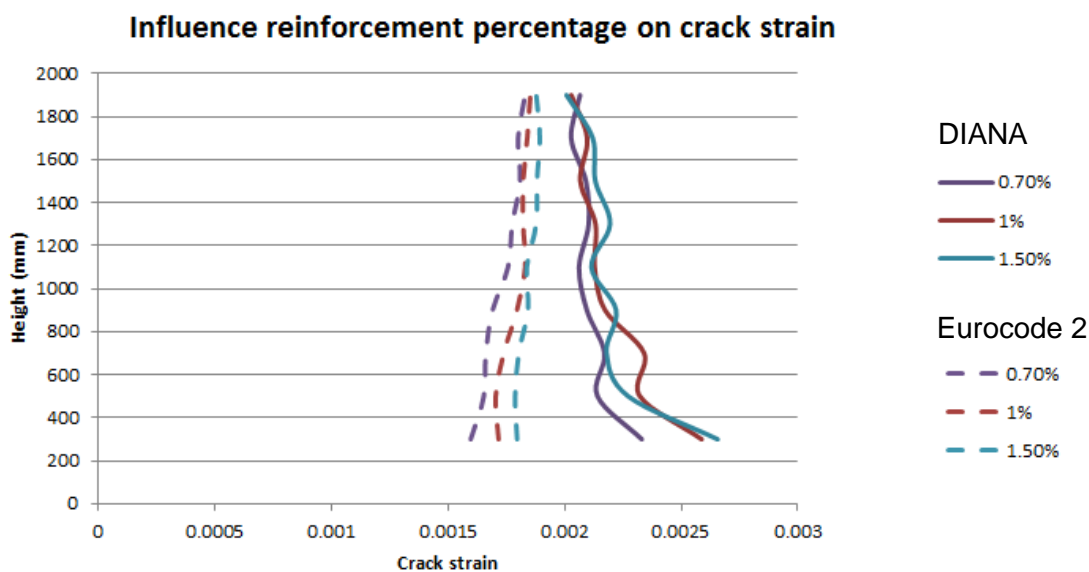


Figure 7-8; Influence reinforcement percentage on crack strain

The differences between the reinforcement percentages are in both the Eurocode 2 and DIANA model not significant. The Eurocode 2 shows a slight increase of crack strain with increasing reinforcement percentage; in the DIANA model this effect is less clear. The average strain is in the DIANA model higher than in the Eurocode 2, this behaviour already have been detected in the comparison of the influence of the cover.

The slight increase of crack strain with increasing reinforcement percentage is explained by the increase of steel area. A larger reinforcement percentage leads to a larger steel area. The concrete tensile area does not change. Therefore the concrete tensile strength will stay the same and will be reached at lower reinforcement stresses. This leads to cracks at a lower reinforcement stress and strain. After this point the crack strain will start to grow with increasing reinforcement stress. Since all the bars are loaded until the same reinforcement stress the crack strain of higher reinforcement percentages are larger.

II

### 7.3 Influence concrete tensile strength

After the influence of reinforcement percentage is discussed, the results of the tensile strength of concrete will be compared. The Eurocode 2 and DIANA results can be found in Figure 7-9.

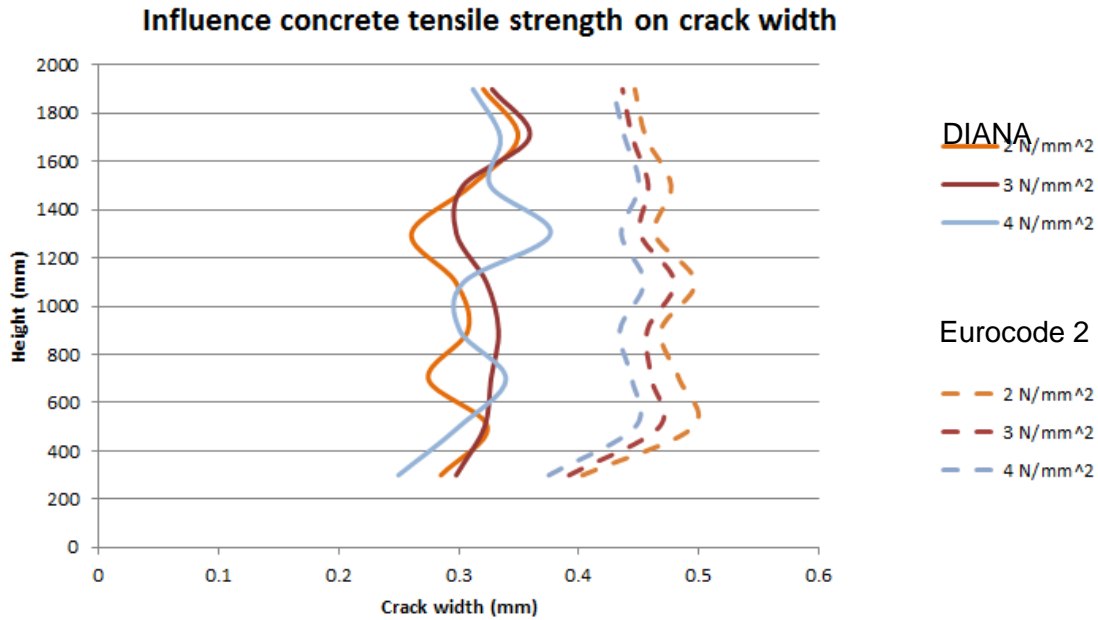


Figure 7-9; Influence of tensile strength on crack width

There is a decrease of crack width with increasing tensile strength in the Eurocode 2. This increase was not found in the results of the DIANA model, the lines of the DIANA results run through each other and no clear influence can be detected.

The crack spacing stays the same for every concrete tensile strength in the Eurocode 2. The results for the crack spacing of the Eurocode 2 and DIANA model are in Figure 7-10.

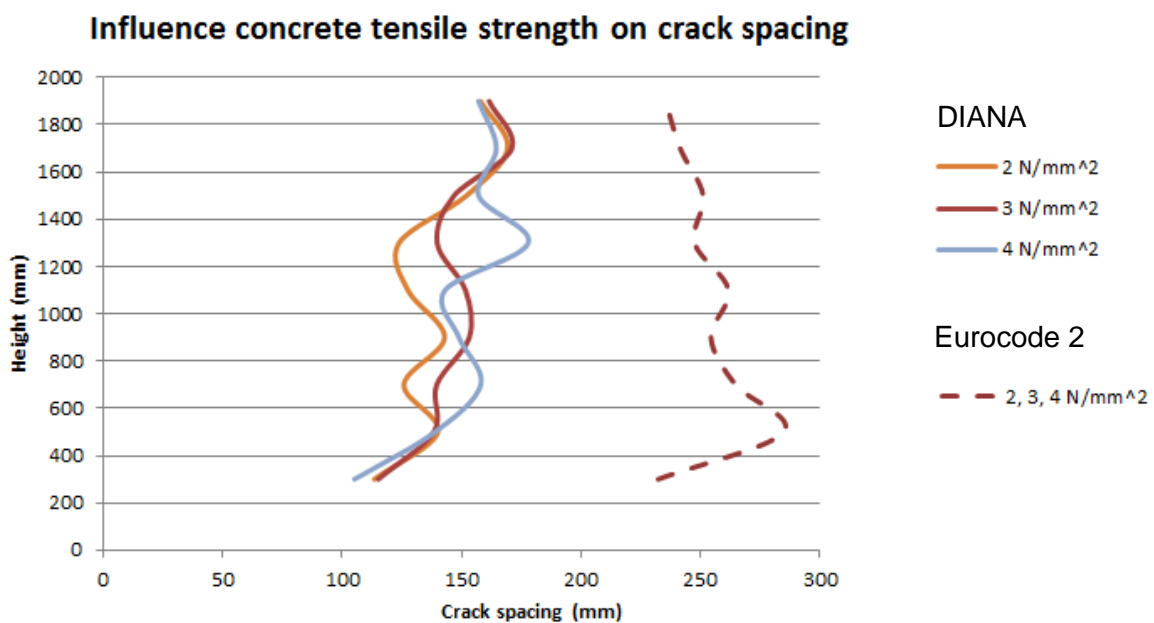


Figure 7-10; Influence tensile strength on crack spacing



In the DIANA crack spacing results, the same scatter was found as has been found for the crack width. There is no distinctive relation between the tensile strength and crack spacing. But difference in crack spacing could be explained by the fact that with higher tensile strength the concrete can take more tensile load. Therefore the reinforcement needs more bonding length after a crack to get the concrete tensile stress in the concrete. When the concrete reaches its tensile strength a new crack can be formed. So a higher tensile strength would lead to bigger crack spacing's.

The concrete tensile strength is one of the parameters in the crack strain term of the Eurocode 2 calculation. The influence of the concrete tensile strength on the crack strain can be found in Figure 7-11.

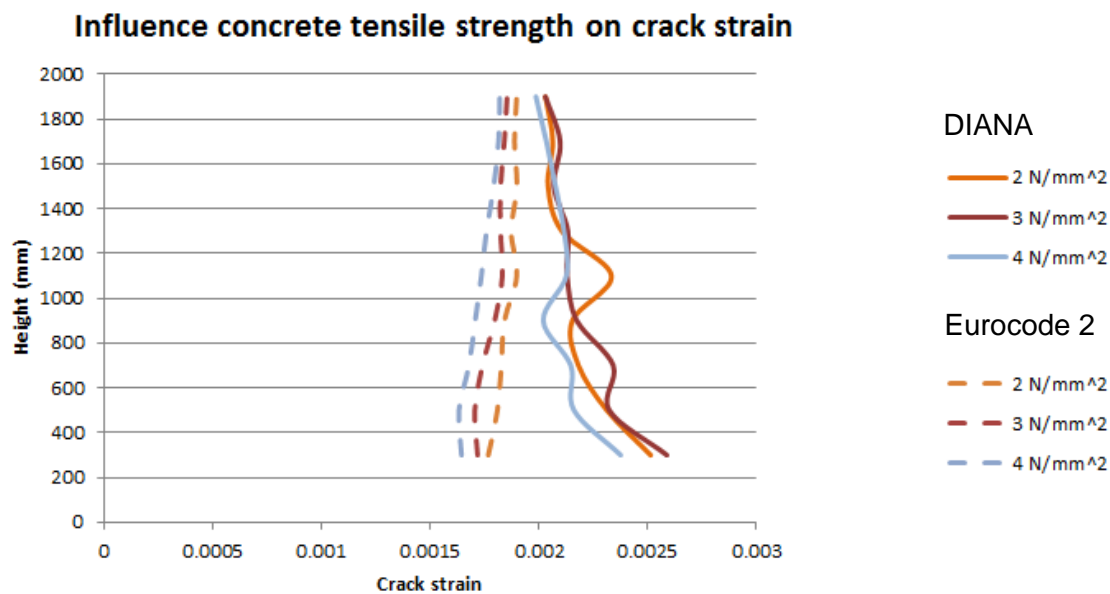


Figure 7-11; Influence tensile strength on crack strain

In the Eurocode 2 the crack spacing does not change with increasing concrete tensile strength, therefore the crack strain has the same relative decrease of the crack strain with increase tensile strength as the crack width. When the results of the DIANA model results for the crack strain are analysed, it can be concluded that the strain stays about the same with increasing concrete tensile strength. So that differs from the Eurocode 2, also the average value of the crack strains differ.

The same reasoning can be used as has been used for the crack strain results of the reinforcement percentage. When the tensile strength of the concrete increases the amount of reinforcement stress needed to reach this tensile strength is also increased. Therefore the cracks appear at higher reinforcement stresses, when the tensile strength is higher. After this moment the crack strain starts to grow. For all the results the same maximum reinforcement stress is used. Therefore the crack strain is less at higher tensile strengths.

## 7.4 Influence reinforcement stress

The last parameter that is compared is the reinforcement stress. The results of the Eurocode and the DIANA model are in Figure 7-12.

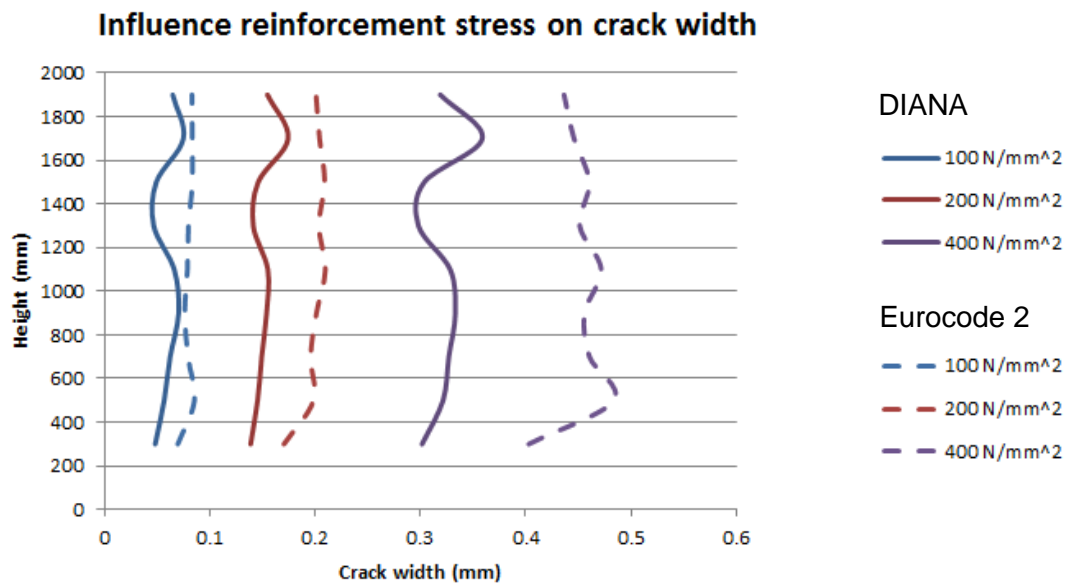


Figure 7-12; Influence reinforcement stress on crack width

In both the Eurocode 2 and the DIANA model the same trend with increasing reinforcement stress has been found. The average crack widths of the Eurocode 2 are larger than the crack widths of the DIANA model. If the increase of reinforcement stress is put out against the crack width the graph in Figure 7-13 can be made.

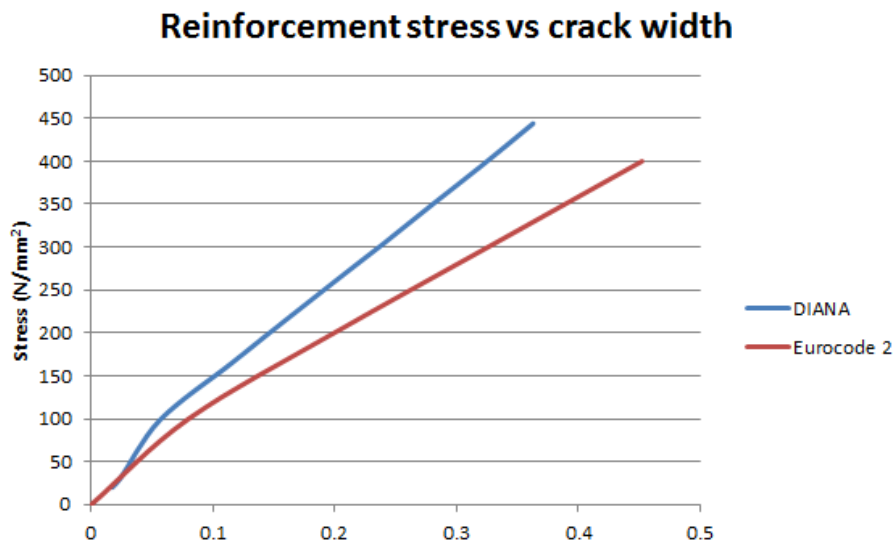


Figure 7-13; Comparison reinforcement stress over crack width

In this graph a clear difference is visible; the Eurocode 2 crack width grows faster than the DIANA model crack width.

The crack spacing results of the Eurocode 2 and the DIANA model (cover 50 mm in Figure 7-3) stays the same with increasing reinforcement stress. Though, the average of these

crack spacing's differ. The average crack spacing of the Eurocode 2 is around 250 millimetres, where the average of the DIANA model is around 150 millimetres.

The crack strain is analysed, because of this significant difference in crack spacing and the fact that the reinforcement stress is a dominant term in crack strain calculation in the Eurocode 2. The results of the crack strain in the Eurocode 2 and DIANA model are in Figure 7-14.

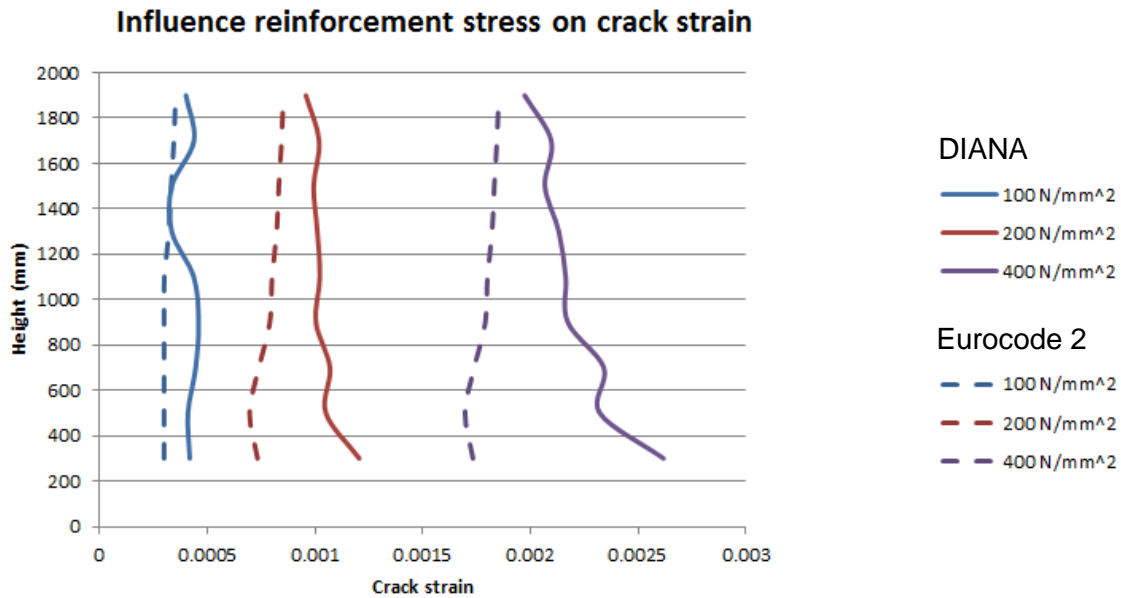


Figure 7-14; Influence reinforcement stress on crack strain

The same relative increase of crack strain with increasing reinforcement stress as has been found in the crack width analysis is present in the results. The average crack strain of the Eurocode 2 is smaller than the average crack strain of the DIANA model, because of the large difference between the crack spacing's. This is compared in Figure 7-15.

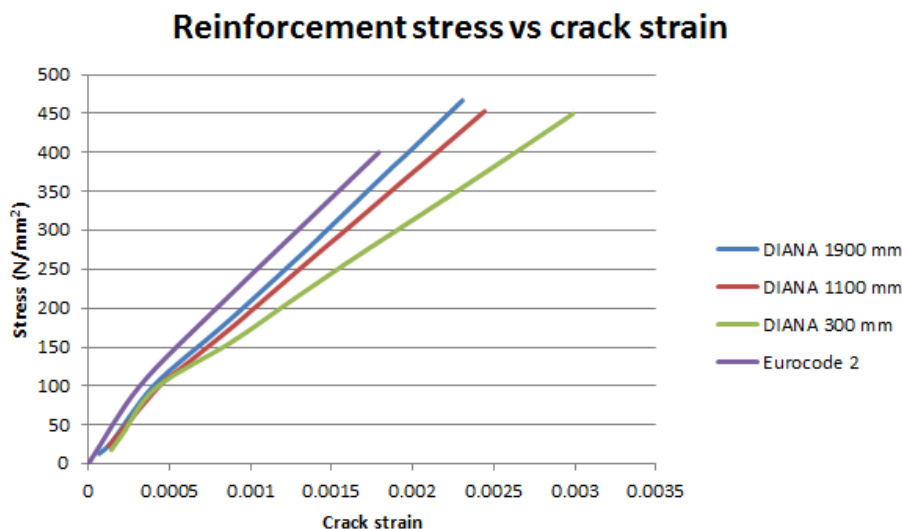


Figure 7-15; Comparison reinforcement stress over crack strain

The crack strain grows faster in the DIANA model than in the Eurocode 2, this effect becomes larger with decreasing construction height. The reason for this effect is the bending moment load as explained in the influence of the cover on the crack strain.

## 7.5 Adjusting Eurocode 2

Since there are some major differences between the Eurocode 2 and DIANA model a modification is made on the Eurocode 2. The largest influences on the Eurocode 2 are the cover in the crack spacing term and the reinforcement stress in the crack strain term.

### 7.5.1 Crack strain

The crack strain term of the Eurocode 2 is:

$$\epsilon_{sm} - \epsilon_{cm} = \frac{\sigma_s - k_t * \frac{f_{ct,eff}}{\rho_{p,eff}} (1 + \alpha_e * \rho_{p,eff})}{E_s} \geq 0.6 \frac{\sigma_s}{E_s}$$

7-1

In the comparison of the crack strain, in the influence of the cover and the reinforcement stress, it appeared that the height and the cover were affecting the crack strain in the DIANA results, but not in the Eurocode 2 results, see Figure 7-15 and Figure 7-18.

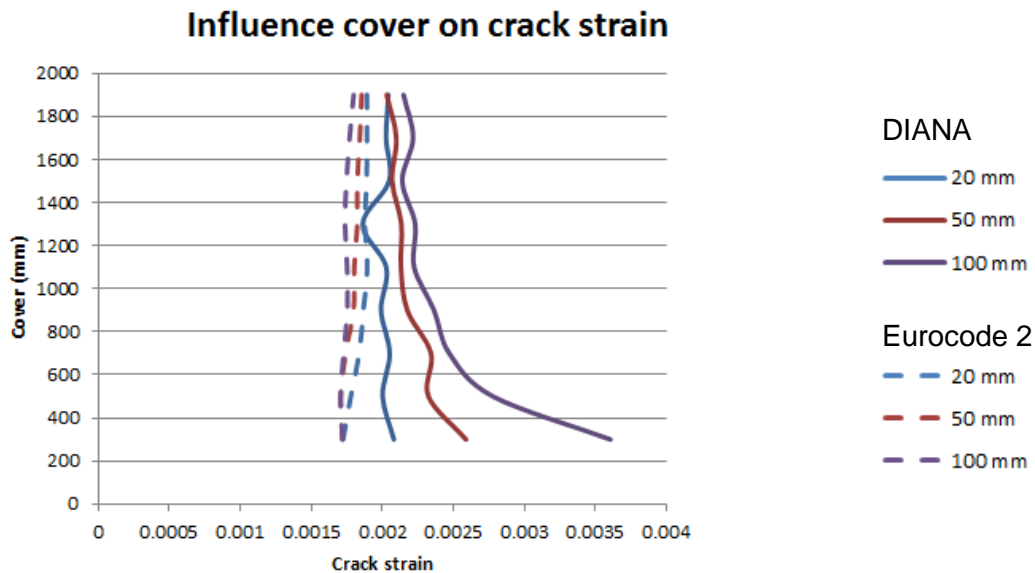


Figure 7-16; Influence cover DIANA model on crack strain

An explanation for this is the fact that the load is a bending moment and the crack strain at reinforcement height, which is calculated in the Eurocode 2, is lower than the crack strain at the outer fibre which is measured in the DIANA results, see Figure 7-17. The cracks should be measured at the outer fibre, because they are at their maximum at the edge.

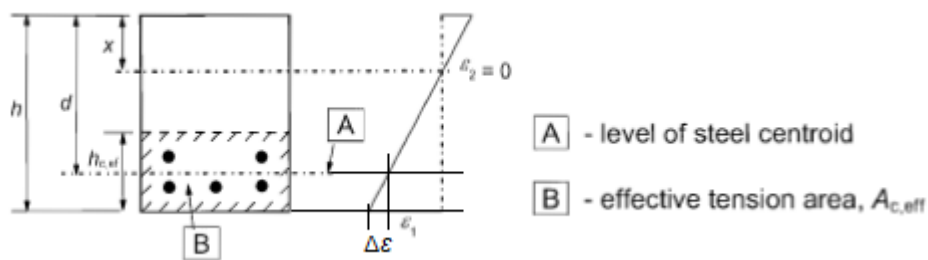


Figure 7-17; Difference ( $\Delta\epsilon$ ) in crack strain reinforcement height and outer fibre

In the Model code 2010 a factor over the complete crack width is used to take bending into account, equation 7-2.

$$(h - x)/(d - x)$$

7-2

Though, the Model code 2010 factors differ from the factors that are found between the Eurocode 2 and the DIANA crack strain results. The values where a cover of 50 millimetres is applied are given in Table 7-1.

Height	Factor model code	Factor DIANA model
300	1.3	1.51
1100	1.07	1.18
1900	1.03	1.09

Table 7-1; Factors model code and adjusted Eurocode 2

The cover also influences this factor, therefore the factors for the other covers are also determined, see Table 7-2.

Height	Cover 100 mm	Cover 70 mm	Cover 50 mm	Cover 20 mm
300	2.1	1.8	1.51	1.21
1100	1.27	1.21	1.18	1.07
1900	1.2	1.13	1.09	1.08

Table 7-2; Factors adjusted Eurocode 2 all covers

To adjust the Eurocode 2 to the DIANA model these factors are taken over the whole crack strain term. An example with a height of 1100 mm and cover of 50 mm is given in Figure 7-18.

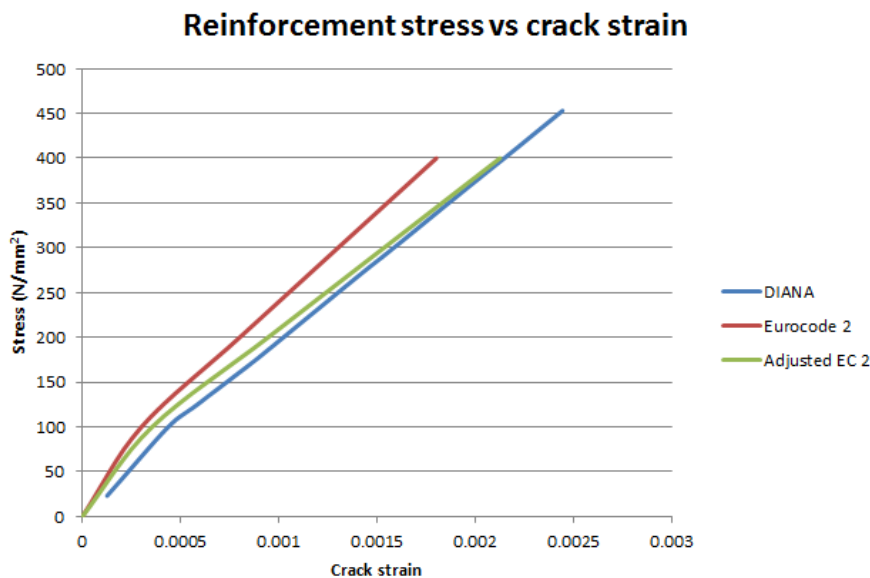


Figure 7-18; Adjusted Eurocode 2 to DIANA model

So it can be concluded that there is a certain factor between the crack strain of the Eurocode 2 and the DIANA model, this factor is influenced by the height and the cover and differs from the additional factor used for bending moment loads in the Model code 2010.

### 7.5.2 Crack spacing

The crack spacing term that is used in the Eurocode 2 is:

$$S_{r,max} = k_3c + k_1k_2k_4\phi/\rho_{p,eff}$$

7-3

In Figure 7-4 quite a significant difference between the crack spacing of the DIANA models and the Eurocode 2 is presented. The individual factors in the crack spacing term of the Eurocode 2 calculation are added to this figure, see Figure 7-20.

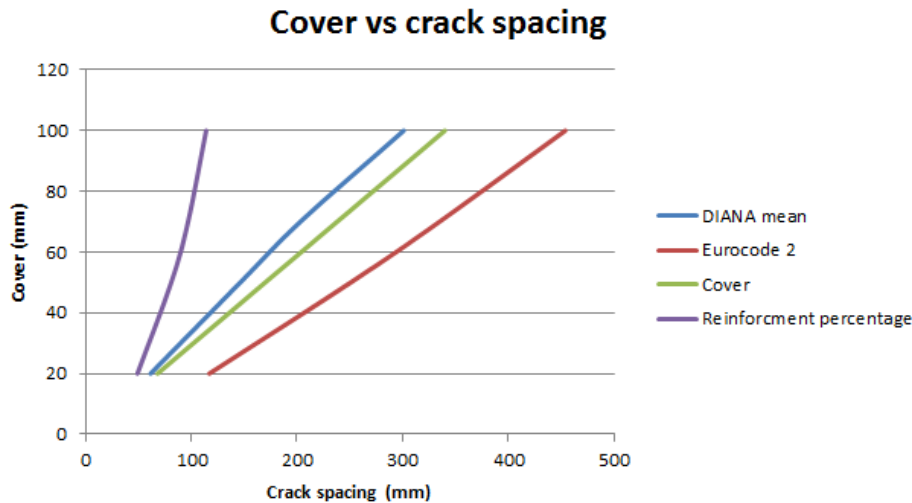


Figure 7-19; Comparison cover over crack spacing with factors Eurocode 2

In this figure the cover term is close to the result of the DIANA model. If the  $k_3$  factor in equation 7-3 is changed from 3.4 to 3 and the other term is completely left out the following results is gained, Figure 7-21.

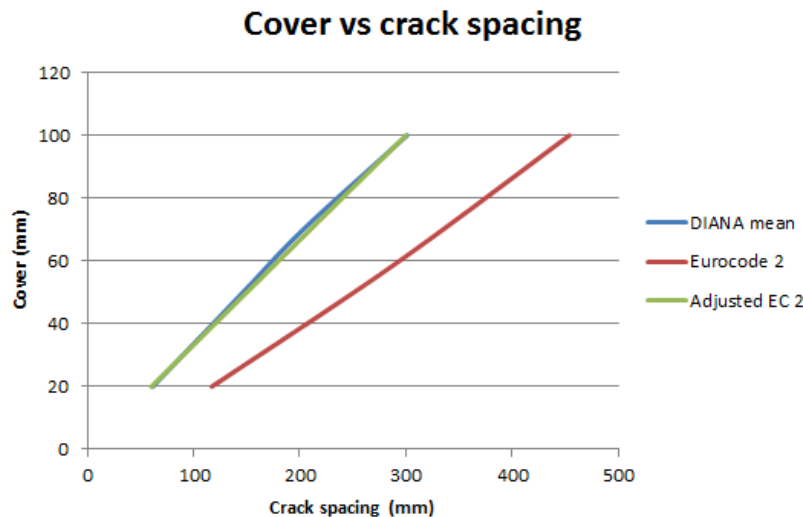


Figure 7-20; Comparison cover over crack spacing with adjusted Eurocode 2

A clear reason for the difference between the results of the Eurocode 2 and the DIANA model is not found, this should be further investigated.

# 8 Conclusions and recommendations

In chapter eight the conclusions are covered first, there after the recommendations are discussed. More extensive answers to the sub questions are given in Appendix E.

## 8.1 Conclusions

The main question of this thesis is:

*Are the current rules in the Eurocode 2 for the calculation of flexural cracks too conservative for large thicknesses that are applied in the concrete lining of immersed tunnels?*

In the Eurocode 2 the crack width of flexural cracks is calculated by multiplying the crack spacing and the crack strain. The crack spacing is the distance between the cracks. In the Eurocode 2 the crack spacing is calculated with the cover and the reinforcement configuration. The crack strain calculated in the Eurocode 2 corresponds with the increase of the strain in the reinforcement steel after cracks have appeared. Cracks appear when the concrete is loaded by its tensile stress. Therefore the crack strain in the Eurocode 2 is dependent on the reinforcement strain and tensile strength of concrete.

Whether the Eurocode 2 is conservative or not is on first-hand checked with codes that are used in other countries. Most of the codes use the same approach as the Eurocode 2 by multiplying the crack strain with the crack spacing. Though, these factors are calculated differently. There are other parameters used and/or parameters are left out and other influence factors are applied. When the results of the crack widths of the codes are compared it seemed that the Eurocode 2 crack width calculation was not conservative relative to the other codes.

For a more reliable conclusion the Eurocode 2 is compared with a DIANA model, which is verified with experiments. The crack widths of the DIANA results are smaller than the crack widths of the Eurocode 2 results. The factor between crack width values is decreasing when the cover increases (factor 1.7 for 20 mm and factor 1.1 for 100 mm). The crack spacing's are also smaller in the DIANA results. The differences in crack spacing's (factor 1.9 for 20 mm and 1.5 for 100 mm) are relatively larger than in the crack widths. The crack strains are larger in the DIANA results.

The influence factors used in the crack spacing calculation are overestimated, but no clear reason is found for this result. The difference in strains is caused by the bending moment load and is influenced by the cover and the construction height. The cracks are measured at the outer fibre of a beam. Therefore the crack strain must also be determined at the outer fibre. The Eurocode 2 calculation for the crack strain determines the strain at reinforcement height, if the structure would be loaded by an axial force the crack strain at outer fibre would be the same. Though, flexural cracks are investigated and therefore a bending moment load is applied. This bending moment load introduces a rotation in the structure. The rotation causes an increase of strain from the centre of the beam to the outer fibres. The strain at the outer fibre is therefore larger than at the reinforcement height and that is why the DIANA crack strain results are larger than the Eurocode 2 results. The ratio between construction

height and the cover is important for the extra strain that the rotation causes, since the rotation is decreasing with increasing height and the difference in crack strain increases with increasing cover.

The sensitivity of the parameters used in the Eurocode 2 is investigated. The cover is the most important factor for the crack spacing and the reinforcement stress is dominant in the crack strain in both the Eurocode 2 and DIANA results. The influence of the concrete tensile strength and reinforcement percentage are small in the Eurocode 2 and the DIANA results. The impact of construction height is minimal, only the crack strain in the DIANA results is affected as has been discussed in the last paragraph.

In short, the Eurocode 2 calculation for flexural cracks is too conservative, because the crack widths in the DIANA model, which is verified with experiments, are smaller than in the Eurocode 2 results. This originates out of the crack spacing which is overestimated substantially. Though, the crack strain is underestimated, but less significant. The large thicknesses that are applied in the concrete lining of immersed tunnels are not the reason for the conservativeness, since the influence of the construction height appeared to be minimal in the sensitivity study.



## 8.2 Recommendations

A few recommendations are given for further research.

### *3-Dimensional*

In this thesis the problem is approached on a 2-dimensional level. All of the parameters of the Eurocode 2 could be examined in the 2-dimensional environment. In the Japanese code and United States code the reinforcement bar spacing is also of importance. With a 3-dimensional this parameter could also be examined. Next to that other 3-dimensional influences could be brought to light.

### *Axial force cracks*

There is calculated with bending moments in this thesis. Though, there are also crack that can appear by axial forces, or internal forces by drying, restraint to shortening or temperature fluxes. These kinds of cracks could also be examined and compared with results for the Eurocode 2.

### *Origin of the Eurocode 2 crack width calculation parameters*

An addition to this thesis could be an investigation towards the origin of the Eurocode 2 parameters in the crack width calculation. Tests have been carried out to determine the parameters and there influence factor. To investigated these tests and determining where the decisions in making the Eurocode 2 crack width calculation are based on, can help improving the Eurocode 2.

### *Immersed tunnels*

Since in designing immersed tunnels the problems with the crack width calculations appeared, the results out of this thesis could be used to do a recalculation in order to see what the effect is in reinforcement usage. Additionally a cost calculation can be carried out reduction on costs could be.

## 9 List of literature

- American Association of State Highway Transportation Officials. (2012). *AASHTO LRFD bridge design specifications, customary U.S. units*. In. Retrieved from Knovel <http://app.knovel.com/hotlink/toc/id:kpAASHTO32/aashto-lrfd-bridge>
- Bakker, K. J., Huijben, J. W., & Vrijling, J. K. (2012). *Bored and immersed tunneling : CIE5305*. Delft: TU Delft.
- Braam, C. R. (1990). *The behaviour of deep reinforced concrete beams : experimental results*. Delft: Delft University of Technology, Concrete Structures Group; Stevin Laboratory.
- Broomfield, J. P. (2007). *Corrosion of steel in concrete: understanding, investigation and repair* (2nd ed.). London: Taylor and Francis.
- China highway planning and design institute of the people's republic of china. (2004). JTG D62-2004. In *Code for Design of Highway Reinforced Concrete and Prestressed Concrete Bridges and Culverts*. Beijing: China Communications Press.
- DIANA FEA BV. (2016). User's Manual Release 10.1. In. Delft.
- International Federation for Structural Concrete. (2013). *Fib model code for concrete structures 2010*. Lausanne, Switzerland: Ernst & Sohn.
- JSCE 2010 concrete committee. (2007). *Standard specification for concrete structures In Design*. Retrieved from <http://www.jsce-int.org/about/guideline>
- Leonhardt, F., & Walther, R. (1962). *Schubversuche an einfeldrigen stahlbetonbalken mit und ohne schubbewehrung zur ermittlung der schubtragfähigkeit und der oberen schubspannungsgrenze*. Berlin: Ernst.
- Lunniss, R., & Baber, J. (2013). *Immersed tunnels*: CRC Press.
- Nederlands Normalisatie instituut. (2011). Eurocode 2: Ontwerp en berekening van betonconstructies - Deel 1-1: Algemene regels en regels voor gebouwen. In. Delft, The Netherlands.
- Vecchio, F., & Shim, W. (2004). Experimental and analytical reexamination of classic concrete beam tests. *Journal of Structural Engineering*, 130(3), 460-469.

## IV Appendix

- A. Immersed tunnels
- B. Corrosion of the reinforcement steel
- C. Experiment Braam extended version
- D. Python file DIANA calculation
- E. Answers sub questions

# A. Immersed tunnels

In the early 1800s the first ideas for building an immersed tunnel came in Great Britain, about crossing the Thames and connecting England and France. But not until 1893 the first immersed tunnel was built in the United States, which was used for sewage. The tunnel was constructed of brick and concrete and was 100 m long and had a diameter of 2.7 m.

The first larger scale transportation tunnel was the Detroit River tunnel, opened in 1910. It was made of two watertight steel tubes, which were placed in a dredged trench and then backfilled with concrete (Figure appendix A-1).

The first significant concrete immersed tunnel was the friedrichshagen tunnel in Germany, which was completed in 1927. About a decade later the



Figure appendix A-1; Detroit river tunnel (Lunniss & Baber, 2013, p. 9)

Dutch adopted the technique, in response of the problems with traffic congestion. This resulted in the construction contract of the Maastunnel in 1937, and was completed in 1942. The reason that the Dutch chose for the usage of concrete, was because the steel prices in Europe were high and with reinforced concrete the rectangular cross section could be introduced. In the decades after the Dutch developed the immersed reinforced concrete tunnel, for example to reduce the longitudinal cracks they developed the segmented tunnel. The immersed tunnels started to get more applied and are still a common form of tunnelling (Figure appendix A-2).

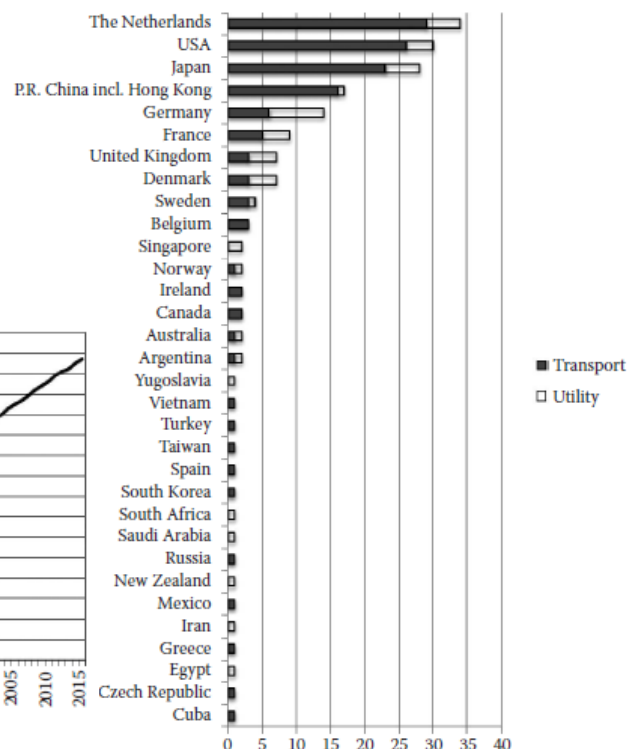
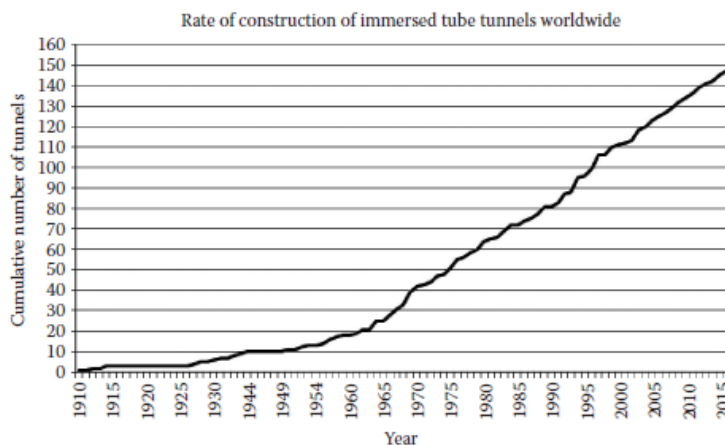


Figure appendix A-2; Number of Tunnels constructed (Lunniss & Baber, 2013, pp. 21, 23)

## Current forms of immersed tunnels

### Monolithic concrete element construction

The monolithic tunnel is a structure with continuous elements of typically 100 to 200 m long. This form of construction provides flexibility for design, since it can be easily adapted to different shapes (Figure appendix A-3). Often a membrane for water tightness is applied since there are risks for cracks over the full depth of the concrete walls in longitudinal direction, since the concrete of the walls is poured when the floor is already hard and this can cause curing cracks.

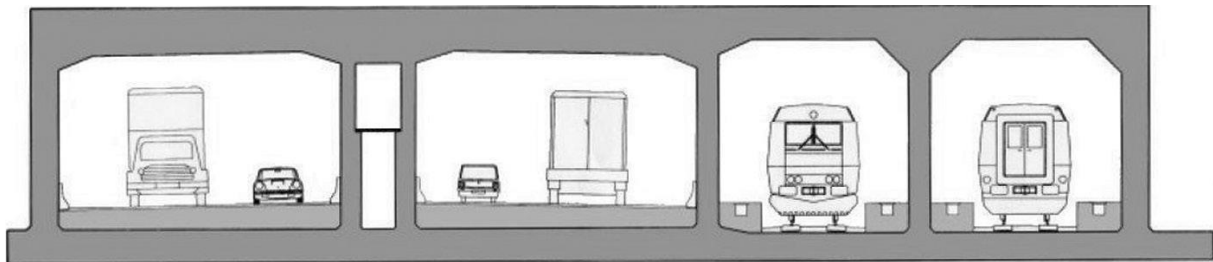


Figure appendix A-3; Concrete tunnel cross-section (Lunniss & Baber, 2013, p. 32)

### Segmental concrete element construction

The segmental concrete element tunnel is developed, because of the problems with leakage in the monolithic tunnel element. Since in longitudinal direction the shrinkage cracks penetrated the whole thickness of the concrete there were leakages. To control the temperature during curing some techniques have been applied, such as a combination of concrete mix design, controlling it with water cooling by pipelines that are cast into the concrete and by insulating the formwork.

### Prestressed concrete

The prestressed concrete tunnel is much like the monolithic concrete tunnel, only there is permanent prestressing applied in longitudinal direction. This can reduce the amount of longitudinal reinforcement and can close the cracks, so leakage is less of a problem. Though it is common that there is still a watertight membrane applied. The downside of this method is that there is much detailing and it is an extra step during construction. Prestressing in transversely direction is sometimes used when it can increase the capacity of the structure, but it is not common.

### Single steel shell / Double steel shell / Composite concrete steel sandwich

Next to that there are tunnels where the main structure is predominantly made of steel or a combination of concrete and steel. Hereby the steel is used as a watertight outer shell and is supported by reinforced concrete. Since the outer shell is of steel it is usually protected against corrosion by for example a cathodic protection.

## Basic sizing

The first sizing of the tunnel is based on the basis layout of the traffic tubes, with the alignment, ventilation system and other measures for fire life safety. First the traffic clearance envelope is defined, after that the other items can be added.

Next to that there are some construction tolerances that are important:

- Element placing tolerance: Steps or angular deviations in the tunnel of about  $\pm 50$  mm (Figure appendix A-4). Depends on the length of the element, longer elements can must have a greater allowance;

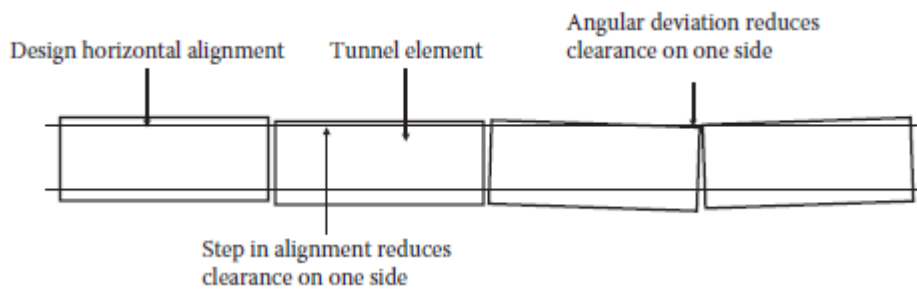


Figure appendix A-4; Horizontal placing tolerance (Lunniss & Baber, 2013, p. 171)

- Settlement tolerance: Unexpected settlements between elements can cause a need for tolerance (Figure appendix A-5); a typical allowance is 25 mm;

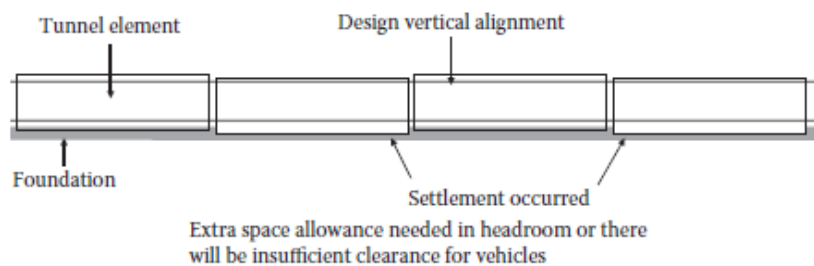
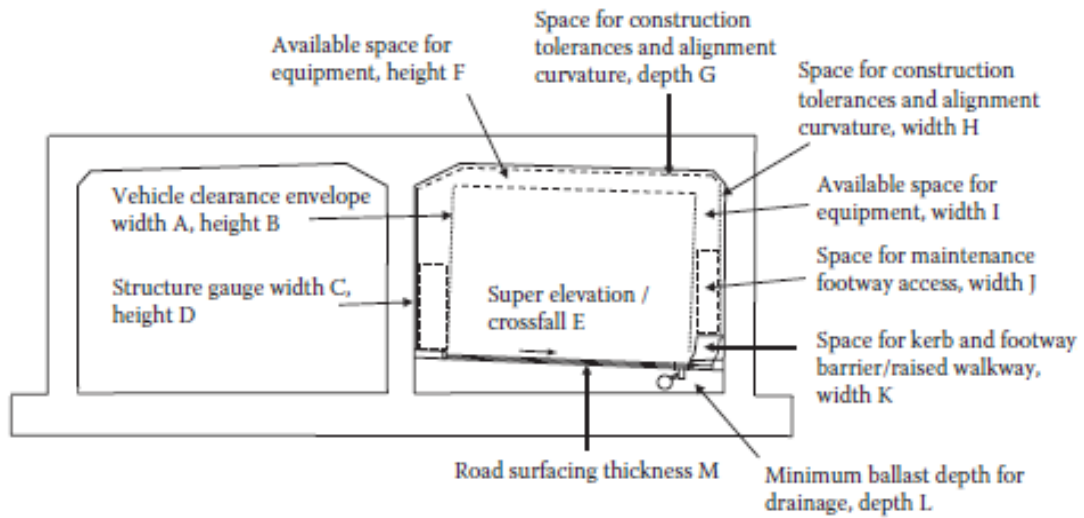


Figure appendix A-5; Settlement tolerance (Lunniss & Baber, 2013, p. 172)

- Surface tolerance: Deviation in the finished surface for the roof may be accommodated in the space for the mechanical and electrical equipment. Variations in the top surface of the base can be levelled with the ballast concrete.

A set of allowances is given in Figure appendix A-6. The numbers can vary depending on the national codes.



Dimension	Typical value	Clearance for
A	$n \times 3.65 \text{ m} + \text{hardstrip width}$	Traffic width: $n = \text{no. of lanes}$ , 3.65 m is typical lane width
B	5.25 m	5.0 m traffic height plus 0.25 m allowance for loose flapping truck tarpaulins
C	$A + H + K$	Total width required
D	$B + E + F + G + L + M$	Total height required
E	2.5%	Minimum carriageway crossfall
F	300 mm	Space for M&E equipment (excluding vent fans which may require additional space unless housed in niches)
G	75 mm	10 mm surface tolerance 25 mm settlement allowance 15 mm alignment curvature 25 mm element placing tolerance
H	80 mm	10 mm concrete surface tolerance 20 mm alignment curvature 50 mm element placing tolerance
I	As required	Space for equipment above footway— not usually critical unless ventilation fans are placed in this space
J	Width as footway Height 2.3 m	Space for maintenance personnel access and car passenger safety in the event of breakdown
K	1.0 m	Minimum footway width
L	600 mm	Minimum depth of ballast to accommodate drainage
M	75–100 mm	Two layers of wearing course with allowance for overlay, unless it is assumed renewal will include planning out of the old surface

Figure appendix A-6; Tolerances for clearance in an immersed tunnel (Lunniss & Baber, 2013, pp. 172, 173)

The stability and buoyancy are important for the sizing, since the tunnel should be able to float and sink. When the amount of space needed in the tunnel is known the structural part can be determined. The thickness of the concrete walls and slabs can be taken for a first assessment with a ratio of span over depth of 10:1. Then can be checked if the factor of safety between the upward force and the downward force is sufficient. This can be easily calculated by:

$$FoS \text{ against uplift} = \frac{\text{Weight of structure}}{\text{Vol of displaced water} * \text{Density water}}$$

A-1

Material	Maximum (kN/m <sup>3</sup> )	Minimum (kN/m <sup>3</sup> )
Water	10.1	9.9
Structural concrete	24.5	23.0
Ballast concrete	23.5	22.5
Backfill (submerged)	10.0	6.5

Figure appendix A-7; Densities of materials (Lunniss & Baber, 2013, p. 180)

In evaluating the buoyancy of the structure the material densities are important. There are two extremes, first the light condition in which the maximum water density is taken and the minimum structure material densities (Figure appendix A-7), second the heavy conditions where it is the other way around. Light weight conditions are used in the calculations where the structure needs to be able to sink and stay submerged, like in the permanent condition. The heavy conditions are used for the situations where the structure should float, like during towing.

Next to the vertical stability there is the stability against overturning. The element can overturn by wind or currents; it's also possible that the cross-section is not in balance. There are two checks for that have to be carried out:

- The metacentric height should be at least one meter above the centre of gravity of the element;
- The righting moment should be large enough to stabilize the element again, if it reaches an angle of typically 30 degrees.



## Loads

### Permanent loadings

The permanent loadings can be important for three different analyses namely, for Structural design, settlement and buoyancy.

#### Self-weight of the tunnel structure

The self-weight of the structure is important for the buoyancy of the element. It won't float if it's too heavy and if it's too light it may not be able to store all sufficient ballast to provide a necessary safety factor for uplift. The sizing of the tunnel is therefore important and mostly based on the buoyancy criteria. When the sizing is known the self-weight can be determined for the structural design and settlement analyses. For the buoyancy it is also important to take the variability of the density of the materials into account, since these together with the size determine the weight.

#### Hydrostatic forces

The hydrostatic forces can cause in several of construction stages a big difference in forces on the tunnel structure. But when the tunnel is submerged the biggest hydrostatic forces will be unleashed on the structure. With depth the forces will increase since the water pressure increases with depth.

#### Permanent ballast

Most of the times the ballast is mass concrete placed in the tunnel or rocks placed in a box on top of the tunnel. The ballast can solve some mistakes that have been made in construction. When the tunnel element is too light, extra dense material can be applied as ballast material. When the tunnel element is too heavy, light weight aggregate can be used in the ballast concrete.

#### Finishing's

With the calculation for buoyancy the finishing's have to be taken into account. Only the parts that are removed during maintenance, for example ventilation equipment, must be excluded.

#### Backfill

Load of the backfill should be taken into account the structural and settlement analyses. Next to that the backfill can contribute to the buoyancy by friction, but is for safety often not included. Fill on top of the tunnel can be seen as permanent loading, if it is not sensitive for scour.

## Variable loads

### Loads by vehicles

The live loading due to road vehicles and trains should be included as variable loads, to name a few:

- Transient vertical loads
- Wheel loads and patch loads
- Braking loads
- Impact loads
- Suction/Pressure loads

### Temperature loads

The seasonal temperature variation causes the tunnel to expand and contract throughout the year. These movements will influence the joints. Also the temperature in the concrete during curing has to be considered, since these can cause cracks through the whole thickness of the walls. And the temperature difference between the inside and outside of the tunnel can cause distortion in the tunnel structure.

### Wave and current loads

The wave and current loads are important for the towing of the structure from its building location to its final location. These loadings are especially important for the reinforcement/prestressing in the longitudinal direction since the wave and current loads can cause bending effects. Deep water swell waves can cause instability of the tunnel and its backfill when the wave height is sufficient to be effective on that depth.

### Ice loads

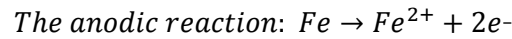
Ice loads isn't a load that is common in calculating the tunnel structure, the only reason to consider it is when historic weather records shows sufficient ice forming at the final location of the tunnel. When it is the case that there is loading of ice, these loads can become quite significant.

### Accidental loads

- Flooding
- Loss of a support
- Ship impact
- Falling and dragging anchor
- Fire
- Explosion
- Propeller scour

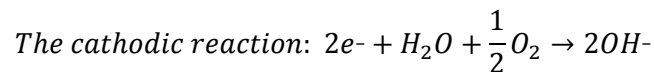
## B. Corrosion of the reinforcement steel

Steel and so steel reinforcement bars corrode when air and water are present. Steel corrodes because it dissolves in water that is present and gives up electrons. First there is an anodic reaction:



B-1

The two electrons that appear need to be consumed to keep an electric balance. This is done by another reaction that consumes the electrons:



B-2

In Figure appendix B-1 these reactions are shown.

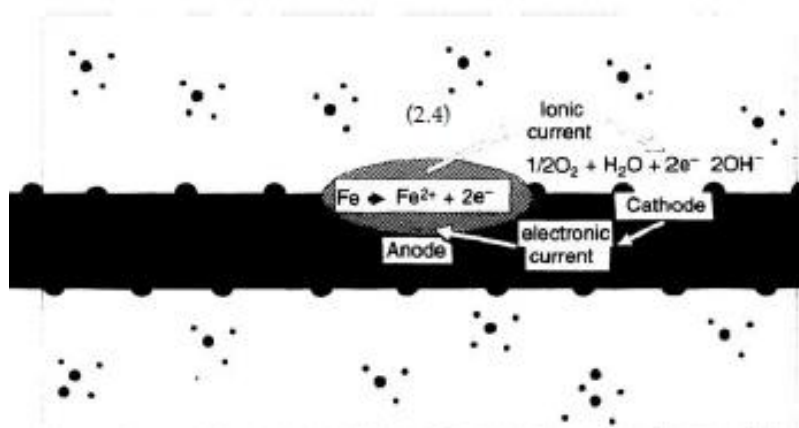
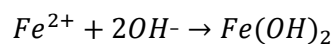


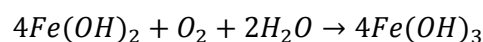
Figure appendix B-1; The cathodic and anodic reactions (Broomfield, 2007, Chapter 2.1)

These reactions are the first step in the process that creates rust. The next step can be expressed in the following manner; the ferrous ion ( $Fe^{2+}$ ) will react with the hydroxyl ions ( $OH^{-}$ ):



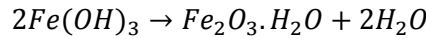
B-3

This is called Ferrous hydroxide, this will then react with water and oxygen:



B-4

This is Ferric hydroxide, this will eventually form rust:



B-5

An overview is given in Figure appendix B-2. This kind of corrosion gives a red/brown colour and has a bigger volume, which can cause the cracks to grow. In low oxygen conditions there is a chance that there is no normal formation of 'red' rust, but 'black' or 'green' rust. Since the anode is starved from oxygen the iron as  $Fe^{2+}$  will stay in the solution, this kind of rust also doesn't expand and will give no increase of cracks. This can be even more dangerous than 'red' rust since it is harder to detect where the steel is damaged.

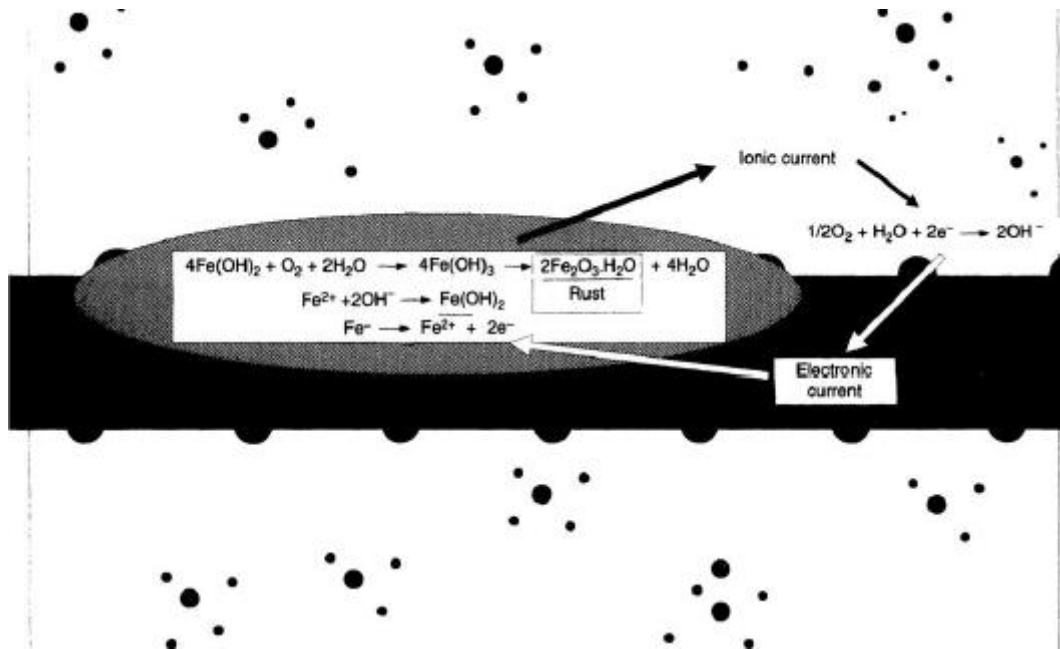


Figure appendix B-2; Corrosion reactions on steel (Broomfield, 2007, Chapter 2.1)

When reinforce concrete is loaded in its tension areas the concrete will crack when it reaches the tensile strength of the concrete. These cracks can cause acceleration of the corrosion, though most of these cracks are small. They do not lead to corrosion because the entrance for chlorides, moisture and carbonation is limited by the alkalinity of the concrete. It can be a problem when the crack becomes bigger. The biggest problem with corrosion in reinforced concrete is not due to the loss of steel, but the formation of rust which leads to expansion and that leads to cracking a spalling of the concrete cover, see Figure appendix B-3.

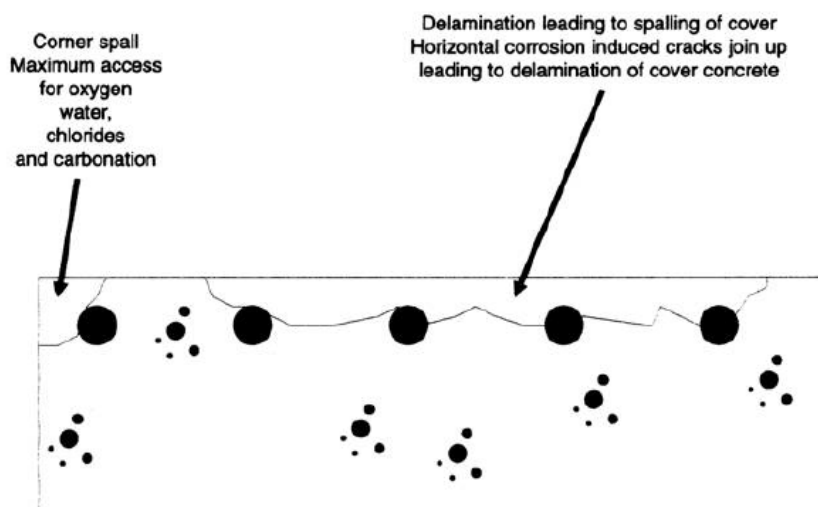


Figure appendix B-3; Corrosion causes cracking (Broomfield, 2007, Chapter 3.4)

To control the danger of corrosion a checklist can be made, see Figure appendix B-4.

<i>Structural form: Segmental concrete tunnel element</i>			
<i>Watertightness: Provided by reinforced concrete and joints</i>			
<i>Structural element</i>	<i>Risk</i>	<i>Mitigation</i>	<i>Criteria and design consideration</i>
Primary concrete structure	Corrosion due to chloride	Cover depth	Design to standard for extreme marine conditions
		w/c ratio	Design to standard, typically <0.4
		Permeability	Design to standard
		Chloride diffusivity	Set target, typically $7 \times 10^{-12} \text{ m}^2/\text{sec}$
		Flexural crack width	Design to standard, typically <0.25 mm
		Protection to prestress	Protection caps to anchorage and duct grouting procedures
	Leakage or corrosion due to through-cracking	Cooling or full section casting	Control risk of cracking to eliminate cracks Needs simulation, based on risk of cracking <0.7 Needs accurate concrete properties from testing to undertake representative simulation
		Carbonation	Coating Example: silane treatment
	ASR	Cover depth	Design to standard, typically 55 mm internal
		Choice of aggregates	Design to standard
	DEF	Concrete mix design	Design to standard
		Limit maximum temperature during curing	<65°C Needs temperature simulation to verify compliance Needs accurate concrete properties from testing to undertake representative simulation
Sulfate attack	Concrete mix	Design to appropriate standard, e.g., BS8500	
	Cover depth	Design to standard, typically 75 mm external	

Figure appendix B-4; Checklist for corrosion in segmental concrete tunnel elements (Lunniss & Baber, 2013, p. 309)

There are several ways to repair and protect the steel from corroding;

- Removal and replacement;
- Coatings;
- Sealers;
- Membranes;
- Barriers;
- Encasement;
- Overlays;
- Corrosion inhibitors;
- Cathodic protection;
- Chloride extraction;
- Realkalization.

One of the most known ones is the cathodic protection; a schematization is given in Figure appendix B-5. There are two forms of cathodic protection;

- Impressed current systems;
- Sacrificial anode systems.

With impressed current cathodic protection the anode reaction is stopped by passing sufficient current from the anode to the reinforcing steel. Only the cathodic reaction will occur. This will generate hydroxyl ions and these will increase the alkalinity of the concrete, which protects the reinforcing steel from chloride attacks.

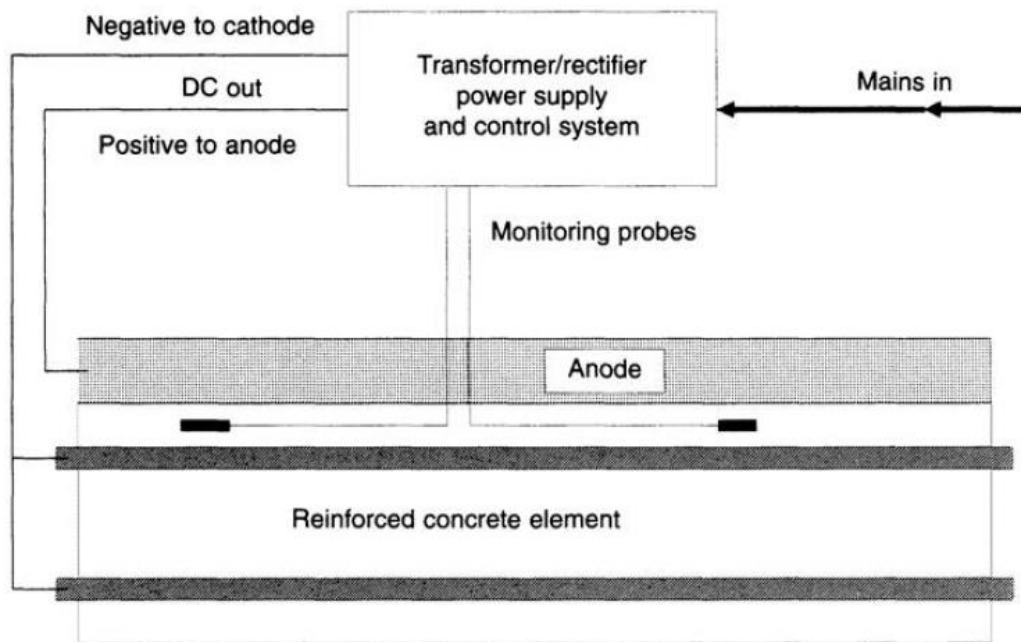


Figure appendix B-5; Schematization of electrochemical protection (Broomfield, 2007, p. Chapter 6.1)

Sacrificial anode cathodic protection is a method where a sacrificial or galvanic anode is directly connected to the steel, without using a power supply. This anode corrodes and produces electrons; this will give the same effect as the impressed current system.

In tunnelling the crack width is important for water tightness and corrosion, for water tightness the concrete should not crack over its full depth, for corrosion the crack width should be limited. It depends on the severity of the environment and sensitivity of the structure but normally this is in the range of 0.2 to 0.4 mm.

## C. Experiment Braam extended version

The parameters of the materials that are used in the experiment of Braam are given in the table below:

Name	Value
Young's modulus concrete	31800 N/mm <sup>2</sup>
Tensile strength concrete	4.08 N/mm <sup>2</sup>
Tensile fracture energy concrete	0.15 N/mm
Compressive strength concrete	55,9 N/mm <sup>2</sup>
Compressive fracture energy concrete	30 N/mm
Yield stress main reinforcement	570 N/mm <sup>2</sup>
Yield stress stirrups and rest	550 N/mm <sup>2</sup>
Diameter first layer	20 mm
Diameter second layer	10 mm

C-1; Parameters for the experiment of Braam

### Geometry

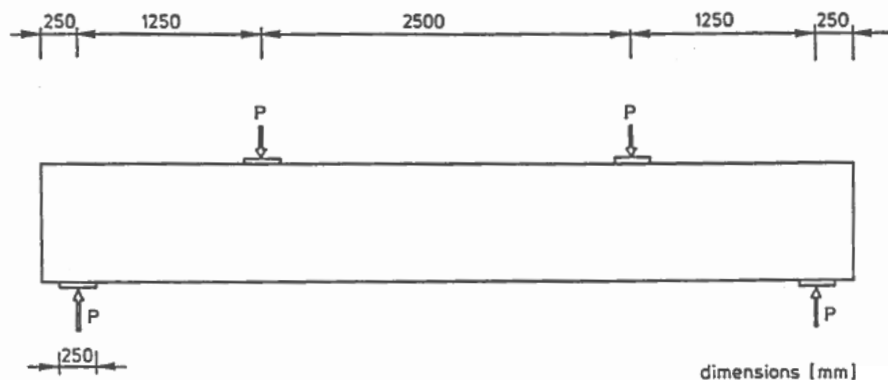


Figure appendix C-1; Geometry of the beam of the experiment of Braam

The beam has a length of 5,5 metres, the distance between the centres of the supports is 5 meter and the distance between the centres of the loads is 2,5 metres.

The height of the beam is 0,8 meters and the width is 0,3 meters.

The tensile reinforcement consists of four bars with each a diameter of 20 millimetres and above those four bars there are two bars with a diameter of 10 millimetres. The stirrups and the compressive reinforcement also have a diameter of 10 millimetres. The cover is 40 millimetres

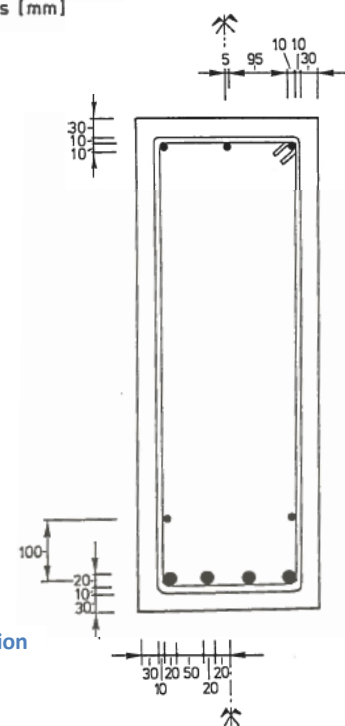


Figure appendix C-2; Cross-section of the experiment of Braam

In DIANA only half of the beam is modelled, because geometry of the beam and the loading is symmetric. The reason this is done is for faster computing of the model.

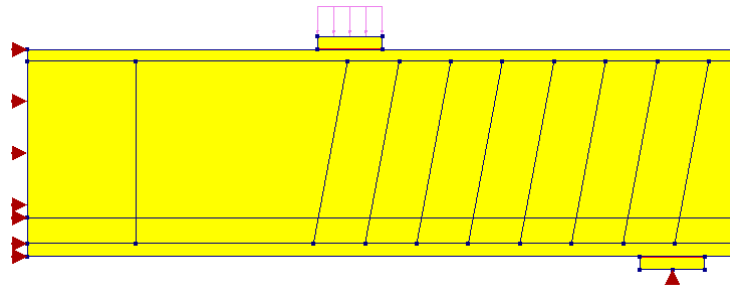


Figure appendix C-3; Geometry DIANA model experiment Braam

This figure shows the concrete, the reinforcement and the load and support configuration. There are eight stirrups used between the load and support point and one between the middle point and the load point.

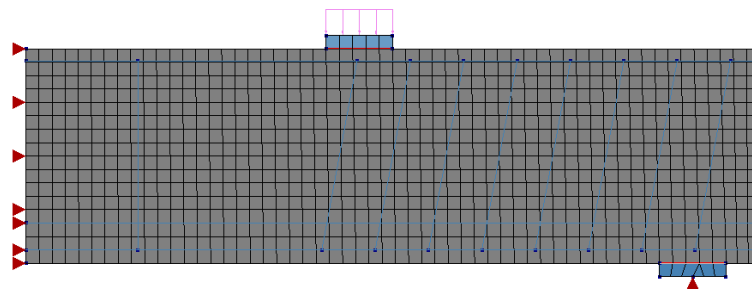


Figure appendix C-4; Mesh of the DIANA model of the experiment of Braam

For the mesh an element size of 50 mm is used.

### Force-displacement

The first check is the force-displacement diagram:

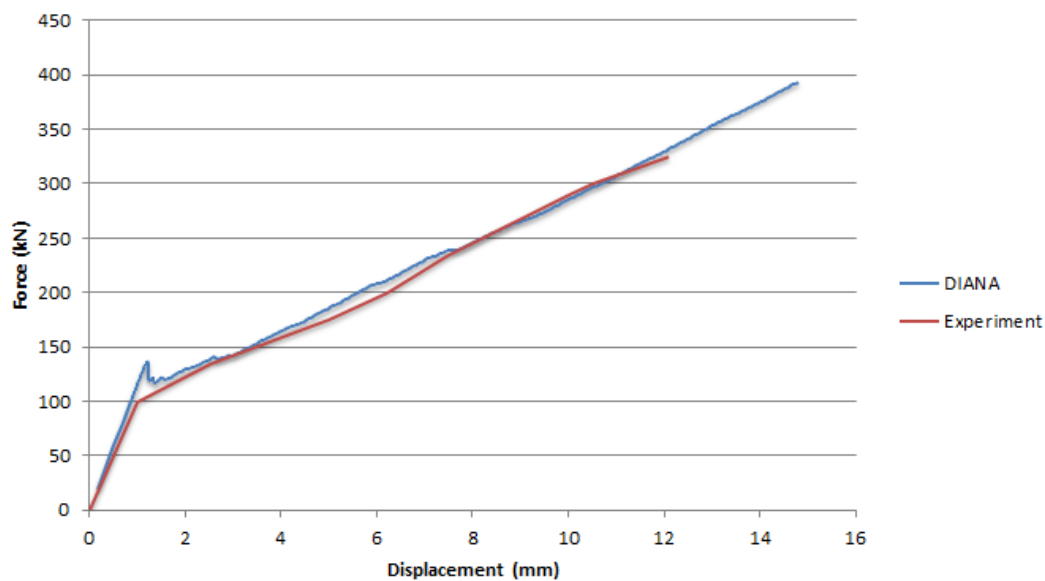


Figure appendix C-5; Force displacement diagram of with result of experiment Braam and DIANA



In this graph the value of the force is the load that is put on each loading point and the displacement is the deflection in the middle of the beam. The linear part of the DIANA model is a bit steeper; this can be the result of a difference in Young's modulus. After the linear part, it can clearly be seen that the DIANA model deviates a little bit from the experiment result. This is caused by the tension stiffening by Hordijk. The tension stiffening by Hordijk is used since this gives the best overall crack patterns. The fit of the force-displacement from the DIANA calculation with the experiment findings are good, since the lines have a similar trend.

To be able to state that the results of the numerical calculation are reliable a check has been carried out on the stability of the calculation. An overview is given of the 'out of balance' factor, the fact or it convergence and after how much iterations and the load for each step.

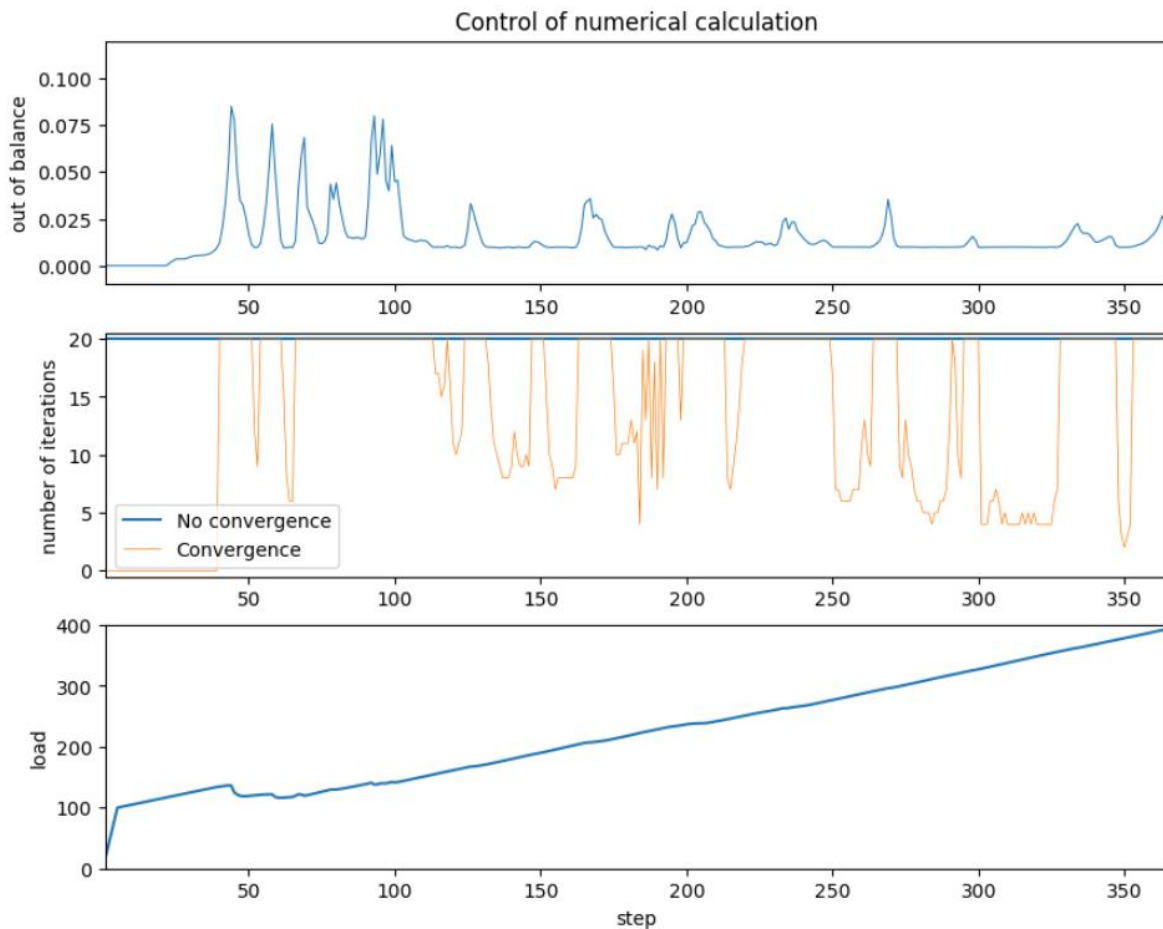


Figure appendix C-6; Control of numerical calculation of experiment Braam

There can be concluded that the numerical calculation has some difficulty converging after the linear part, especially when the cracks are formed. Though, the 'out of balance' factor doesn't get out of proportion. As the calculation continues the balance get better.

## Crack pattern

There are four load stages during the experiments, 218 kN, 368 kN, 468 kN and 668 kN. For each of these load stages the cracks between the loading points are recorded, see Figure 5-5. All of these crack patterns will be compared with the results in the DIANA model.

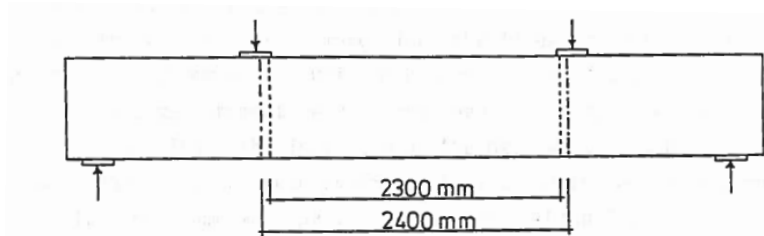


Figure appendix C-7; Part of the beam where crack patterns are recorded

The crack pattern from the experiment is for the loading stage of 468 kN is as follows:

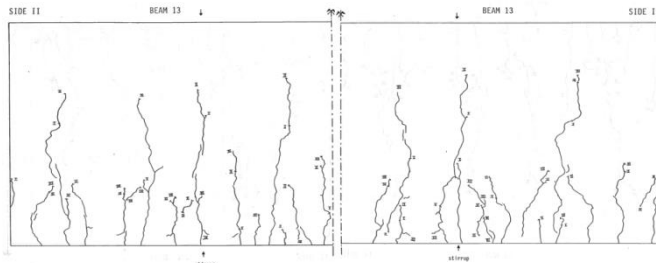


Figure appendix C-8; Crack pattern experiment 468 kN

The crack pattern that has been found for the loading stage of 468 kN in DIANA is:

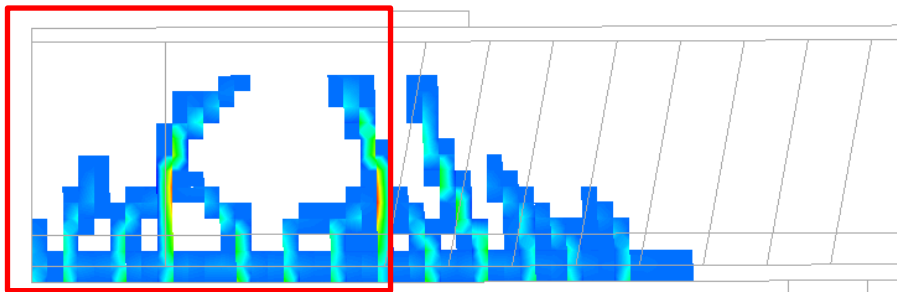


Figure appendix C-9; Crack pattern 462 kN in DIANA

When the two are compared, the red outlined area of the DIANA result (Figure appendix C-9) with half of the crack pattern of the experiment (Figure appendix C-8), it can be concluded that the experiment has more cracks than the DIANA model.

When the mesh is made smaller in the area where the experiment reviews the crack pattern, see Figure appendix C-10, the crack pattern will improve. An element size of 10 mm is applied at the edges that are indicated with the red lines.

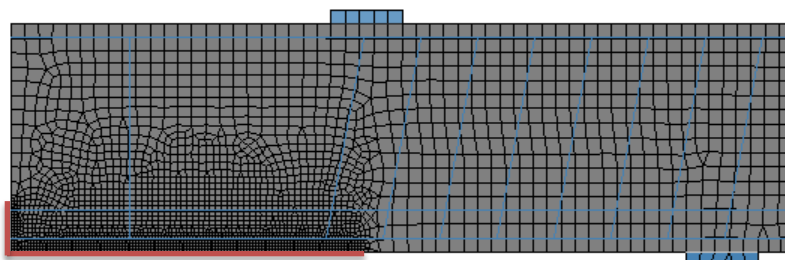


Figure appendix C-10; Change in mesh for better crack pattern

The crack pattern is now as follows:

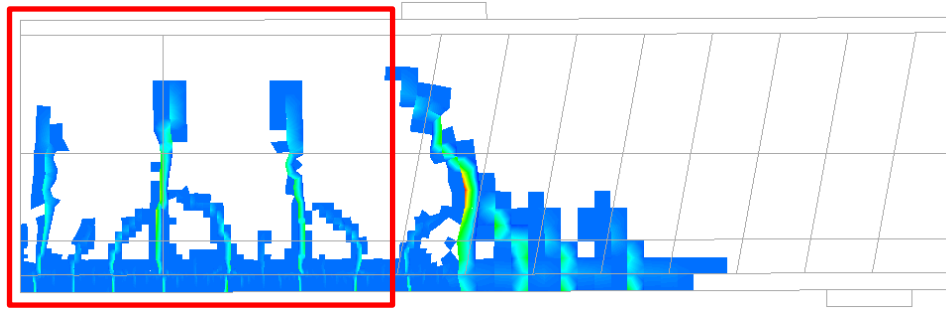


Figure appendix C-11; Improved crack pattern

It can be seen that the crack pattern is more detailed; this is because the mesh have been made smaller. This more detailed crack pattern gives a better comparison with the crack pattern that has been found in the experiment

When the mesh is made smaller the force-displacement diagram deviates, at the point where the cracks appear, a little bit more from the line of the experiment.

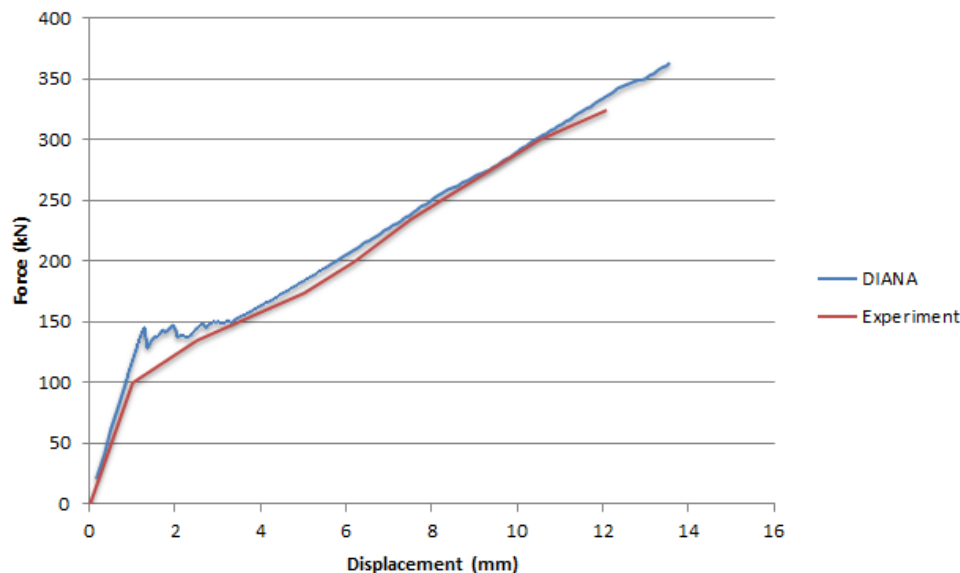


Figure appendix C-12; Force-displacement diagram improved model

So it can be concluded that when the mesh is made smaller the crack pattern improves but the force-displacement diagram deviates a little bit more from the experiment. The smaller mesh has an impact on the bandwidth ( $h$ ) and the Hordijk tension softening is dependent on this bandwidth. This clarifies the fact that a change is appearing. Since the calculation of the two models (small and large mesh) have a comparable progression of the 'out of balance' graph and so this cannot be the reason for the difference. For the control of the numerical calculation of the smaller mesh see Figure appendix C-13.

To be able to compare the other crack patterns the model with the smaller mesh is used, because this gives the better crack patterns and the difference in the force-displacement diagram are not substantially.

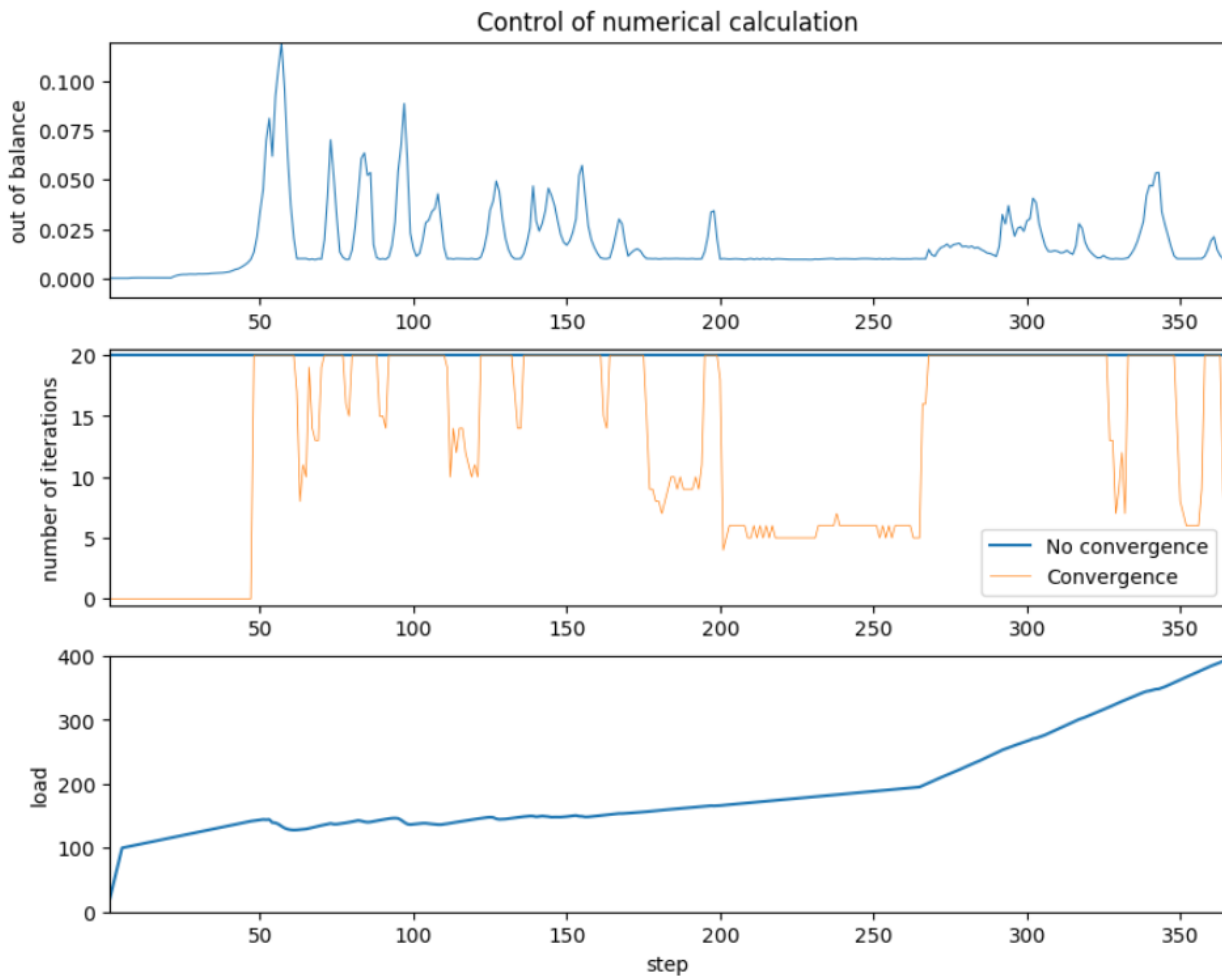


Figure appendix C-13; Control of numerical calculation of smaller mesh, experiment Braam

Each loading stage will now be reviewed with their crack pattern.

The first loading stage has a load of 218 kN, since there are two loading points each point gets a load of 109 kN. In the load-displacement diagram it can be seen that this is just after the first cracks appear, because of the nod in the line. The DIANA model deviates here from the experiment. It could be expected that in this stage the crack pattern will differ from each other.

In Figure appendix C-14 the crack pattern of the experiments from both sides of the beam are presented.

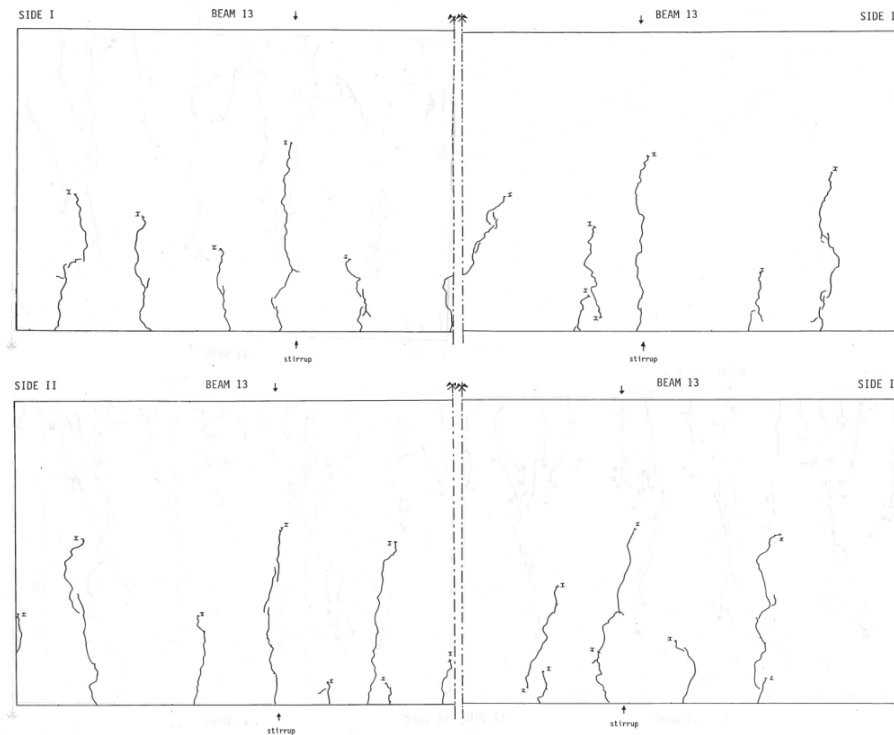


Figure appendix C-14; Crack pattern beam 218 kN

The results of the DIANA model gives no cracks at this load, but if the stresses in the concrete are examined it can be concluded that the tensile stress ( $4.08 \text{ N/mm}^2$ ) of concrete is just reached, see Figure appendix C-15.

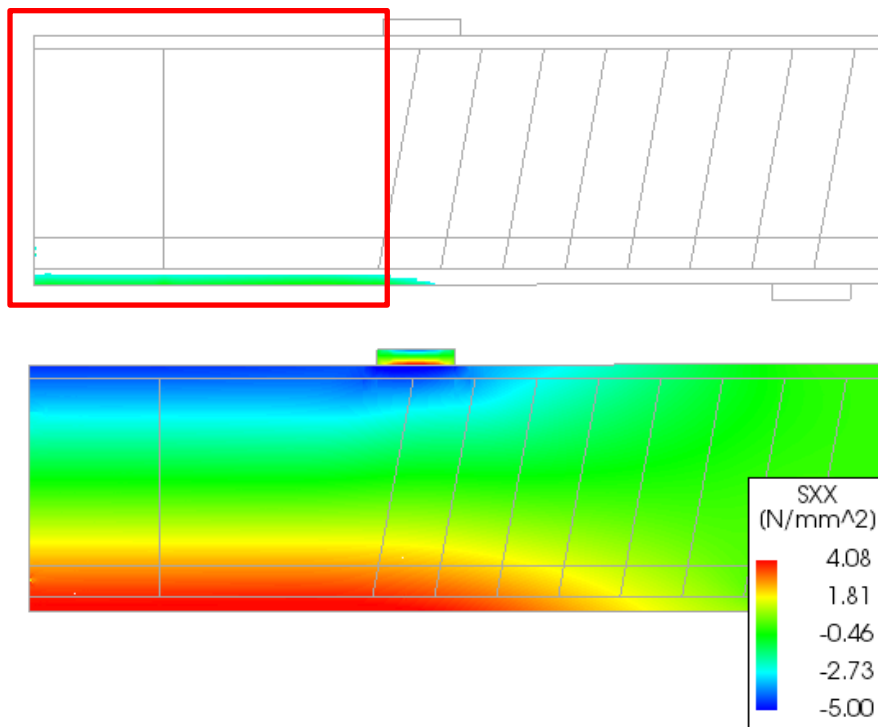


Figure appendix C-15; Crack width and stresses in concrete DIANA model with load of 220 kN

First cracks appear at 272 kN in this model with the following crack pattern, see Figure appendix C-16.

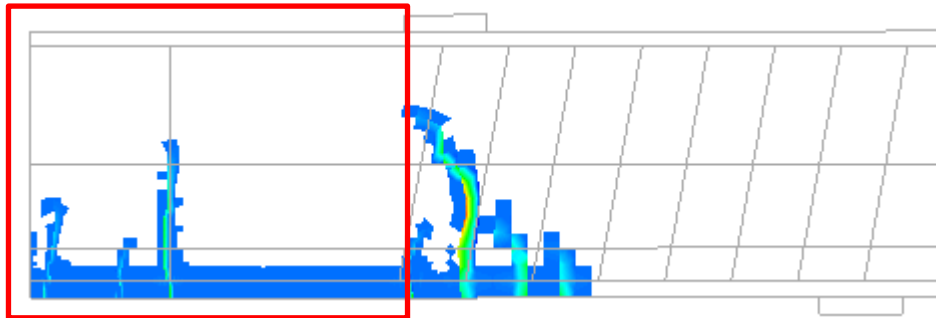


Figure appendix C-16; Crack pattern at 272 kN

It can be concluded that the crack pattern at this stage isn't comparable, which was expected since the tension softening causes a deviation between the force-displacement diagrams of the experiment and the DIANA model.

For the second loading stage a force of 368 was applied, this is 184 kN on each load point.

In Figure appendix C-17 the crack pattern of the experiment are shown:

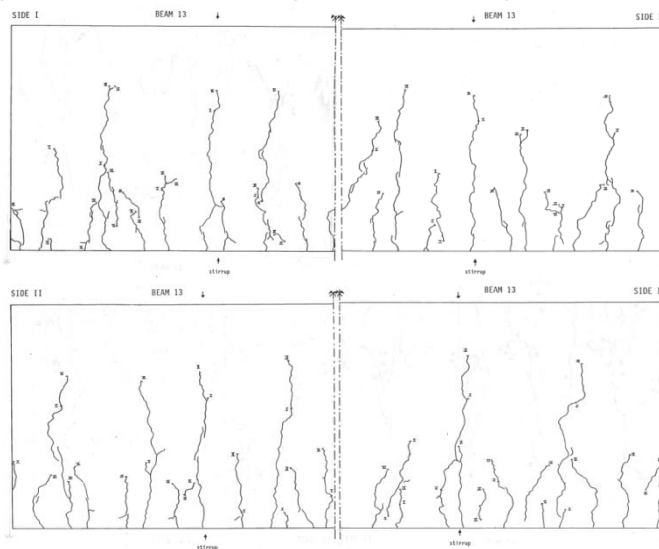


Figure appendix C-17; Crack pattern beam 368 kN

The crack pattern in DIANA gives the following figure:

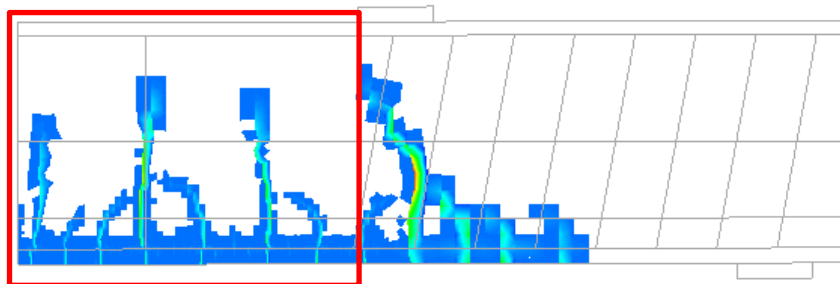


Figure appendix C-18; Crack pattern beam DIANA model 372 kN

The part from the middle to the loading point in the DIANA model, see Figure appendix C-18, can be compared with half of the crack pattern of the experiments, see Figure appendix C-17. The progress of cracking in concrete is different in every beam. For instance if the left and right side of the two sides of the beam are compared, there can be seen that there are differences in crack patterns. This is because the material is not isotropic, though in the DIANA model an isotropic material is assumed. So there cannot be expected that the crack patterns are spot on. The fact that the crack patterns of the experiment have a comparison with the crack pattern in the DIANA model is satisfying.

The next loading stage is 468 kN, so a load of 234 kN each load point.

The crack pattern of the experiment:

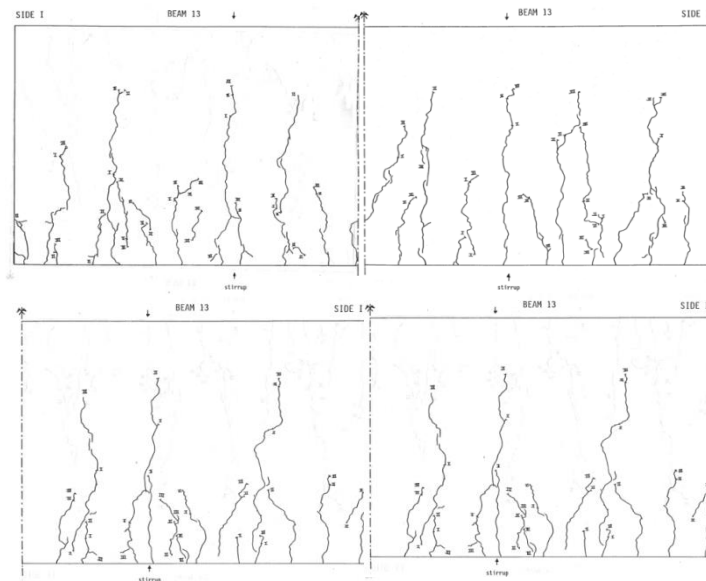


Figure appendix C-19; Crack pattern beam 468 kN

The crack pattern in DIANA:

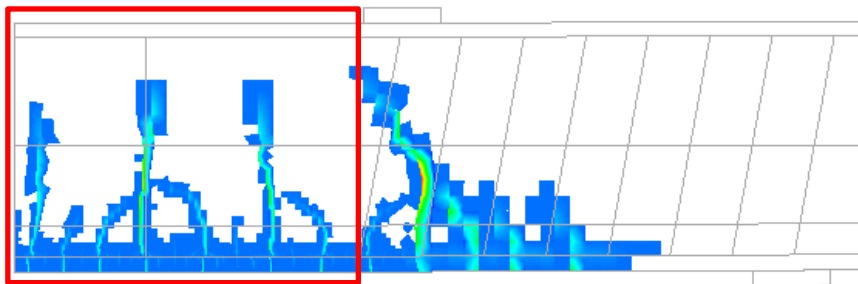


Figure appendix C-20; Crack pattern beam DIANA model 468 kN

The difference between crack patterns of the experiments of the second loading stage and the third are not that big, the cracks have developed a little bit.

The last loading stage of 668 kN, 334 kN on each load point, has also similar outcomes for the experimental and DIANA model in the force-displacement diagram.

The crack pattern of the experiment:

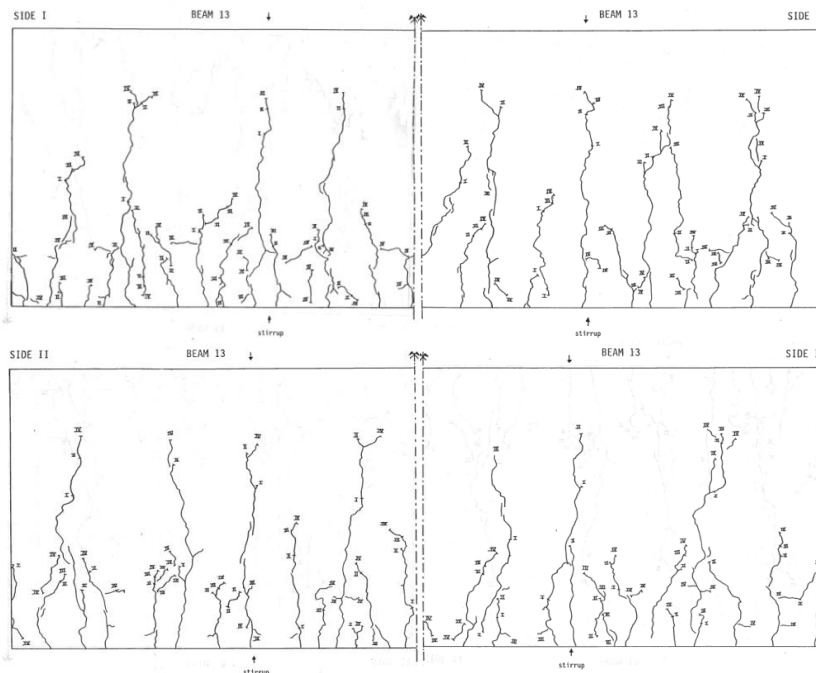


Figure appendix C-21; Crack pattern beam 668 kN

The crack pattern in DIANA:

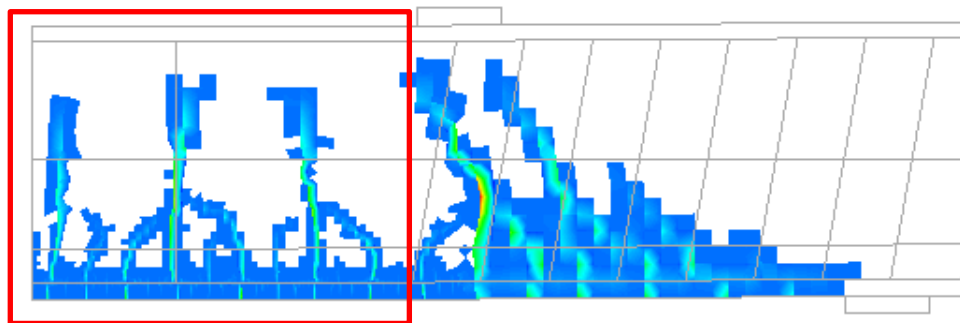


Figure appendix C-22; Crack pattern beam DIANA model 668 kN

Here the cracks are getting wider and extend a bit and no new cracks are formed, in both the experiments and the DIANA model. Based on the crack patterns the DIANA model gives a good estimation.



### Crack width

After the crack patterns the crack widths are checked. The crack width is determined with the displacement in x-direction over the complete crack spacing. In Figure 5-9 it is shown between which points the displacement is measured, indicated with the red dots.

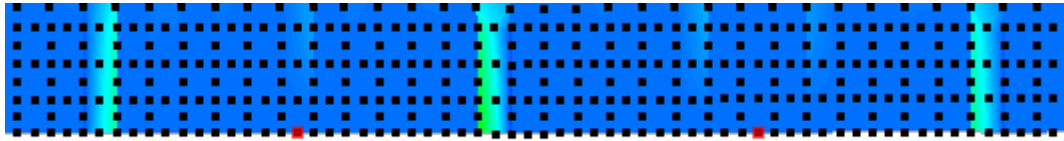


Figure appendix C-23; Check of crack widths

In the DIANA model there are seven cracks that can be clearly indicated, the displacement in x-direction between the red indication lines and the crack spacing are determined, see Figure appendix C-24.

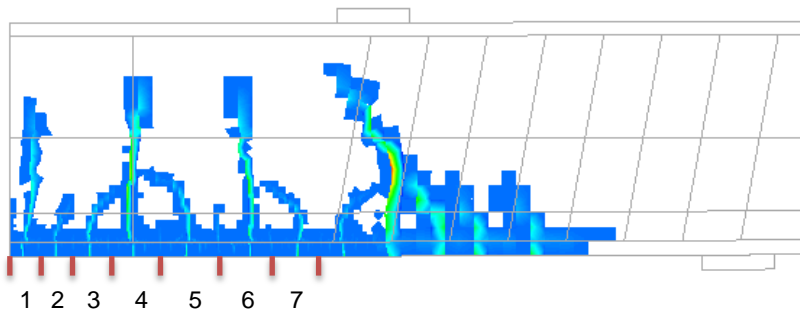


Figure appendix C-24; Crack width and crack spacing

In the experiment the crack width is at every load stage analysed. This has been done at several of heights, see Figure appendix C-25. The two measures closest to the outer fibre have been used for the crack width, since the cracks at the surface are of interest.

An example of an overview of the experiment results is given in Figure appendix C-26, these are the results of loading stage three. The red indicated numbers are used in the comparison with the result of DIANA. The maximum crack width has been taken, since the small cracks that have been taken into account in the mean of the experiment are not visible in the DIANA model. Therefore the crack width of DIANA will be closer to the maximum crack width of the experiments.

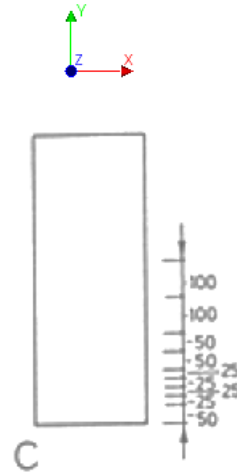


Figure appendix C-25; Measure heights of the crack widths

loading stage	line no.	$l_m$	$w_{min}$	$w_{max}$	$w_m$	c.v.	$w_k$	$w_k/w_m$	$w_{max}/w_m$	
		[mm]	[mm]	[mm]	[mm]	[-]	[mm]	[-]	[-]	
3	1	52	88	0.01	0.22	0.103	0.51	0.19	1.83	2.14
	2	51	90	0.01	0.24	0.104	0.47	0.18	1.77	2.31
	3	47	98	0.01	0.23	0.117	0.44	0.20	1.73	1.97
	4	47	98	0.01	0.24	0.101	0.56	0.19	1.92	2.38
	5	49	94	0.01	0.25	0.089	0.67	0.19	2.10	2.82
	6	43	107	0.01	0.25	0.086	0.88	0.21	2.45	2.90
	7	25	184	0.01	0.31	0.126	0.75	0.28	2.24	2.45
	8	17	271	0.01	0.28	0.149	0.51	0.27	1.84	1.88
	9	16	288	0.01	0.16	0.083	0.49	0.15	1.80	1.94

Figure appendix C-26; Results of crack width experiment braam

The results of the crack widths at the different loads are presented in Figure appendix C-27.

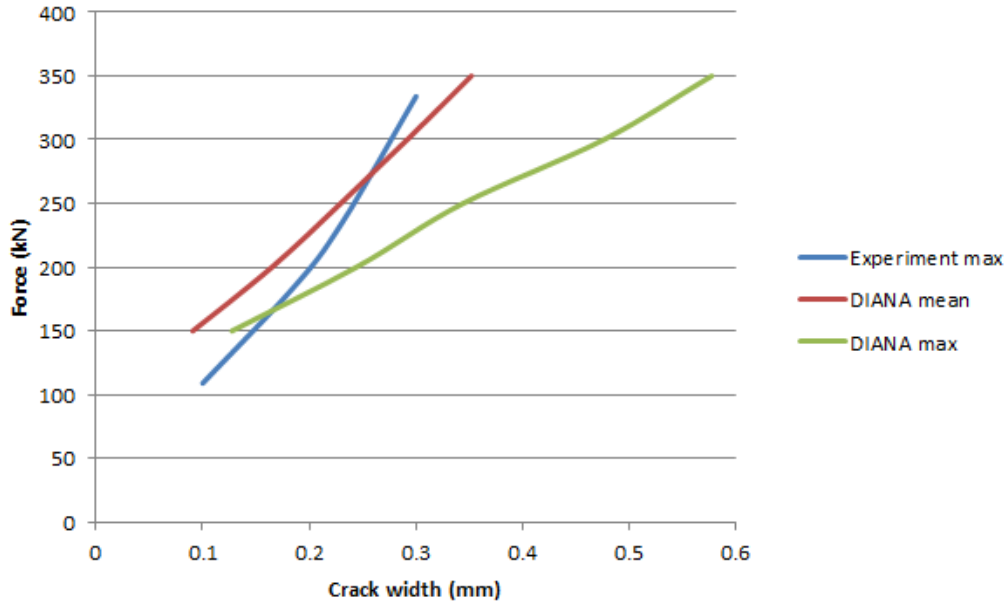


Figure appendix C-27; Crack width comparison experiment Braam

The DIANA model overestimates the crack width especially at higher loads. This could be the case due to small cracks that appear around the bigger cracks in the experiments at higher loads; these small cracks do not appear in the DIANA model and may be the reason that the cracks are bigger. Differences in the crack widths of the DIANA model and the experiment also can be explained by the small difference in the force displacement comparison, the cracks appear at a higher load which is as explained the result of the tension softening. Nevertheless, it can be concluded that the mean of the DIANA model is comparable with the maximum of the experiments.

The mean crack spacing in the experiment is around 90 mm; in the DIANA model a crack spacing of 150 mm is found.

## D. Python file DIANA calculation

This is an example of the python file, this python file is used for the influence of the cover. DIANA version 10.1 is used.

### **#Parameters**

```
Height=[300,500,700,900,1100,1300,1500,1700,1900]
Cover=[20,50,70,100]
Diameter=[16,25,25,30,35,35,40,40,40]
Steel_Area=[402,982,1963,3534,4810,6734,8800,11310,13820]
Perimeter=[100,157,314,471,550,770,880,1130,13820]
Load=[75,200,420,760,1050,1660,2000,2800,3400]
```

```
Ten_Strength=3
E_Con=30000
Poison_Con=0.2
Com_Strength=30
G_F=73*pow(Com_Strength,0.18)/1000
G_C=250*G_F
E_Steel=200000
Poison_Steel=0.3
Strenght_Steel=500
```

```
for j in range(len(Cover)):
    for i in range(len(Height)):
```

### **#start project**

```
newProject( "Afstuderen TU/Beam/Beam"+str(Height[i])+"C"+str(Cover[j]), 100 )
setModelAnalysisAspects( [ "STRUCT" ] )
setModelDimension( "2D" )
setDefaultMeshOrder( "QUADRATIC" )
setDefaultMesherType( "HEXQUAD" )
setDefaultMidSideNodeLocation( "ONSHAP" )
setUnit( "LENGTH", "MM" )
setUnit( "FORCE", "N" )
```

### **#Geometry**

```
createSheet( "Concrete", [[ 0, 0, 0 ],[ Height[i]*5, 0, 0 ],[ Height[i]*5, Height[i], 0 ],[ 0,
Height[i], 0 ] ] )
createSheet( "Support", [[ Height[i]*0.5, 0, 0 ],[ Height[i]*0.5, -50, 0 ],[ Height[i]*0.75,
-50, 0 ],[ Height[i]*0.75, 0, 0 ] ] )
createSheet( "Load", [[ Height[i]*2.25, Height[i], 0 ],[ Height[i]*2.25, Height[i]+50, 0
],[ Height[i]*2.5, Height[i]+50, 0 ],[ Height[i]*2.5, Height[i], 0 ] ] )
createLine( "Main reinforcement", [ 0, Cover[j], 0 ], [ Height[i]*5, Cover[j], 0 ] )
createLine( "Stirrup 1", [ Height[i]*0.5, 0, 0 ], [ Height[i]*0.1, Height[i], 0 ] )
arrayCopy( [ "Stirrup 1" ], [ Height[i]/7.5, 0, 0 ], [ 0, 0, 0 ], [ 0, 0, 0 ], 15 )
createLine( "Composed", [ 0, Height[i]/2, 0 ], [ Height[i]*5, Height[i]/2, 0 ] )
fitAll( )
```

**#Materials****#Concrete**

```

addMaterial( "Concrete", "CONCR", "TSCR", [] )
setParameter( "MATERIAL", "Concrete", "LINEAR/ELASTI/YOUNG", E_Con )
setParameter( "MATERIAL", "Concrete", "LINEAR/ELASTI/POISON", Poison_Con )
setParameter( "MATERIAL", "Concrete", "MODTYP/TOTCRK", "ROTATE" )
setParameter( "MATERIAL", "Concrete", "TENSIL/TENCRV", "HORDYK" )
setParameter( "MATERIAL", "Concrete", "TENSIL/TENSTR", Ten_Strength )
setParameter( "MATERIAL", "Concrete", "COMPRS/COMCRV", "PARABO" )
setParameter( "MATERIAL", "Concrete", "COMPRS/COMSTR", Com_Strength )
setParameter( "MATERIAL", "Concrete", "COMPRS/GC", G_C )
setParameter( "MATERIAL", "Concrete", "TENSIL/GF1", G_F )
setParameter( "MATERIAL", "Concrete", "COMPRS/REDUCT/REDCRV", "VC1993" )
setParameter( "MATERIAL", "Concrete", "COMPRS/REDUCT/REDMIN", 0.6 )
addGeometry( "Concrete geometry", "SHEET", "MEMBRA", [] )
setParameter( "GEOMET", "Concrete geometry", "THICK", Height[i]/2.5 )
addElementData( "Element data 1" )
setParameter( "DATA", "Element data 1", "/INTEGR", [] )
setParameter( "DATA", "Element data 1", "INTEGR", "HIGH" )
clearReinforcementAspects( [ "Concrete" ] )
setElementClassType( "SHAPE", [ "Concrete" ], "MEMBRA" )
assignMaterial( "Concrete", "SHAPE", [ "Concrete" ] )
assignGeometry( "Concrete geometry", "SHAPE", [ "Concrete" ] )
assignElementData( "Element data 1", "SHAPE", [ "Concrete" ] )

```

**#Steel plate**

```

addMaterial( "Steel", "MCSTEL", "ISOTRO", [] )
setParameter( "MATERIAL", "Steel", "LINEAR/ELASTI/YOUNG", E_Steel )
setParameter( "MATERIAL", "Steel", "LINEAR/ELASTI/POISON", Poison_Steel )
addGeometry( "Steel geometry", "SHEET", "MEMBRA", [] )
setParameter( "GEOMET", "Steel geometry", "THICK", Height[i]/2.5 )
clearReinforcementAspects( [ "Load" ] )
setElementClassType( "SHAPE", [ "Load" ], "MEMBRA" )
assignMaterial( "Steel", "SHAPE", [ "Load" ] )
assignGeometry( "Steel geometry", "SHAPE", [ "Load" ] )
assignElementData( "Element data 1", "SHAPE", [ "Load" ] )
clearReinforcementAspects( [ "Support" ] )
setElementClassType( "SHAPE", [ "Support" ], "MEMBRA" )
assignMaterial( "Steel", "SHAPE", [ "Support" ] )
assignGeometry( "Steel geometry", "SHAPE", [ "Support" ] )
assignElementData( "Element data 1", "SHAPE", [ "Support" ] )

```

**#Reinforcement**

```

addMaterial( "Bond Slip Reinforcement", "REINFO", "REBOND", [] )
setParameter( "MATERIAL", "Bond Slip Reinforcement", "REBARS/ELASTI/YOUNG",
E_Steel )
setParameter( "MATERIAL", "Bond Slip Reinforcement", "REBARS/PLATYP", "VMISES"
)
setParameter( "MATERIAL", "Bond Slip Reinforcement", "REBARS/PLASTI/YLDSTR",
Strenght_Steel )
setParameter( "MATERIAL", "Bond Slip Reinforcement", "RESLIP/DSNY", 1000 )

```

```

setParameter( "MATERIAL", "Bond Slip Reinforcement", "RESLIP/DSSX", 1000 )
setParameter( "MATERIAL", "Bond Slip Reinforcement", "RESLIP/SHFTYP", "BONDS4"
)
setParameter( "MATERIAL", "Bond Slip Reinforcement", "RESLIP/BONDS4/SLPVAL",
Com_Strength )
setParameter( "MATERIAL", "Bond Slip Reinforcement", "RESLIP/BONDS4/DIAMET",
Diameter[i] )
addGeometry( "Bond Slip geometry", "RELIN", "REBAR", [] )
setParameter( "GEOMET", "Bond Slip geometry", "REITYP", "REITRU" )
setParameter( "GEOMET", "Bond Slip geometry", "REITRU/CROSSE", Steel_Area[i] )
setParameter( "GEOMET", "Bond Slip geometry", "REITRU/PERIME", Perimeter[i] )
addElementData( "Element data 2" )
setParameter( "DATA", "Element data 2", "./INTERF", [] )
setParameter( "DATA", "Element data 2", "INTERF", "TRUSS" )
setReinforcementAspects( [ "Main reinforcement" ] )
assignMaterial( "Bond Slip Reinforcement", "SHAPE", [ "Main reinforcement" ] )
assignGeometry( "Bond Slip geometry", "SHAPE", [ "Main reinforcement" ] )
assignElementData( "Element data 2", "SHAPE", [ "Main reinforcement" ] )
setReinforcementDiscretization( [ "Main reinforcement" ], "ELEMENT" )

```

#### #Stirrups

```

addMaterial( "Stirrups", "REINFO", "VMISES", [] )
setParameter( "MATERIAL", "Stirrups", "LINEAR/ELASTI/YOUNG", E_Steel )
setParameter( "MATERIAL", "Stirrups", "PLASTI/YLDTYP", "NONE" )
setParameter( "MATERIAL", "Stirrups", "PLASTI/HARDI1/YLDSTR", Strenght_Steel )
addGeometry( "Stirrups geometry", "RELIN", "REBAR", [] )
setParameter( "GEOMET", "Stirrups geometry", "REIEMB/CROSSE", Steel_Area[i]/3 )
setReinforcementAspects( [ "Stirrup 1", "Stirrup 2", "Stirrup 3", "Stirrup 4", "Stirrup
5", "Stirrup 6", "Stirrup 7", "Stirrup 8", "Stirrup 9", "Stirrup 10", "Stirrup 11", "Stirrup
12", "Stirrup 13", "Stirrup 14", "Stirrup 15", "Stirrup 16" ] )
assignMaterial( "Stirrups", "SHAPE", [ "Stirrup 1", "Stirrup 2", "Stirrup 3", "Stirrup 4",
"Stirrup 5", "Stirrup 6", "Stirrup 7", "Stirrup 8", "Stirrup 9", "Stirrup 10", "Stirrup 11",
"Stirrup 12", "Stirrup 13", "Stirrup 14", "Stirrup 15", "Stirrup 16" ] )
assignGeometry( "Stirrups geometry", "SHAPE", [ "Stirrup 1", "Stirrup 2", "Stirrup 3",
"Stirrup 4", "Stirrup 5", "Stirrup 6", "Stirrup 7", "Stirrup 8", "Stirrup 9", "Stirrup 10",
"Stirrup 11", "Stirrup 12", "Stirrup 13", "Stirrup 14", "Stirrup 15", "Stirrup 16" ] )
resetElementData( "SHAPE", [ "Stirrup 1", "Stirrup 2", "Stirrup 3", "Stirrup 4", "Stirrup
5", "Stirrup 6", "Stirrup 7", "Stirrup 8", "Stirrup 9", "Stirrup 10", "Stirrup 11", "Stirrup
12", "Stirrup 13", "Stirrup 14", "Stirrup 15", "Stirrup 16" ] )
setReinforcementDiscretization( [ "Stirrup 1", "Stirrup 2", "Stirrup 3", "Stirrup 4",
"Stirrup 5", "Stirrup 6", "Stirrup 7", "Stirrup 8", "Stirrup 9", "Stirrup 10", "Stirrup 11",
"Stirrup 12", "Stirrup 13", "Stirrup 14", "Stirrup 15", "Stirrup 16" ], "ELEMENT" )
addGeometry( "Composed geometry", "LINE", "COMLIN", [] )
setParameter( "GEOMET", "Composed geometry", "DISTAN/THICK", Height[i] )
setElementClassType( "SHAPE", [ "Composed" ], "COMLIN" )
assignGeometry( "Composed geometry", "SHAPE", [ "Composed" ] )

```

#### #Load

```

addSet( "GEOMETRYLOADSET", "Geometry load case 1" )
createLineLoad( "Load", "Geometry load case 1" )

```

```

setParameter( "GEOMETRYLOAD", "Load", "FORCE/VALUE", Load[i]/-
0.25/Height[i]*1000 )
setParameter( "GEOMETRYLOAD", "Load", "FORCE/DIRECT", 2 )
attach( "GEOMETRYLOAD", "Load", "Load", [[ Height[i]*2.375, Height[i]+50, 0 ]] )

```

### **#Support**

```

createVertex( "Vertex 1", [ Height[i]*0.625, -50, 0 ] )
projection( "SHAPEEDGE", "Support", [[ Height[i]*0.625, -50, 0 ]], [ "Vertex 1" ], [ 0, 0,
-1 ], True )
removeShape( [ "Vertex 1" ] )
addSet( "GEOMETRYSUPPORTSET", "Geometry support set 1" )
createPointSupport( "Side", "Geometry support set 1" )
setParameter( "GEOMETRYSUPPORT", "Side", "AXES", [ 1, 2 ] )
setParameter( "GEOMETRYSUPPORT", "Side", "TRANSL", [ 0, 1, 0 ] )
setParameter( "GEOMETRYSUPPORT", "Side", "ROTATI", [ 0, 0, 0 ] )
attach( "GEOMETRYSUPPORT", "Side", "Support", [[ Height[i]*0.625, -50, 0 ]])
createLineSupport( "Mid", "Geometry support set 1" )
setParameter( "GEOMETRYSUPPORT", "Mid", "AXES", [ 1, 2 ] )
setParameter( "GEOMETRYSUPPORT", "Mid", "TRANSL", [ 1, 0, 0 ] )
setParameter( "GEOMETRYSUPPORT", "Mid", "ROTATI", [ 0, 0, 0 ] )
attach( "GEOMETRYSUPPORT", "Mid", "Concrete", [[ Height[i]*5, 0.5*Height[i], 0 ]])
createPointSupport( "Rein", "Geometry support set 1" )
setParameter( "GEOMETRYSUPPORT", "Rein", "AXES", [ 1, 2 ] )
setParameter( "GEOMETRYSUPPORT", "Rein", "TRANSL", [ 1, 0, 0 ] )
setParameter( "GEOMETRYSUPPORT", "Rein", "ROTATI", [ 0, 0, 0 ] )
attach( "GEOMETRYSUPPORT", "Rein", "Main reinforcement", [[ Height[i]*5, Cover[j],
0 ]])

```

### **#Interface**

```

addMaterial( "Interface", "INTERF", "NONLIF", [] )
setParameter( "MATERIAL", "Interface", "LINEAR/IFTYP", "LIN2D" )
setParameter( "MATERIAL", "Interface", "LINEAR/ELAS2/DSNY", 1000000 )
setParameter( "MATERIAL", "Interface", "LINEAR/ELAS2/DSSX", 0.1 )
setParameter( "MATERIAL", "Interface", "NONLIN/NLEL8/NOTENS", [ 0.001, 0 ] )
setParameter( "MATERIAL", "Interface", "NONLIN/NLEL8/NOSHTE", [ 0.001, 0 ] )
addGeometry( "Interface geometry", "LINE", "STRINT", [] )
setParameter( "GEOMET", "Interface geometry", "THICK", Height[i]/2.5 )
createLineConnection( "Interface" )
setParameter( "GEOMETRYCONNECTION", "Interface", "CONTYP", "INTER" )
setParameter( "GEOMETRYCONNECTION", "Interface", "MODE", "AUTO" )
attachTo( "GEOMETRYCONNECTION", "Interface", "SOURCE", "Support", [[
Height[i]*0.625, 0, 0 ]])
attachTo( "GEOMETRYCONNECTION", "Interface", "SOURCE", "Load", [[
Height[i]*2.375, Height[i], 0 ]])
setElementClassType( "GEOMETRYCONNECTION", "Interface", "STRINT" )
assignMaterial( "Interface", "GEOMETRYCONNECTION", "Interface" )
assignGeometry( "Interface geometry", "GEOMETRYCONNECTION", "Interface" )
resetElementData( "GEOMETRYCONNECTION", "Interface" )

```

**#Mesh**

```

createVertex( "Vertex 1", [ Height[i]*2.25, 0, 0 ] )
projection( "SHAPEEDGE", "Concrete", [[ Height[i]*2.5, 0, 0 ]], [ "Vertex 1" ], [ 0, 0, -1
], True )
removeShape( [ "Vertex 1" ] )
createVertex( "Vertex 1", [ Height[i]*5, 0.25*Height[i], 0 ] )
projection( "SHAPEEDGE", "Concrete", [[ Height[i]*5, 0.5*Height[i], 0 ]], [ "Vertex 1"
], [ 0, 0, -1 ], True )
removeShape( [ "Vertex 1" ] )
setElementSize( [ "Concrete", "Load", "Support", "Composed" ], Height[i]/10, -1,
True )
setMesherType( [ "Concrete", "Load", "Support", "Composed" ], "HEXQUAD" )
setMidSideNodeLocation( [ "Concrete", "Load", "Support", "Composed" ], "ONSHAP"
)
setElementSize( "Concrete", 1, [[ Height[i]*3.625, 0, 0 ],[ Height[i]*5, 0.125*Height[i],
0 ]], 10, 0, True )
generateMesh( [] )
hideView( "GEOM" )
showView( "MESH" )

```

**#Analysis**

```

addAnalysis( "Analysis Beam "+str(Height[i])+"C"+str(Cover[j]) )
addAnalysisCommand( "Analysis Beam "+str(Height[i])+"C"+str(Cover[j]), "NONLIN",
"Structural nonlinear" )
setAnalysisCommandDetail( "Analysis Beam "+str(Height[i])+"C"+str(Cover[j]),
"Structural nonlinear", "EXECUT(1)/LOAD/STEPS/EXPLIC/SIZES", "0.100000(2)
0.005(50) 0.02(100)" )
addAnalysisCommandDetail( "Analysis Beam "+str(Height[i])+"C"+str(Cover[j]),
"Structural nonlinear", "EXECUT(1)/LOAD/STEPS/EXPLIC/ARCLLEN" )
setAnalysisCommandDetail( "Analysis Beam "+str(Height[i])+"C"+str(Cover[j]),
"Structural nonlinear", "EXECUT(1)/LOAD/STEPS/EXPLIC/ARCLLEN", True )
setAnalysisCommandDetail( "Analysis Beam "+str(Height[i])+"C"+str(Cover[j]),
"Structural nonlinear", "EXECUT(1)/ITERAT/MAXITE", 10 )
setAnalysisCommandDetail( "Analysis Beam "+str(Height[i])+"C"+str(Cover[j]),
"Structural nonlinear", "EXECUT(1)/ITERAT/CONVER/DISPLA", False )
setAnalysisCommandDetail( "Analysis Beam "+str(Height[i])+"C"+str(Cover[j]),
"Structural nonlinear", "EXECUT(1)/ITERAT/CONVER/FORCE/NOCONV", "CONTIN" )
addAnalysisCommandDetail( "Analysis Beam "+str(Height[i])+"C"+str(Cover[j]),
"Structural nonlinear", "EXECUT(1)/ITERAT/LINESE" )
setAnalysisCommandDetail( "Analysis Beam "+str(Height[i])+"C"+str(Cover[j]),
"Structural nonlinear", "EXECUT(1)/ITERAT/LINESE", True )
setAnalysisCommandDetail( "Analysis Beam "+str(Height[i])+"C"+str(Cover[j]),
"Structural nonlinear", "EXECUT(1)/ITERAT/MAXITE", 10 )
setAnalysisCommandDetail( "Analysis Beam "+str(Height[i])+"C"+str(Cover[j]),
"Structural nonlinear", "OUTPUT(1)/SELTYP", "USER" )
addAnalysisCommandDetail( "Analysis Beam "+str(Height[i])+"C"+str(Cover[j]),
"Structural nonlinear", "OUTPUT(1)/USER" )
addAnalysisCommandDetail( "Analysis Beam "+str(Height[i])+"C"+str(Cover[j]),
"Structural nonlinear", "OUTPUT(1)/USER/DISPLA(1)/TOTAL/TRANSL/GLOBAL" )

```

```

addAnalysisCommandDetail( "Analysis Beam "+str(Height[i])+"C"+str(Cover[j]),
"Structural nonlinear", "OUTPUT(1)/USER/STRAIN(1)/TOTAL/GREEN" )
addAnalysisCommandDetail( "Analysis Beam "+str(Height[i])+"C"+str(Cover[j]),
"Structural nonlinear", "OUTPUT(1)/USER/STRAIN(2)/CRACK/GREEN" )
addAnalysisCommandDetail( "Analysis Beam "+str(Height[i])+"C"+str(Cover[j]),
"Structural nonlinear", "OUTPUT(1)/USER/STRAIN(3)/CRKWDT/GREEN" )
addAnalysisCommandDetail( "Analysis Beam "+str(Height[i])+"C"+str(Cover[j]),
"Structural nonlinear", "OUTPUT(1)/USER/STRAIN(4)/CRKWDT/GREEN/PRINCI" )
addAnalysisCommandDetail( "Analysis Beam "+str(Height[i])+"C"+str(Cover[j]),
"Structural nonlinear", "OUTPUT(1)/USER/STRAIN(5)/TOTAL/GREEN/PRINCI" )
addAnalysisCommandDetail( "Analysis Beam "+str(Height[i])+"C"+str(Cover[j]),
"Structural nonlinear", "OUTPUT(1)/USER/STRESS(1)/TOTAL/CAUCHY/GLOBAL" )
addAnalysisCommandDetail( "Analysis Beam "+str(Height[i])+"C"+str(Cover[j]),
"Structural nonlinear", "OUTPUT(1)/USER/STRESS(2)/TOTAL/CAUCHY/PRINCI" )
addAnalysisCommandDetail( "Analysis Beam "+str(Height[i])+"C"+str(Cover[j]),
"Structural nonlinear", "OUTPUT(1)/USER/STRESS(3)/TOTAL/MOMENT/LOCAL" )
addAnalysisCommandDetail( "Analysis Beam "+str(Height[i])+"C"+str(Cover[j]),
"Structural nonlinear", "OUTPUT(1)/USER/STRESS(4)/TOTAL/FORCE/LOCAL" )
addAnalysisCommandDetail( "Analysis Beam "+str(Height[i])+"C"+str(Cover[j]),
"Structural nonlinear", "OUTPUT(1)/USER/FORCE(1)/REACTI/TRANSL" )
addAnalysisCommandDetail( "Analysis Beam "+str(Height[i])+"C"+str(Cover[j]),
"Structural nonlinear", "OUTPUT(1)/USER/STRESS(5)/TOTAL/TRACTI/LOCAL" )
addAnalysisCommandDetail( "Analysis Beam "+str(Height[i])+"C"+str(Cover[j]),
"Structural nonlinear", "OUTPUT(1)/USER/STRAIN(6)/TOTAL/TRACTI/LOCAL" )
setAnalysisCommandDetail( "Analysis Beam "+str(Height[i])+"C"+str(Cover[j]),
"Structural nonlinear", "OUTPUT(1)/SELECT/MODSEL", "USER" )
setAnalysisCommandDetail( "Analysis Beam "+str(Height[i])+"C"+str(Cover[j]),
"Structural nonlinear", "OUTPUT(1)/SELECT/ELEMEN(1)/RNGNRS", "\"Concrete\"
\"Interface 1\" \"Interface\" \"Composed\"" )
runSolver( "Analysis Beam "+str(Height[i])+"C"+str(Cover[j]) )
showView( "RESULT" )

```

### **#Save**

```

saveProjectAs( "C:/Users/905583/Documents/Afstuderen
TU/Beam/Beam"+str(Height[i])+"C"+str(Cover[j])+".dpf" )
closeProject( )

```



## E. Answers sub questions

### Sub questions:

- How is crack width calculated in the Eurocode 2, and where are these calculations based on?
- How is crack width calculated in other codes, and what are the differences with the Eurocode 2?
- How does DIANA determine the location of the crack?
- How can the crack width be determined in DIANA?
- Can DIANA predict the crack width found in experiments?
- How do the parameters that are used in the Eurocode 2 crack width calculation influence the outcome of both the Eurocode 2 and the DIANA calculations?
- Are the outcomes of the DIANA and Eurocode 2 of the crack width comparable, if not which explanations can be given for the difference?
- What is the influence of the construction height on the crack width?

*How is crack width calculated in the Eurocode 2, and where are these calculations based on?*

The crack width calculation is the multiplication of the so called crack spacing and crack strain. The crack strain is the increase of the strain in the reinforcement steel after cracks appear which happens when the concrete tensile strength has been reached. The crack spacing is determined by the cover, diameter and the ratio between the effective tensile area of the concrete and the reinforcement steel area. On most of these parameters influence factors are applied, these values take into account long or short term loading, the distribution of the strain and the bond properties.

*How is crack width calculated in other codes, and what are the differences with the Eurocode 2?*

In most of the other codes about the same approach for the calculation of the cracks is applied. Though, the influence factors differ quite a lot. The Model code 2010 is of the investigated codes the most comparable with the Eurocode 2, only the factors differ from each other. The Japanese code and Chinese code show some differences, for instance in both codes there is no reduction term that includes the tensile strength of concrete when the crack strain is calculated, in the Chinese code the cover is not included in the crack spacing calculation and in the Japanese code the spacing between the reinforcement bars is included, but the effective reinforcement percentage is left out. The code of the United States is a totally different approach than what is used in the Eurocode 2. The spacing between the reinforcement bars is checked with a certain criterion. In this criterion there is a factor that is dependent on the maximum allowable crack width. When the criterion is approved the cracks will not become bigger than the maximum allowable crack width. It appeared in the calculations that the Eurocode 2 is less conservative if compared to the other codes.

*How does DIANA determine the location of the crack?*

DIANA FEA has several of material models, for the determination of cracks there are smeared and discrete crack models. For discrete crack models the location of the crack has to be known, this was not the case, so a smeared crack model is used. There are two kinds of smeared crack models; the total strain crack model and the multi directional fixed crack model. The total strain crack model uses stress-strain curves in the calculation of the structure; the multi directional fixed crack model is applied for temperature and maturity dependent cracking. Since the cracks are formed by external forces the total strain crack model is used. In this model the stress-strain relations of the tensile behaviour and compressive behaviour of the material has to be given. When the tensile strength is reached softening of the material will appear and eventually a crack will appear in the structure, the tension stress in the material directly around the crack disappears and increases with increasing distance of the crack, a new crack will appear at the point where the tensile strength is reached again. In this way the crack pattern is formed and the location of the cracks are found.

#### *How can the crack width be determined in DIANA?*

In this thesis the crack width is calculated by the displacement in x direction, so perpendicular to the crack, over the crack spacing. If the displacement was taken over the element of the crack the same results were found. For practical reasons the displacement between the crack spacing is taken, since the crack spacing also could be determined in that way.

#### *Can DIANA predict the crack width found in experiments?*

In the validation of the experiments the force-displacement line is first compared. Since this is a check whether the DIANA model reacts the way it should be reacting. The force-displacement lines of all the three experiments were comparable with the DIANA models. The second check was the crack pattern, these are also comparable with each other, but small cracks that appear in the experiments are not always visible in the DIANA models. At last the crack width is compared; in this comparison the mean of the DIANA models is around the value of the maximum of the experiments. So there is a correlation, but the DIANA model prediction is bigger than the experiment results. Since the mean of the DIANA crack widths is comparable with the maximum of the experiments; the mean of the DIANA crack widths is used in the comparison with the Eurocode 2.

#### *How do the parameters that are used in the Eurocode 2 crack width calculation influence the outcome of both the Eurocode 2 and the DIANA calculations?*

The influence of the cover is quite significant in the Eurocode 2 as well as in the DIANA calculations; there is a large increase of crack width and crack spacing with increasing cover.

The influence of the reinforcement percentage in the Eurocode 2 is less significant, though a slight decrease of crack width and crack spacing with increasing reinforcement percentage has been seen. The crack strain reacts in an opposite manner, the strain increases with increasing reinforcement percentage. The influence of the reinforcement percentage in the DIANA calculations is small; no real influence could be detected in the crack width as in the

crack spacing. Only in the crack strain a small increase with increasing reinforcement percentage is detected.

The influence of the concrete tensile strength in the Eurocode 2 is that the crack width decreases with increasing concrete tensile strength. This results from the same relative change in the crack strain. In the DIANA model there is no clear influence of the concrete tensile strength.

The influence of the reinforcement steel stress is next to the cover a significant factor in the Eurocode 2 and DIANA calculations. A great increase of crack width is the results of an increase of reinforcement stress. This increase is relatively the same as the crack strain, because the crack spacing does not change.

All together the most important factors in the Eurocode 2 and the DIANA calculations are the cover and reinforcement steel stress.

*Are the outcomes of the DIANA and Eurocode 2 of the crack width comparable, if not which explanations can be given for the difference?*

The crack widths are somewhat comparable; the crack width in the Eurocode 2 is larger than the crack width in the DIANA calculations. The difference between these two is a certain value. This difference is the cause of a different outcome of the crack spacing and crack strain in the two calculations. The difference of the crack spacing is relatively bigger than the difference between the crack widths. Though, the crack strain is bigger in the DIANA calculations than in the Eurocode 2 calculations, so this slightly counteracts the influence of the crack spacing. In the end the difference between the crack spacing's is bigger than the difference between crack strains so that is why the crack width is larger in the Eurocode 2. If the crack strain is modified with a certain bending influence factor, which is influenced by the height of the beam and the cover, the crack strain could be adjusted to the DIANA calculations. When the crack spacing term of the Eurocode 2 is modified to the DIANA calculations outcomes, only the cover stays in the calculations with a certain factor over it. This is because of the fact that the reinforcement percentage did not really have an influence on the crack spacing in the DIANA calculations.

*What is the influence of the construction height on the crack width?*

The influence of increasing construction height is in all the results of the Eurocode 2 negligible, there is no real change with increasing construction height. But in the DIANA calculations there is a slight decrease of crack strain with increasing construction height.